

## Self-organization in active distributed media: scenarios for the spontaneous formation and evolution of dissipative structures

B. S. Kerner and V. V. Osipov

Usp. Fiz. Nauk 160, 1–73 (September 1990)

Various scenarios for self-organization in a wide range of nonequilibrium physical, chemical, and biological systems are examined. It is stressed that in many systems small-amplitude dissipative structures never form: At the instant at which the homogeneous state stratifies, large-amplitude dissipative structures appear abruptly. These large-amplitude structures are striations, spots, or blobs. Methods for the construction of such dissipative structures and for studying their stability are discussed for an arbitrary departure of the system from equilibrium. Many self-organization scenarios do not involve an instability of the dissipative structures of a given type and are instead determined by a local breakdown effect. In real systems, self-organization is determined by the spontaneous appearance and subsequent evolution of autosolitons (localized dissipative structures). The conditions under which turbulence arises in such systems in the absence of a flow are discussed. This turbulence is a complicated picture of the random appearance and disappearance of interacting autosolitons in various parts of the system. In gaseous and semiconductor plasmas, dissipative structures can arise in the form of numerous current filaments or electric-field domains. Their formation is unrelated to the shape of the current-voltage characteristic of the system. There is a discussion of certain self-organization phenomena in systems in which static dissipative structures may be accompanied by pulsating dissipative structures and autowaves. Corresponding effects in systems with flows (or fluxes of material) are also discussed. The general results of self-organization theory are used to explain the properties of the dissipative structures which have been observed and studied in numerical and experimental studies of physical systems of various types in recent years.

### I. INTRODUCTION

Among the most vivid phenomena in nonlinear physics is the spontaneous or stimulated formation of spatially inhomogeneous states in nonequilibrium systems (Refs. 1–25, for example). Such states are presently called “dissipative structures” (DSs) or “autostructures.”<sup>1)</sup> As the excitation level is varied, the nature of the DS changes, either smoothly or abruptly. Prigogine suggested the name “self-organization” for the spontaneous formation and evolution of DSs.<sup>2)</sup> Self-organization is associated with a manifestation of collective (or cooperative) effects which occur in nonequilibrium systems. Haken has suggested the name “synergetics” for this field of science.<sup>5,6)</sup>

Striations in a gas discharge are a classic example of the formation and evolution of DSs.<sup>14)</sup> The formation of ionization striations was apparently observed by Michael Faraday back in the 19th century.<sup>14b)</sup> Another classic example of self-organization is the formation and evolution of Bénard cells in a viscous liquid heated from below.<sup>3,4)</sup> Self-organization is observed in many nonequilibrium systems, differing completely in nature, including hydrodynamic systems,<sup>2)</sup> chemical and biological systems,<sup>3–8,10–12,16,17)</sup> semiconductor plasmas,<sup>31,32)</sup> semiconductor<sup>33–35)</sup> and gas-discharge structures,<sup>14,15,36,37)</sup> composite superconductors,<sup>19,38)</sup> and nonlinear optical media.<sup>41)</sup> Self-organization is also observed in the propagation of flame fronts,<sup>13,20)</sup> during the melting and

crystallization of solids,<sup>39)</sup> and in chemical reactions at surfaces.<sup>40)</sup>

In ideally homogeneous distributed media, the spontaneous formation of DSs stems from a stratification of their homogeneous state, i.e., from the growth of fluctuations with some particular wave number  $k_0 \neq 0$ . In the active distributed media which we will be discussing in this review, the stratification occurs because a positive feedback operates through one of the parameters—the “activator”—and leads to a growth of this activator. The growth of the activator is controlled by another parameter of the system—the “inhibitor”—for which there is a negative feedback.<sup>3)</sup> Both the activation processes and the inhibition processes are of course completely different in nature in different physical, chemical, and biological active systems (§§1, 7, 8).

Steady-state DSs usually form in active distributed media in which the inhibition process is of longer range than the activation process.<sup>3,5,8,11,12)</sup> In other words, in these media the length scale of the variation of the inhibitor,  $L$ , is much larger than the length scale of the variation of the activator,  $l$ . The homogeneous state becomes stratified because the relation  $L \gg l$  prevents the inhibitor from effectively suppressing a local growth of the activator in a region of size  $d \approx (lL)^{1/2}$  (Subsection 1.1).

That a flame front might stratify, essentially because of the relation  $L \gg l$ , was pointed out back in 1944 by Zel'do-

vich.<sup>43</sup> In 1952, Turing analyzed the condition for the stratification of a homogeneous state on the basis of an axiomatic model of morphogenesis.<sup>44</sup> Analysis of that model leads to the general conclusion that it becomes an easier matter to satisfy the stratification condition as the quantity  $\varepsilon = l/L$  becomes smaller (Subsection 1.1). It later became clear that it was specifically the combination of a short-range activation process and a long-range inhibition process—i.e., the condition  $l \ll L$ —which was pertinent to the formation of DSs in a wide range of active distributed media, including gas discharges,<sup>45,46</sup> several chemical and biological systems,<sup>3,5,8,11,12</sup> hot semiconductor plasmas and gaseous plasmas,<sup>47-51</sup> homogeneous semiconductors and semiconductor structures (transistor, p-n, p-i-n, etc., structures),<sup>33b,34,35,52-58</sup> nonequilibrium gas mixtures,<sup>59-61</sup> and the ionospheric  $F$  layer.<sup>62</sup>

Various approaches have now been developed for analyzing the evolution of small-amplitude DSs. Under certain condition (Subsection 1.4), such structures may form near the point at which the homogeneous state of a system stratifies. The goal of these approaches is to make use of the small amplitude of the DSs to construct some equations simpler than the original equations for describing the self-organization processes.

### 1.1. THEORY OF SMALL-AMPLITUDE DISSIPATIVE STRUCTURES

It was back in 1944 that Landau derived an equation describing the appearance of small-amplitude DSs in a moving viscous liquid at Reynolds numbers near the critical value.<sup>1</sup> Simplified equations were subsequently derived for describing the properties of small-amplitude DSs in various systems, including hydrodynamic systems, by many investigators, including Kuramoto and Tsuzuki,<sup>63</sup> Nitzan and Ortoleva,<sup>64</sup> Sivashinsky,<sup>13</sup> Newell and Whitehead,<sup>65</sup> Segel,<sup>66</sup> Siggia and Zippelius,<sup>67</sup> Swift and Hohemberg,<sup>68</sup> Gertsberg and Sivashinsky,<sup>69</sup> and Malomed.<sup>70</sup> Haken proposed a method by which a certain choice of “order parameter” of the system and the use of a “subordination principle” of decaying modes make it possible to derive equations for the evolution of this order parameter: so-called generalized Ginzburg–Landau equations.<sup>5,6</sup> It follows from an analysis of these and many other equations describing small-amplitude DSs that the formation and evolution of DSs are related to a fluctuational restructuring of these systems, i.e., to the growth of fluctuations of a certain type at certain critical excitation levels of the system. In other words, fluctuations are assigned a decisive role in the selection of one of the possible stable states of the system:<sup>3-9</sup> “an ordering through fluctuations.”<sup>3</sup> A picture of self-organization drawn from an analysis of the various equations describing small-amplitude DSs is presented in monographs by Nicolis and Prigogine<sup>3</sup> and Haken<sup>5,6</sup> and also in many reviews (e.g., Refs. 9, 13, 71–74).

As has already been mentioned, the methods used to derive equations describing the properties of small-amplitude DSs rest on the assumption that at excitation levels above but close to the critical level (which corresponds to the stratification point of the homogeneous state,  $A = A_c$ ) the amplitude of the DSs is small to the extent that the excitation level is close to the critical level. In other words, it is small to the extent that the quantity  $\beta = (A - A_c)/A_c \ll 1$  is

small (Refs. 1, 3, 5, 6, 9, 13, and 63–74). This assumption, as natural as it might seem, frequently turns out to be unjustified. In many real active distributed media the stratification of the homogeneous state of the medium results in the *abrupt* appearance—i.e., right at the point  $A = A_c$ —of large-amplitude DSs, whose magnitude does not depend on the distance above the critical excitation level (the value of  $\beta$ ) and is determined instead by the nonlinearities of the system. This effect stems directly from the long-range nature of the inhibition in comparison with the activation, i.e., from the small value of the quantity  $\varepsilon = l/L$ . Large-amplitude DSs appear abruptly at the point  $A = A_c$  because the condition  $L \gg l$  causes an avalanche growth of the activator in the course of the stratification, in certain regions of the system of size  $d \approx (lL)^{1/2} \ll L$ . In certain systems, the amplitude of the DSs which form is higher, the smaller the quantity  $\varepsilon = l/L$  (Subsection 1.5.2).

### 1.2. THEORY OF LARGE-AMPLITUDE DISSIPATIVE STRUCTURES IN ACTIVE DISTRIBUTED MEDIA

This theory was derived in Refs. 75–77 by the authors of the present review. It has been used to study the shape, stability, and evolution of various types of large-amplitude DSs. It does not make use of the assumption that the excitation is only slightly above the critical level; i.e., it does not assume that the quantity  $\beta = (A - A_c)/A_c$  is small. It does make use of the small value of the ratio  $\varepsilon = l/L$ . It thus becomes possible to analyze self-organization phenomena in active systems at arbitrary excitation levels (§§2-6 and 12). It follows (in particular) from that analysis that self-organization in real systems usually results from a dynamic, rather than fluctuational, restructuring of the DSs.<sup>78</sup>

### 1.3. DYNAMIC RESTRUCTURING OF DISSIPATIVE STRUCTURES

This dynamic restructuring occurs because at certain critical levels of the excitation of a system the solution describing dissipative structures of a given type disappears (Subsection 12.2). The dynamic restructuring of DSs is not related to the presence of fluctuations in the system. It occurs in a deterministic way as a result of a local breakdown<sup>78</sup> in certain regions of the DSs (Subsection 2.1). In other words, fluctuations may not play an important role in the selection of the particular type of DS which forms. The presence of fluctuations in real systems leads to a finite probability for the occurrence of a local breakdown, before the corresponding critical excitation levels of the system are reached.

### 1.4. SELF-ORGANIZATION AND AUTOSOLITONS

In real systems, the formation of DSs is usually not determined by a stratification of a state near a homogeneous state and is instead associated with a spontaneous formation of autosolitons. Autosolitons are localized DSs in the form of solitary nonequilibrium regions which may be static, pulsating, or traveling. The theory of autosolitons and the properties of these entities were reviewed in Ref. 25. The spontaneous formation of autosolitons in real systems stems from a local breakdown which occurs near the small local inhomogeneities<sup>78,79</sup> which are always present in a real system (Subsection 4.1). The spontaneous formation of autosolitons and their subsequent evolution determine the self-organization scenarios which are observed experimentally (§4).

## 1.5. TURBULENCE AND AUTOSOLITONS

In active distributed media, even in the absence of flows (convective fluxes), a turbulence can arise in the form of inhomogeneous oscillations which are random in time and space. In certain systems, such a turbulence may be linked with an interaction of autowaves, e.g., spiral autowaves,<sup>7,8,10,11,17</sup> while in other systems it may be linked with the complex nature of the interaction of static or pulsating autosolitons (striations, in the 1D case).<sup>80,81</sup> In the latter case, the picture of the turbulence may be a random disappearance and nucleation of autosolitons at various spatial points<sup>79,82,83</sup> (§9).

Self-organization phenomena have recently been studied experimentally in many physical systems. For example, DSs in the following forms have been observed and studied: emitting regions of a hot electron-hole plasma in GaAs (Ref. 31), thermal-diffusion striations in a photogenerated hot electron-hole plasma in Ge (Ref. 84), resistive domains in composite superconductors,<sup>38</sup> the glowing multiple-thread formations which occur during extrinsic breakdown of GaAs (Ref. 32), the avalanche breakdown of  $\alpha$ -SiC p-n junctions<sup>34</sup> and Si p-i-n structures,<sup>35</sup> the current filaments in forward-biased, gold-doped Si p-i-n structures,<sup>33a</sup> the glowing current filaments in various structures containing gas-discharge layers,<sup>36,37,57</sup> including structures containing a high-resistivity compensated semiconductor,<sup>85</sup> and also the inhomogeneously emitting pattern in an electronic analog of a model of an active distributed system with diffusion.<sup>86,87</sup> Extremely detailed studies have been made of the shape and evolution of DSs experimentally,<sup>31,34,36,38,57,85-87</sup> analytically,<sup>11b,17,88-91</sup> and numerically.<sup>8b,11b,17,57,92-113</sup> The results found in these studies agree completely with the conclusions which follow from the theory derived in Refs. 75-78 for self-organization in active distributed media.

The present review is devoted to an examination of this extremely nontrivial picture of self-organization in active distributed media of various types. We focus on self-organization phenomena which do not depend on the size of the system or the conditions at its boundaries and are instead determined by the bulk properties of the distributed medium (which is sufficiently large, in at least one direction). In other words, we will not be discussing such very simple self-organization phenomena as the formation and evolution of a current filament or a field domain in a system with an S-shaped or N-shaped current-voltage characteristic, since their properties depend in a fundamental way on the size of the system, on the conditions at the boundaries of the system, and on the parameters of the external circuit.<sup>21-24</sup>

### 1. STRUCTURES NEAR THE POINT AT WHICH THE HOMOGENEOUS STATE STRATIFIES

#### 1.1. Turing instability

The long-range nature of the inhibitor and the activator is determined by diffusion processes in many physical, chemical, and biological distributed media. Such media are accordingly called "active systems with diffusion."<sup>3,7,8,11,12,25</sup> The properties of DSs in such systems are described by equations of the type

$$\tau_\theta \frac{\partial \theta}{\partial t} = l^2 \Delta \theta - q(\theta, \eta, A), \quad (1.1)$$

$$\tau_\eta \frac{\partial \eta}{\partial t} = L^2 \Delta \eta - Q(\theta, \eta, A), \quad (1.2)$$

where  $\theta$  and  $\eta$  are the values of the activator and the inhibitor;  $\tau_\theta$ ,  $\tau_\eta$ , and  $l$ ,  $L$  are the time and length scales of the variation of the activator and the inhibitor; and  $A$  is a control parameter (or bifurcation parameter), which characterizes the excitation level in a physical system. Formally, the existence of a negative feedback through the inhibitor and of a positive feedback through the activator  $\theta$  means that in a certain range of  $A$  we have

$$Q'_\eta \equiv \frac{\partial Q}{\partial \eta} > 0, \text{ and } q'_\theta \equiv \frac{\partial q}{\partial \theta} < 0. \quad (1.3)$$

Under conditions (1.3), it follows from Eqs. (1.1) and (1.2) that with  $\theta = \text{const}$  fluctuations  $\delta\eta$  will die out, while with  $\eta = \text{const}$  fluctuations  $\delta\theta$  will grow.

According to Eqs. (1.1) and (1.2), the homogeneous state of the system ( $\theta = \theta_h$  and  $\eta = \eta_h$ ) is determined by the equations

$$q(\theta_h, \eta_h, A) = 0, \quad Q(\theta_h, \eta_h, A) = 0. \quad (1.4)$$

A self-organization can occur in a monostable active system, in which the functional dependences  $\eta_h(A)$  and  $\theta_h(A)$  are single-valued. According to (1.3) and (1.4), the latter assertion is valid if

$$q'_\theta Q'_\eta - q'_\eta Q'_\theta > 0. \quad (1.5)$$

A homogeneous state of a monostable active system may spontaneously stratify. Linearizing Eqs. (1.1) and (1.2) with respect to fluctuations  $\delta\theta$ ,  $\delta\eta \propto \exp(-\gamma t + i\mathbf{k}\mathbf{r})$  near the homogeneous state, we find a dispersion relation. From this relation it follows that the stability is disrupted (Re  $\gamma < 0$ ) if one of the following inequalities holds<sup>41</sup>:

$$\tau_\eta (q'_\theta + k^2 l^2) + \tau_\theta (Q'_\eta + k^2 L^2) < 0, \quad (1.6)$$

$$k^4 l^2 L^2 + k^2 l^2 Q'_\eta + k^2 L^2 q'_\theta + q'_\theta Q'_\eta - q'_\eta Q'_\theta < 0. \quad (1.7)$$

According to (1.3), the first of these inequalities holds in systems with  $\alpha = \tau_\theta / \tau_\eta \ll 1$ , with respect to fluctuations with  $k = 0$  and with a particular frequency

$$\Omega \equiv \text{Im } \gamma = \omega_0 = (\tau_\theta \tau_\eta)^{-1/2} (q'_\theta Q'_\eta - q'_\eta Q'_\theta)^{1/2}. \quad (1.8)$$

Near the threshold for its satisfaction, condition (1.7) is satisfied for fluctuations with  $\text{Im } \gamma \equiv \omega = 0$  and with certain special wave numbers near<sup>5)</sup>

$$k = k_0 = (lL)^{-1/2} (q'_\theta Q'_\eta - q'_\eta Q'_\theta)^{1/4}, \quad (1.9)$$

in which case we have

$$q'_\theta < -\varepsilon^2 Q'_\eta - 2\varepsilon (q'_\theta Q'_\eta - q'_\eta Q'_\theta)^{1/2}. \quad (1.10)$$

Stratification condition (1.10), i.e., the condition for an instability of the homogeneous state of the system with respect to an aperiodic growth of fluctuations with  $k = k_0$ , holds by virtue of the relation  $q'_\theta < 0$ , according to (1.3) and (1.5). This condition can be satisfied more easily, the smaller the value of  $\varepsilon = l/L$ .

A condition for the stratification of active systems with diffusion was derived by Turing<sup>44</sup> in an analysis of an axiomatic model explaining the process of morphogenesis. Turing's ideas stimulated analytic and numerical studies of var-

ious axiomatic models of biological and chemical systems which can be described by Eqs. (1.1) and (1.2) (Refs. 3-8, 10-12, and 17). One particular model in this category is the classical Gierer-Meinhardt model of morphogenesis,<sup>92,93</sup> for which we would have

$$q = \theta - B - A\theta^2\eta^{-1}, \quad Q = \eta - C\theta^2, \quad (1.11)$$

Another model in this category is one proposed by Prigogine's Brussels school (the "brusselator"),<sup>3</sup> for which we would have

$$q = \theta - (B + \theta^2\eta)(1 + A)^{-1}, \quad Q = \eta\theta^2 - A\theta. \quad (1.12)$$

Yet another is the model with a "cubic nonlinearity"<sup>11b</sup> of the type<sup>6</sup>

$$q = \theta^3 - \theta - \eta, \quad Q = \theta + \eta + \frac{2}{3^{3/2}} - A. \quad (1.13)$$

Conditions (1.3) hold for these models. The second of conditions (1.3) holds for the model in (1.11) under the condition  $A > A_0 = CB$ , for the model in (1.12) under the condition  $A > A_0 = 1$ , and for the model in (1.13) in a limited range of the control parameter  $A$ :  $A_0 < A < A'_0$ . The value  $A = A_0$  or  $A = A'_0$  corresponds to a point with  $q'_\theta = 0$ . In chemical and biological reactions, a positive feedback through the activator implies a self-production of activator substance. Real processes involving a self-production of a substance and the equations which describe them are exceedingly complicated and extremely controversial.<sup>3-6,7b,8,11</sup>

Equations (1.1) and (1.2), which make use of expressions (1.11)-(1.13), are the simplest axiomatic models of such reactions.

Independently, research has developed on the processes which lead to the stratification of the homogeneous state of physical systems. In the 1950s and 1960s, for example, the physical reason for the stratification of gas discharges was

identified.<sup>14</sup> It turned out that the stratification of a gas discharge and the formation of striations in it can be treated, on the basis of general considerations,<sup>45</sup> as consequences of a Turing instability. Equations like (1.1) and (1.2) also describe the DSs in many other real physical systems,<sup>25</sup> including the "hot spots" in semiconductor structures<sup>52</sup> (Subsections 7.2 and 7.3); the avalanche-current filaments in p-n junctions<sup>34</sup> (Subsection 7.1), p-i-n structures, and gas-discharge structures<sup>57,112,113</sup>; and also the multifilament or multidomain states in various composite structures with a "latent" S-shaped or N-shaped current-voltage characteristic, including structures which contain an active layer of a semiconductor, a superconductor, or a material which undergoes a metal-insulator or other type of phase transition (§7).

The threshold for the satisfaction of condition (1.10) for a given value of  $\varepsilon$  determines the critical excitation level  $A = A_c$ , at which the homogeneous state of the system stratifies. As  $\varepsilon \rightarrow 0$ , condition (1.10) becomes the same as the second of conditions (1.3); i.e., it becomes satisfied as  $A_c \rightarrow A_0$ , at which we have  $q'_\theta = 0$ . There exists a certain maximum value  $\varepsilon = \varepsilon_m$  above which condition (1.10) cannot be satisfied at any value of the parameter  $A$  (Fig. 1, a and b). For the model in (1.11), it follows from (1.10) that the relationship between  $A_c$  and  $\varepsilon$  is<sup>115</sup>

$$A_c = (1 + \varepsilon)^2(1 - 2\varepsilon - \varepsilon^2)^{-1}A_0 \quad (A_0 = CB) \quad (1.14)$$

and is shown in Fig. 1a. It can be seen from (1.14) that under the condition  $\varepsilon > \varepsilon_m = \sqrt{2} - 1 \approx 0.41$  Turing's stratification condition (1.10) does not hold. For the model in (1.12), the relationship between  $\varepsilon$  and  $A_c$  is

$$\varepsilon = (A_c^{1/2} - 1)(1 + A_c)^{-1/2}B^{-1} \quad (1.15)$$

and is shown in Fig. 1a. From (1.15) we find  $\varepsilon_m = B^{-1}$ . For

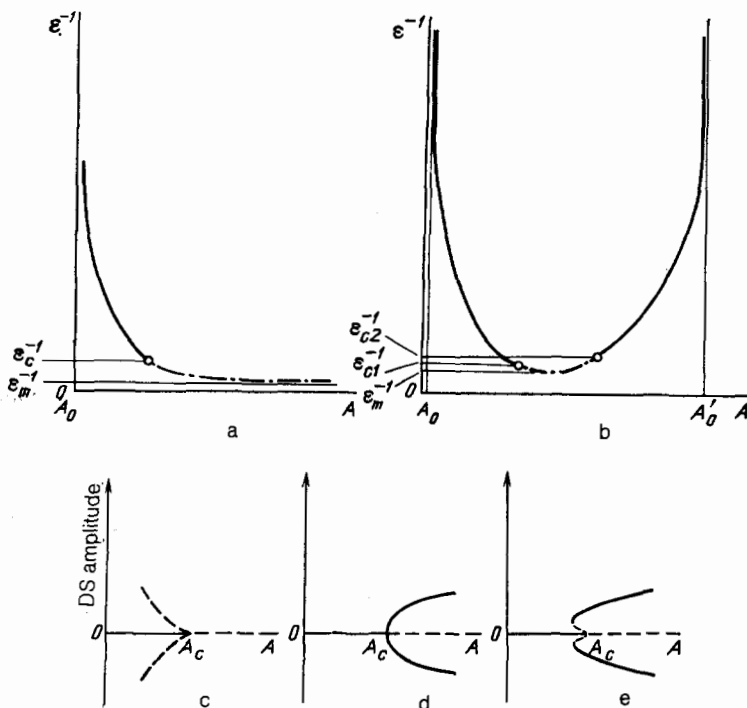


FIG. 1. The critical excitation level ( $A = A_c$ ) as functions of the quantity  $\varepsilon = l/L$  (a, b) and bifurcation diagrams (c, d). a—For V and A systems; b—for N and H systems. The solid parts of the curves in parts a and b correspond to a subcritical branching of the solutions (c), which is realized under the condition  $\varepsilon < \varepsilon_c$ ; the dot-dashed parts of the curves correspond to a supercritical branching of the solutions (d), which is realized at  $\varepsilon > \varepsilon_c$ . The diagram in part e corresponds to values of  $\varepsilon$  which are close to  $\varepsilon_c$  but which satisfy  $\varepsilon < \varepsilon_c$  (the corresponding small regions are shown schematically by the circles in parts a and b). The dashed lines in parts c-e are the parts of the curves which correspond to unstable states.

the model in (1.13), the relationship between  $\varepsilon$  and  $A$  is as shown in Fig. 1b. The various types of behavior of  $\varepsilon$  as a function of  $A$  (Fig. 1, a and b) found for models (1.11)–(1.13) are characteristic of the entire class of monostable active systems.

## 1.2. Conditions for the stratification of active systems with a "cross" diffusion

In Subsection 1.1 we discussed active systems with a diffusion which can be described by Eqs. (1.1) and (1.2). In those systems, the positive feedback through the activator which results in the stratification is determined by the nonlinearities of the systems, i.e., by the functional dependence  $q(\theta, \eta)$  in (1.11). More generally, active distributed media are described by equations of the type

$$\frac{\partial X_i}{\partial t} = \sum_{j=1}^N \nabla (D_{ij} \nabla X_j) - g_i(X_1, \dots, X_N, A), \quad (1.16)$$

where  $X_i$  are the concentrations of chemical substances, gas particles, electrons, holes, or ions; the temperature; etc.<sup>3,5,8,17,25</sup> Physical<sup>47,59,60,61,62,75,76</sup> and chemical<sup>8b,108,116</sup> active systems in which the stratification is determined by diffusion processes or, more precisely, by a dependence of the cross diffusion coefficients  $D_{ij}$  with  $i \neq j$  on the parameters of the system,  $X_i$ , constitute a special class.

Examples of these systems with a cross diffusion are gaseous and electron-hole plasmas in semiconductors heated by electromagnetic radiation or by an electric field.<sup>47-51</sup> The distributions of the density  $n$  and the effective temperature  $T$  of hot electrons are described by balance equations for the number of particles,

$$\frac{\partial n}{\partial t} = -\operatorname{div} \mathbf{j}_e + G - n\tau_r^{-1}, \quad (1.17)$$

and for their average energy,

$$\frac{3}{2} \frac{\partial nT}{\partial t} = -\operatorname{div} \mathbf{j}_e + W_j - P. \quad (1.18)$$

Here  $\mathbf{j}_e$  and  $\mathbf{j}_e$  are the flux densities of the particles and their energy;  $G$  and  $\tau_r$  are the rate of generation and the lifetime of the electrons;  $W_j$  is the power transferred to the electrons from the external source;  $P = n(T - T_l)\tau_\varepsilon^{-1}$  is the power transferred from the electrons to the lattice or to the atoms of the gas;  $\tau_\varepsilon$  is the relaxation time of the electron energy; and  $T_l$  is the temperature of the semiconductor lattice or of the gas atoms. We wish to stress that Eqs. (1.17) and (1.18) can be derived rigorously from a Boltzmann kinetic equation.<sup>117-119</sup>

To learn about the physics of the stratification of the homogeneous state of a system with a cross diffusion, we consider a symmetric electron-hole plasma, in which the electrons and the holes have the same properties. In this case we have<sup>47,51</sup>

$$\mathbf{j}_e = -\nabla(nD(T)) = -D\nabla n - (1 + \alpha)DnT^{-1}\nabla T, \quad (1.19)$$

$$\begin{aligned} \mathbf{j}_e = & -\left(\frac{5}{2} + \alpha\right) \nabla(TnD(T)) = -\left(\frac{5}{2} + \alpha\right) [TD\nabla n \\ & + (2 + \alpha)Dn\nabla T], \end{aligned} \quad (1.20)$$

where  $D(T) \propto T^{1+\alpha}$  is the diffusion coefficient of the electrons and holes. Using (1.19) and (1.20), we can rewrite Eqs. (1.17) and (1.18) in the form<sup>7)</sup> (Ref. 76)

$$\tau_r \frac{\partial n}{\partial t} = L^2 \Delta \frac{nD(T)}{D^0} + G\tau_r - n, \quad (1.21)$$

$$\frac{3}{2} \tau_\varepsilon^0 \frac{\partial nT}{\partial t} = l^2 \Delta \frac{TnD(T)}{D^0} + W_j \tau_\varepsilon^0 - n(T - T_l) \frac{\tau_\varepsilon^0}{\tau_\varepsilon(T)}, \quad (1.22)$$

where  $D^0 = D(T_l)$ ,  $\tau_\varepsilon^0 = \tau_\varepsilon(T_l)$ ,  $L = (D^0 \tau_r)^{1/2}$  is the carrier diffusion length, and  $l = [(5/2 + \alpha)D^0 \tau_\varepsilon^0]^{1/2}$  is the relaxation length of the hot-carrier energy. In the case with both  $G$  and  $\tau_r$  constant, with  $W_j$  independent of  $n$  and  $T$  (Subsection 8.1), the homogeneous state of the electron-hole plasma is determined from the following equations, as can be seen from (1.21) and (1.22):

$$n = n_h = G\tau_r, \quad T = T_h = T_l + W_j \tau_\varepsilon (G\tau_r)^{-1}. \quad (1.23)$$

In other words, this homogeneous state is unique. The reason is that  $\tau_\varepsilon$  cannot increase more rapidly than  $T^{1/2}$  in a semiconductor; i.e.,  $s = \partial \ln \tau_\varepsilon / \partial \ln T \leq 1/2$  (Ref. 21). Linearizing Eqs. (1.21) and (1.22) with respect to fluctuations  $\delta n, \delta T \propto \exp(-\gamma t + i\mathbf{k}\mathbf{r})$ , we find the dispersion relation<sup>47</sup>

$$\begin{aligned} \gamma^2 \cdot \frac{3}{2} \tau_r \tau_\varepsilon - \gamma \left[ k^2 L^2 \tau_\varepsilon (5 + 3\alpha + \alpha^2) \right. \\ \left. + \frac{3\tau_\varepsilon}{2} + \tau_r \left( 1 - s + s \frac{T_l}{T} \right) \right] + k^4 l^2 L^2 \\ \left. + k^2 \left\{ L^2 \left[ (1 + \alpha + s) \frac{T_l}{T} - (\alpha + s) \right] \right. \right. \\ \left. \left. + l^2 (2 + \alpha) \right\} + s \frac{T_l}{T} + 1 - s = 0. \end{aligned} \quad (1.24)$$

It follows from (1.24) that an electron-hole plasma is stable with respect to homogeneous fluctuations (with  $k = 0$ ). The meaning is that in this case, without spatial derivatives in Eqs. (1.21) and (1.22), an instability does not arise, in contrast with the case in the systems discussed in Subsection (1.1).

The homogeneous state of an electron-hole plasma may stratify because the condition  $\varepsilon = l/L \approx (\tau_\varepsilon/\tau_r)^{1/2} \ll 1$  usually holds in a semiconductor. It follows from (1.24) that in the case  $\alpha + s > 0$  an instability occurs<sup>8)</sup> with respect to an aperiodic growth of fluctuations with  $k = k_0 \approx (lL)^{-1/2}$ , in which case we have  $T > T_l (1 + \alpha + s)(\alpha + s)^{-1}$ . The stratification of the electron-hole plasma stems from the presence in Eq. (1.21) of a term corresponding to the last term in (1.19). The latter term describes a cross diffusion or, more precisely, an effect of the carrier temperature distribution on the carrier density distribution. The physics of the stratification of electron-hole plasmas is analyzed in more detail in Refs. 47 and 76.

The mechanism for the stratification of the homogeneous state of a system with cross diffusion is thus fundamentally different from Turing's stratification mechanism in active systems with diffusion (Subsection 1.1). Formally, these subsystems can be described in a common language, with the help of the concepts of activator and inhibitor. In this case, the temperature plays the role of activator, while the inhibitor is a certain function of the carrier temperature and density:

$$\theta = \frac{T}{T_l}, \quad \eta = \frac{nD(\theta)}{n_h D^0} \equiv n\varphi^{-1}(\theta). \quad (1.25)$$

Using (1.25), we can put Eqs. (1.21) and (1.22) in the form<sup>75,76</sup>

$$\frac{3}{2} \tau_e^0 \frac{\partial \eta \varphi(\theta)}{\partial t} = f^2 \Delta(\eta \theta) - q(\theta, \eta, A), \quad (1.26)$$

$$\tau_r \frac{\partial \eta \varphi(\theta)}{\partial t} = L^2 \Delta \eta - Q(\theta, \eta), \quad (1.27)$$

where

$$q = \eta(\theta - 1) \varphi(\theta) \frac{\tau_e^0}{\tau_e(\theta)} - A, \quad (1.28)$$

$$Q = \eta \varphi(\theta) - 1, \quad A = \frac{W_f \tau_e^0}{n_h T_i}$$

Using (1.28), we easily see that stratification conditions (1.9) and (1.10) agree within  $\varepsilon^2 \ll 1$  with the corresponding conditions which follow from (1.24).

### 1.3. Classification of active distributed media

It follows from the analysis of active systems with diffusion that the particular type of instability which occurs in these systems depends on the value of  $\alpha = (\tau_\theta / \tau_\eta)$  or  $\varepsilon = l/L$  (Subsection 1.1); i.e., it depends on the extent to which the activator is slow and of long range in comparison with the inhibitor.

Under the conditions  $\varepsilon \ll 1$  and  $\alpha > 1$ , condition (1.6)—for the appearance of uniform oscillations—does not hold, but stratification condition (1.10) does. In other words, the condition for the instability of the homogeneous state of the system with respect to the growth of fluctuations with a special wave number  $k = k_0$ , i.e., (1.9), is satisfied. For this reason, systems in which the inhibition (or retardation) is faster than the activation (or excitation) but is of longer range are called “K systems.”<sup>25,120</sup>

In systems with  $\varepsilon > 1$  but  $\alpha \ll 1$ , condition (1.10), for the stratification of the homogeneous state, does not hold, but condition (1.6), for the appearance of uniform oscillations with a special frequency  $\omega = \omega_0$  [see (1.8)], does. Systems in which the inhibition is of shorter range than the activation but slower are thus called “Ω systems.”<sup>9)</sup>

Systems with  $\varepsilon \ll 1$  and  $\alpha \ll 1$  or, more precisely, systems in which the inhibition is slower and of longer range are called “KΩ systems.”

An important characteristic, which determines the properties of both autosolitons<sup>25</sup> and more-complex types of dissipative structures (DSs), is the local-coupling curve, i.e., the functional dependence  $\eta(\theta)$ , which satisfies the equation

$$q(\theta, \eta, A) = 0 \text{ при } A = \text{const}, \quad (1.29)$$

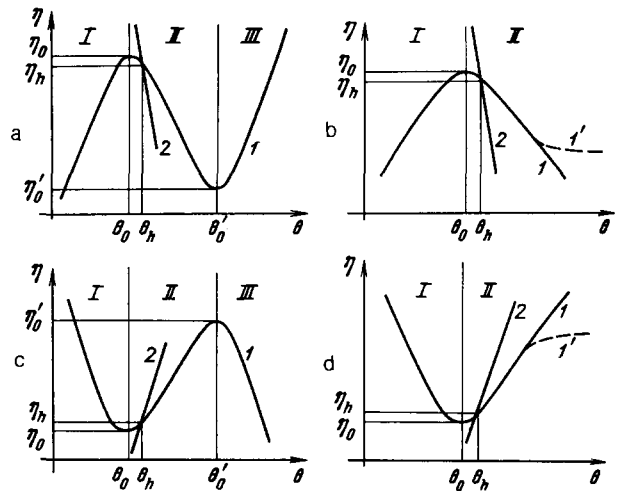


FIG. 2. 1—Basic types of local-coupling curves; 2—basic types of state-equation curves. Dashed lines 1' in parts b and d show systems with “degenerate” local-coupling curves.<sup>25</sup>

Another such important characteristic is the “state-equation” curve, i.e., the functional dependence  $\eta(\theta)$ , which follows from the equation

$$Q(\theta, \eta, A) = 0 \text{ при } A = \text{const}. \quad (1.30)$$

The points at which these curves intersect determine the homogeneous state of this system ( $\theta = \theta_h, \eta = \eta_h$ ) according to (1.4). In a case in which the local-coupling and state-equation curves intersect at one point, the systems are called “monostable.” If there are instead three such points, the system is a “flip-flop” or a “bistable system,” since two of these points usually correspond to stable homogeneous states. The particular features of DSs and self-organization in systems of those types are discussed in §6 below.

It follows<sup>25</sup> from conditions (1.3) and (1.5) that the local-coupling curve in an active system has an N, A, H, or V shape (Fig. 2). Such systems are thus called “N, A, H, and V systems.” The complete names of the various systems—reflecting the response time and range of the activator and the inhibitor and the form of the local-coupling curve, are given in Table I. The DSs which are realized in them and the effects which determine their restructuring, i.e., the self-organization scenarios, are generalized in Table II.

In N and H systems, we have a zero derivative  $q'_\theta = 0$  at two points,  $\theta = \theta_0$  and  $\theta'_0$  (Fig. 2, a and c), while in A and V systems we have this at a single point,  $\theta = \theta_0$  (Fig. 2, b and d). We denote the value of A at which we have  $\theta_h = \theta_0$  or  $\theta'_0$

TABLE I.

Shape of local-coupling curve	Name of system		
	K systems: The inhibition is of long range and is fast (in comparison with the activation)	Ω systems: The inhibition is of short range and is slow (in comparison with the activation)	KΩ systems: The inhibition is of long range and is slow (in comparison with the activation)
N (Fig. 2a)	KN systems	ΩN systems	KΩN systems
H (Fig. 2c)	KH systems	ΩH systems	KΩH systems
A (Fig. 2b)	KA systems	ΩA systems	KΩA systems
V (Fig. 2d)	KV systems	ΩV systems	KΩV systems

TABLE II.

Name of system	Type of dissipative structure (DS)	Effects determining restructuring of DS	Subsections of this paper in which the self-organization scenarios are discussed
KN, KH	Static, wide	I–VI	3.1, 4.1–4.3, 5.1, 5.3, 5.4
KA, KV	Static, peak	I–III, V, VI	3.2, 4.1–4.3, 5.2, 5.3, 5.4
QN, QH	Traveling autosolitons and other autowaves	II, VI	11.1
KQN, KQH	Wide static, pulsating; traveling autosolitons and other autowaves	I–VI	3.1, 4.1–4.3, 5.1, 5.3, 5.4, 11.2–11.6
KQA, KQV	Peak static, pulsating, traveling	I–III, V, VI	3.2, 4.1–4.3, 5.2, 5.3, 5.4, 11.2–11.6

I—*Local breakdown* in static, pulsating, or traveling autosoliton, in striations, or in certain regions of a more-complicated type of DS (Subsections 2.1.1 and 5.1) and autowaves. II—*Local breakdown in oscillating "tail"* of static (Subsections 1.2 and 5.3), pulsating, or traveling autosoliton. III—*"Pumping" of activator* between striations (Subsection 2.2), spots, blobs, or other fragments of DSs (Subsection 5.1) and autowaves. IV—*"Corrugation" of walls* of static (Subsection 2.3), pulsating striations or other extended regions of DSs (Subsections 5.1–5.3) and autowaves in two- or three-dimensional systems. V—*Granulation* of static (Subsection 2.3), pulsating striations or other extended regions of DSs (Subsections 5.1–5.3) and autowaves in two- or three-dimensional systems. VI—*Spontaneous appearance near a small local inhomogeneity* of static (Subsection 4.1), pulsating, traveling autosoliton or a more-complicated type of DS and autowaves.

by  $A_0$  or  $A'_0$ , respectively. It can be seen from (1.10) or (1.6) that the quantities  $A_c$  and  $A'_c$ , which determine the boundaries of the region in which the conditions for instability of the homogeneous state of the system hold, are the same as  $A_0$  and  $A'_0$ , respectively, within  $\varepsilon \ll 1$  or  $\alpha \ll 1$ .

The properties of the DSs which are realized in various active distributed media are general properties, by which we mean that they do not depend on the specific activation (or excitation) or inhibition (or retardation) mechanism, nor do they depend on the processes which determine their speed and range. The distributions of the activator and the inhibitor may be determined not only by diffusion processes (Subsections 1.1 and 1.2) but also by long-range couplings of another nature which can be described by integral operators.<sup>125–130</sup> In particular, equations of the following type are used to model phenomena in active systems with long-range coupling:<sup>9,125,131–133</sup>

$$\tau_\theta \frac{\partial \tilde{\theta}}{\partial t} = -\tilde{\theta} + H \left( \int_{-\infty}^{\infty} \Phi(x' - x) \tilde{\theta}(x', t) dx' - A - a\tilde{\eta} \right), \quad (1.31)$$

$$\tau_\eta \frac{\partial \tilde{\eta}}{\partial t} = \tilde{\theta} - \tilde{\eta}, \quad (1.32)$$

where  $H(y) = 1$  for  $y \geq 0$  and  $H(y) = 0$  for  $y < 0$ , and the function  $\Phi(x)$  describes a short-range activation and a long-range inhibition.<sup>25</sup> The term  $a\tilde{\eta}$  in the argument of the function  $H(y)$  describes the variation in the excitation threshold of the medium. The response time here is determined by Eq. (1.32). Under the condition  $\alpha = \tau_\theta / \tau_\eta > 1$ , Eqs. (1.31) and (1.32) thus describe distributed media which fall in the category of K systems, while under the condition  $\alpha \ll 1$  they describe media which fall in the category of KΩ systems (Table II).

In nonlinear optical resonators excited by external radiation, diffraction DSs form as isolated or interacting autoso-

litons.<sup>107</sup> The activation process here involves an intensification of the electromagnetic radiation as the result of a nonlinearity of the absorption coefficient or refractive index of the medium in the resonator. The inhibition process involves field oscillations caused by diffraction effects. The oscillations of the diffraction pattern propagate a distance considerably greater than the width of the main maximum, which determines the characteristic length scale of the variation of the radiation in the resonator. In other words, the inhibition process here is of longer range than the activation process. For this reason, such systems<sup>107</sup> fall in the category of K or KΩ systems.

In systems with a cross diffusion, as was mentioned back in Subsection 1.2, a homogeneous state undergoes stratification at  $\varepsilon \ll 1$ . Such systems are therefore usually K systems (§8 and Table II); under certain conditions they are KΩ systems. The latter is the case, for example, if the recombination time of the electrons and holes in the nondegenerate electron-hole plasma which we were discussing back in Subsection 1.2 is a decreasing function of the temperature or an increasing function of the carrier density.<sup>51</sup>

In order to identify the particular category in which a specific system falls and therefore the properties of the DSs and the possible self-organization scenarios, it is necessary to identify explicitly the quantities  $\theta$  and  $\eta$  which serve as activator and inhibitor. We wish to stress that in some cases these quantities may be exceedingly complicated functions of the real physical parameters of the system (see, for example, Subsection 1.2 and Refs. 50b and 51). The next step is to determine the time and length scales of the variation of the parameters  $\theta$  and  $\eta$  and the relations between them. It is then necessary to analyze the shape of the local-coupling curve, found from (1.29). The latter relation follows from the equation for the activator in the steady-state, homogeneous case. This procedure is carried out in §§7 and 8 for certain physical systems (see also Refs. 25, 50b, and 51).

#### 1.4. Small-amplitude dissipative structures

Near the stratification point  $A = A_c$ , Eqs. (1.1) and (1.2) have small-amplitude quasiharmonic solutions in the one-dimensional case. Their fundamental mode is<sup>5)</sup> (Ref. 3)

$$\theta(x) - \theta_h = \Delta\theta_m \cos(k_0 x), \quad \Delta\theta_m^2 = \kappa^{-1}(A - A_c), \quad (1.33)$$

where the quantity  $\kappa$  depends on the functions  $q(\theta, \eta, A)$  and  $Q(\theta, \eta, A)$  and the value of  $\varepsilon$  (Ref. 3, 134, and 135). In the limit  $\varepsilon \rightarrow 0$ , the expression for  $\kappa$  is<sup>135</sup>

$$\kappa = (q_{\theta\theta}^{\prime})^2 \left[ (Q_{\theta}^{\prime})^2 (q_{\theta}^{\prime} Q_{\eta}^{\prime} - q_{\eta}^{\prime} Q_{\theta}^{\prime}) (-q_{\eta}^{\prime} Q_{\theta}^{\prime}) \frac{dq_{\theta}^{\prime}}{dA} \right]^{-1}. \quad (1.34)$$

As was mentioned in Subsection 1.3, in the limit  $\varepsilon \rightarrow 0$ , we have  $A_c \rightarrow A_0$ ; i.e.,  $A_c$  approaches the value  $A = A_0$ , which is the value at which we have  $q_{\theta}^{\prime} = 0$ . It follows that at values of  $A$  near  $A_c$  we have a derivative  $dq_{\theta}^{\prime}/dA < 0$ . Making use of this result along with condition (1.3) and (1.5), we find from (1.34) that at small values of  $\varepsilon$  we have  $\kappa < 0$ . It can be seen from (1.33) that in the case  $\kappa < 0$  inhomogeneous states exist at  $A < A_c$ . In other words, a subcritical branching of solutions occurs (Fig. 1c), and in the course of this branching small-amplitude states are unstable.<sup>3</sup> At a certain  $\varepsilon = \varepsilon_c$ , a subcritical branching may be replaced by a supercritical branching (Fig. 1d). For the model of (1.12) with  $B = 2$ , for example, we have  $\varepsilon_c \sim 0.1$ , but even at  $\varepsilon > \varepsilon_m = 0.5$  a stratification of the homogeneous state does not occur, regardless of the value of  $A$  (Fig. 1a; Subsection 1.1). For the model of an electron-hole plasma discussed in Subsection 8.2 we have a value  $\varepsilon_m \approx 0.31$ , and the supercritical branching of solutions (Fig. 1d) occurs at  $\varepsilon > \varepsilon_{c1}$  or  $\varepsilon > \varepsilon_{c2}$ , where  $\varepsilon_{c1} \approx 0.27$  and  $\varepsilon_{c2} \approx 0.23$  (Fig. 1b).

It follows from these examples that a supercritical branching of solutions (Fig. 1d) in the course of which small-amplitude DSs are stable is realized in an extremely narrow interval of  $\varepsilon$  values, i.e., of values of the parameters of the system, even at excitation levels  $A$  close to the critical level  $A_c$ . Since the supercritical branching of solutions is replaced at  $\varepsilon = \varepsilon_c$  (Fig. 1d) by a subcritical branching (Fig. 1c), it is clear that at values of  $\varepsilon$  close to but smaller than  $\varepsilon_c$  the bifurcation diagram has the form shown in Fig. 1e.

As was mentioned back in the Introduction, the properties of small-amplitude DSs in models of various physical systems, including hydrodynamic, have been the subject of very many studies (see, for example, Refs. 2b, 3, 5, 6, 9, 63–74, and 136). In the theory for such DSs, the small value of the amplitude of the DSs is exploited to derive equations which are simpler than the original system of fundamental nonlinear equations describing the specific physical system. Some particular examples of these simplified equations are<sup>6,9,72,74,136,137</sup>

$$\tau \frac{\partial u}{\partial t} = \beta u + c|u|^2 u - \mu|u|^4 u + \gamma \Delta u \quad (1.35)$$

and

$$\tau \frac{\partial u}{\partial t} = \beta u + cu^2 - \mu u^3 - \gamma(k_0^2 + \Delta)^2 u, \quad (1.36)$$

where  $\beta = (A - A_c)A_c^{-1}$  and  $\text{Re } \gamma > 0$ . Equation (1.35) with  $c > 0$  and  $\mu > 0$  was proposed by Petviashvili and Sergeev.<sup>137</sup> A derivation of Eq. (1.36) is given in a monograph

by Haken. With  $c = 0$  and  $\mu > 0$ , this equation becomes the equation which Swift and Hohenberg derived in order to describe the Bénard problem.<sup>68</sup> Equations of the type in (1.35) and (1.36) are called “generalized Ginzburg–Landau equations,”<sup>6,74</sup> since with real coefficients ( $c, \mu, \gamma$ ) they follow from the equation

$$\tau \frac{\partial u}{\partial t} = -\frac{\delta F}{\delta u^*}, \quad (1.37)$$

where the “free energy”  $F$  has the meaning of a Lyapunov functional. The problem of seeking stable steady states, i.e., stable small-amplitude DSs, reduces to a search for the minima of  $F$  (Ref. 74).

We wish to stress that equations of the type in (1.35) and (1.36) describe the properties of only small-amplitude DSs, including autosolitons, which may form at excitation levels near the critical level, i.e., at  $|\beta| = |A - A_c|A_c^{-1} \ll 1$ . Small-amplitude autosolitons, which are sometimes called “localized autostructures” or “particles,”<sup>74</sup> are realized only in systems in which the bifurcation diagram is approximately the same as that in Fig. 1e or—more precisely—when small-amplitude DSs form as a result of a stratification, despite the subcritical branching, at the point  $A = A_c$ . At the beginning of this subsection it was shown that a situation of this sort (Fig. 1e) is realized only at values of  $\varepsilon = l/L$  smaller than, but very close to  $\varepsilon_c$ . In turn, the value of  $\varepsilon_c$  is determined by the nonlinearities of the system, more precisely, by the particular functions  $q(\theta, \eta)$  and  $Q(\theta, \eta)$  in (1.1) and (1.2). It follows that solutions in the form of small-amplitude autosolitons are allowed by models which describe the properties of active systems in a small neighborhood of  $A = A_c$  and with parameter values meeting some very stiff requirements. These stiff requirements would be difficult to meet experimentally.

It was stressed in Subsections 1.1 and 1.2 that it becomes easier to satisfy the conditions for the instability of the homogeneous state as  $\varepsilon$  or  $\alpha$  becomes smaller. We know from the qualitative theory of differential equations<sup>26</sup> that under the condition  $\tau_{\theta} \ll \tau_{\eta}$  small-amplitude quasiharmonic oscillations with a frequency  $\omega = \omega_0$  [see (1.8)] are unstable, and large-amplitude relaxation oscillations appear abruptly in the system at  $A = A_c$ . These oscillations consist of sequential combinations of intervals of slow and fast motions with time scales  $\tau_{\eta}$  and  $\tau_{\theta}$ , respectively.<sup>26</sup>

It was mentioned at the beginning of this subsection that under the condition  $\varepsilon \ll 1$  there is a hard regime of the spontaneous formation of DSs (Fig. 1, a–c), in which large-amplitude DSs appear abruptly at the stratification point (Subsection 1.5). In such DSs, the inhibitor  $\eta$  varies smoothly (with a length scale  $L$ ) in space, and the distribution of the activator  $\theta$  is a high-contrast pattern, i.e., the activator varies sharply in certain regions with a size of the order of  $l$  (§12). We derived a theory for these large-amplitude DSs making use of the small value of the quantity  $\varepsilon = l/L$  in Refs. 75–77. This theory, based on an analysis of an initial system of fundamental equations, of the type presented in Subsections 1.1 and 1.2, describes the shape, stability, and evolution of DSs under arbitrary excitation conditions, for the actual nonlinearities of the system. The basic results of this theory and the basic self-organization scenarios which follow from it are presented below.



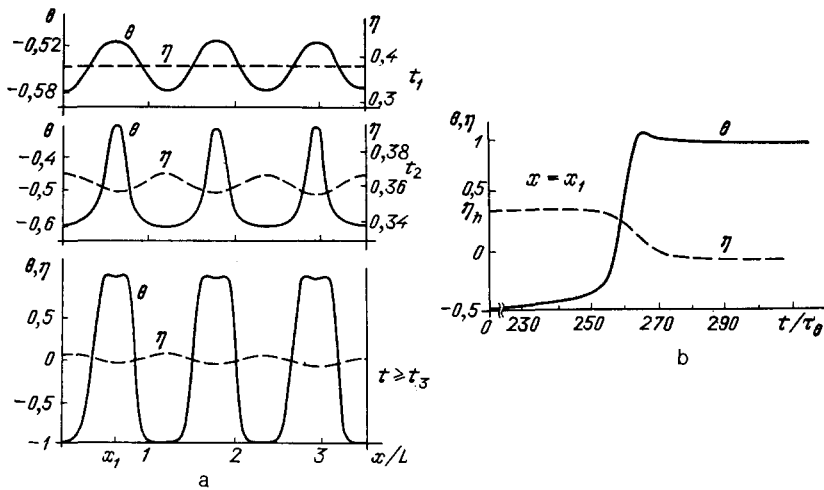


FIG. 3. Kinetics of the spontaneous formation of wide striations. a—Distributions of  $\theta$  and  $\eta$  at various times ( $t_1 = 220 \tau_\theta$ ,  $t_2 = 250 \tau_\theta$ ,  $t_3 = 370 \tau_\theta$ ) b—the functional dependence  $\theta(t)$  at the center of the striations which form ( $x = x_1$ ). These are the results of a numerical solution of Eqs. (1.1), (1.2), and (1.13) with  $A = 0.21$ ,  $\varepsilon = 0.033$ , and  $\alpha = 1$  carried out in Ref. 100.

### 1.5. Kinetics of the formation of one-dimensional DSs, i.e., striations

It was mentioned in Subsections 1.1 and 1.2 that the stratification of the homogeneous state at the point  $A = A_c$  stems from an aperiodic growth of fluctuations of period  $\mathcal{L}_0 = 2\pi k_0^{-1} \approx 2\pi(lL)^{1/2}$ .

1.5.1. A large-amplitude DS forms abruptly at the stratification point  $A = A_c$  in KN and KH systems by virtue of the condition  $\varepsilon \ll 1$  (Fig. 3a,  $t > t_3$ ). In these systems, the inhibitor  $\eta$  varies slowly near  $\eta = \eta_s \neq \eta_h$ , while the activator distribution usually consists of broad striations<sup>76</sup> in which  $\theta(x)$  varies sharply from  $\theta_{\min} \approx \theta_{s1}$  to  $\theta_{\max} \approx \theta_{s3}$  in certain regions of size  $\sim l$  (the walls of the striations). [Equations determining the values of the inhibitor in the striation walls,  $\eta_s$ , the quantity  $\theta_{s1}$  and  $\theta_{s3}$ , and the functions  $\theta(x)$  and  $\eta(x)$  in the striations are given in §12.]

In other words, the shape of the DSs which form in the stratification is fundamentally different from quasiharmonic, i.e., fundamentally different from the shape of a critical fluctuation (a mode with  $k \approx k_0$ ), whose growth leads to the formation of DSs. By this we mean that under the condition  $\varepsilon \ll 1$  the analysis of the DS which arises cannot be restricted to a small number of interacting modes, with the growing fluctuation<sup>10)</sup> with  $k \approx k_0$  chosen as the main one, even near the critical point ( $A = A_c$ ). The reason is the extremely nontrivial nonlinear effect which is manifested at the stratification point of the homogeneous state of the system during the formation of the DS. The short-wavelength modes with  $k \gg k_0$  which are strongly damped in the linear

theory begin to grow when the nonlinear interaction of the modes is taken into account, and as the critical fluctuation with  $k \approx k_0$  grows. Beginning at a certain time, the growth rate of these short-wavelength modes becomes higher than that of the critical fluctuation. This effect has been observed in numerical studies (Fig. 3), and it follows, in particular, from an analytic study of the kinetics of the current stratification in a transistor.<sup>138</sup>

1.5.2. Dissipative structures in KA and KV systems have some fundamental distinguishing features. During the stratification of the homogeneous state in such systems, large-amplitude peak striations of two types form. One type is narrow<sup>75</sup> (Fig. 4a), and the other wide<sup>98,139</sup> (Fig. 4b). Regardless of the small value of  $\varepsilon = l/L \ll 1$ , the width of the narrow peak striations is on the order of  $l$ , and that of the wide ones on the order of  $L$ . The amplitude of the peak striations (the value of  $\theta_{\max}$ ) increases with decreasing  $\varepsilon$  (Refs. 75, 81, 140, and 141). The amplitude of the wide peak striations can reach a huge value even if  $\varepsilon$  is not very small.<sup>98</sup> Wide peak striations may be realized in systems in which  $Q(\theta, \eta, A)$  in (1.2) is not a rapidly increasing function of  $\theta$  (Refs. 98 and 139).

The narrow peak striations, with a period  $\mathcal{L}_p = \mathcal{L}_0$ , are often unstable<sup>75</sup> (Subsection 3.2). The period of the stable peak striations which form during stratification may thus be considerably larger than  $\mathcal{L}_0 = 2\pi k_0^{-1}$ . There is a distinctive feature in the formation of the narrow peak striations. Let us assume that at the time  $t \geq 0$  the excitation level of the system exceeds the critical value  $A = A_c$  by a small amount. As a result of the growth of a critical fluctuation

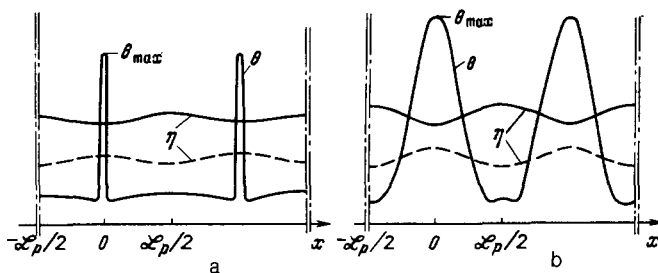


FIG. 4. Two types of peak striations. a—Narrow; b—wide. The solid and dashed lines show  $\eta$  for  $\Lambda$  and  $V$  systems, respectively.

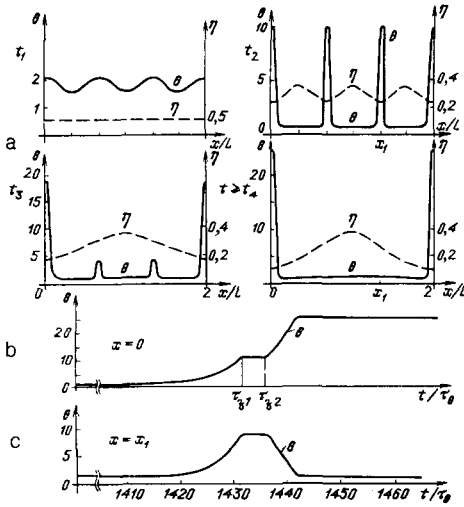


FIG. 5. Kinetics of the spontaneous formation of narrow peak striations. a—Distributions of  $\theta$  and  $\eta$  at various times ( $t_1 = 1324 \tau_\theta$ ,  $t_2 = 1433 \tau_\theta$ ,  $t_3 = 1439 \tau_\theta$ ,  $t_4 = 1460 \tau_\theta$ ) b, c—the functional dependence  $\theta(t)$  at the points  $x = 0$  and  $x = x_1$ . Shown here are results of a numerical solution of Eqs. (1.1), (1.2), and (1.12) with  $A = 1.1$ ,  $B = 2$ ,  $\varepsilon = 2.24 \cdot 10^{-2}$ , and  $\alpha = 1$  in Ref. 82.

with a period  $\mathcal{L}_0 = 2\pi k_0^{-1}$ , after a time delay  $\tau_{del1}$ , peak striations with a period  $\mathcal{L}_0$  form in the system (Fig. 5,  $t = t_2$ ). A DS of this sort is a metastable state. As a result of a "pumping" instability<sup>75</sup> (Subsection 2.2), this state, after a certain time ( $\tau_{del2} - \tau_{del1}$ ; Fig. 5b) which is associated with the growth of a fluctuation of greater period, takes the form of peak striations with a period  $\mathcal{L}_p > \mathcal{L}_0$  (Fig. 5,  $t = t_4$ ). The period of the striations continues to increase in the course of their spontaneous formation until stable striations form.<sup>11</sup> The latter consist of a periodic sequence of peak autosolitons which interact in a relatively weak fashion. The shape of these autosolitons (Fig. 4) was analyzed in Refs. 75, 98, and 139 and was reviewed in Ref. 25.

The conclusion regarding the instability of the striations of period  $\mathcal{L}_0 = 2\pi k_0^{-1}$  applies more to  $\Lambda$  in V systems, in which wide peak striations form<sup>98</sup> (Fig. 4b), since the very width of these striations,  $\sim L$ , is greater than  $\mathcal{L}_0$  under the condition  $\varepsilon \ll 1$ .

## 2. EFFECTS DETERMINING THE RESTRUCTURING OF STRIATIONS

### 2.1. Local breakdown in striations<sup>75,76,78</sup>

Periodic striations with a period  $\mathcal{L}_p > L$  are essentially a periodic sequence of interacting autosolitons (Fig. 6a). At certain values of the excitation level, a local breakdown can occur in the striations, as in autosolitons.<sup>25</sup> In other words, there may be a sharp change in the activator in certain local regions of a DS, which leads to an increase in the number of striations in the system.

2.1.1. A local breakdown can occur between striations (Fig. 6a) or at the center of striations (Fig. 7a), i.e., in regions in which  $\eta(x)$  and  $\theta(x)$  vary smoothly, in  $N$  and  $\bar{N}$  systems. In these regions, the relationship between  $\eta$  and  $\theta$  is determined by (1.29); i.e., it corresponds to a local-coupling curve (Subsection 12.1). The functional dependence  $\theta(\eta)$  corresponding to the local-coupling curve (Fig. 2, a and c) is S-shaped (Figs. 6b and 7b). A local breakdown occurs because as the striations evolve with changing excitation level  $A$  the value of the inhibitor at the center of the striations,  $\eta_m$ , reaches an extremum  $\eta'_0$  (Fig. 7b), or the value of the inhibitor between striations,  $\eta_t$ , reaches an extremum  $\eta_0$  (Fig. 6b).

In the first case, as  $A$  varies further there is a sharp decrease in the activator from  $\theta_m \approx \theta_0$  to  $\theta \approx \theta_d$ , while  $\eta_m \approx \eta'_0$  remains essentially constant (Fig. 7, a and b). As a result of this local breakdown (shown schematically by the arrows in Fig. 7, a and b), the striations divide. A local breakdown of the same type (shown schematically by the arrow in Fig. 7c) leads to a division of the hot autosoliton discussed in Subsection 3.5 of the review in Ref. 25.

In the second case, a further variation in  $A$  results in a local breakdown between striations, i.e., in a sharp increase in the activator, from the value  $\theta_t \approx \theta_0$  to  $\theta \approx \theta'_d$ , at  $\eta_t \approx \eta_0$  (this local breakdown is shown schematically by the arrows in Fig. 6, a and b).

A similar local breakdown (shown schematically by the arrow in Fig. 6c) leads to a division of a cold autosoliton.<sup>25</sup>

These local-breakdown effects at the center of striations or between striations occur because at certain critical value  $A = A_d^{(N)}$  or  $A'_d^{(N)}$  the solution in the form of  $N$  striations in a sample of size  $\mathcal{L}$ , i.e., the solution in the form of striations of period  $\mathcal{L}_p = \mathcal{L}/N$ , disappears. This result follows formally directly from the procedure used to construct periodic striations, which is set forth in §12. Also in that section are

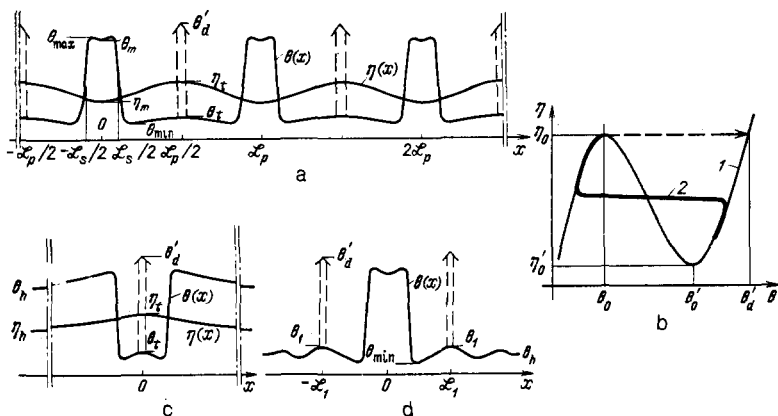


FIG. 6. Diagram used in explaining the local breakdown between striations of period  $\mathcal{L}_p \geq L$  (a), at the center of a cold autosoliton (c), and in the "tails" of a hot autosoliton (d). Part b shows the local-coupling curve (curve 1) for  $N$  systems and the actual  $\eta(\theta)$  dependence (2) in striations (a) and in autosolitons (c, d) near critical excitation levels of the system,  $A_d^{(N)}$ ,  $A'_d^{(N)}$ , and  $\tilde{A}_d$ , respectively. The arrows schematically show local breakdown, i.e., a local increase in the activator from  $\theta \approx \theta_0$  to  $\theta \approx \theta'_d$  in an avalanche fashion (part b).

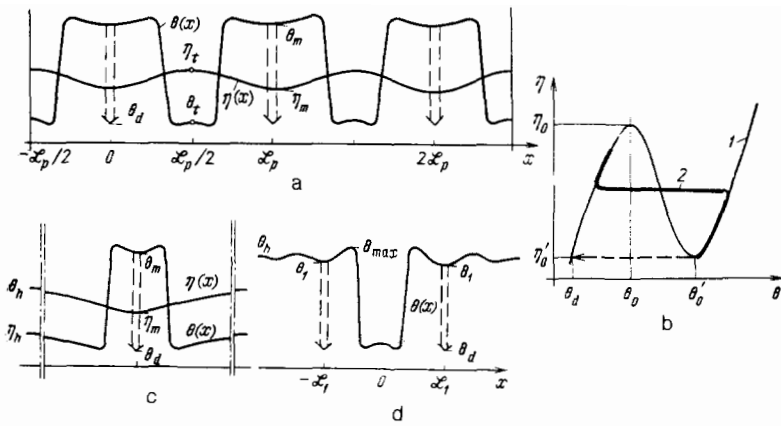


FIG. 7. Diagram used in explaining local breakdown at the center of striations of period  $\mathcal{L}_p \gtrsim L$  (a), at the center of a hot autosoliton (c), and in the "tails" of a cold autosoliton. (d). Part b shows the local-coupling curve (curve 1) for  $N$  systems and the true  $\eta(\theta)$  dependence (2) in striations (a) and in autosolitons (c, d) near critical excitation levels  $A_d^{(N)}$ ,  $A_d$ , and  $A'_d$ , respectively, of the system. The arrows schematically show local breakdown, i.e., a local decrease in the activator from  $\theta \approx \theta'_0$  to  $\theta \approx \theta_d$  in an avalanche fashion (part b).

equations which determine, within  $\varepsilon \ll 1$ , the values of  $A = A_d^{(N)}$  and  $A'_d^{(N)}$  and the critical width of the striations at these points. It also follows from the procedure for constructing the striations that a set of solutions in the form of striations of various periods corresponds to a single value of  $A$ .

There is an upper limit  $\mathcal{L}_{\max}$ , on the period of the striations; this value depends on  $A$ . For a specific system, this dependence can be found from the equations in Subsection 12.2.

The qualitative dependence<sup>12</sup>  $\mathcal{L}_{\max}(A)$  (Fig. 8a) follows from the fact that at  $A < A_c$  and  $A > A'_c$  an autosoliton,<sup>25</sup> i.e., a solitary state which may be thought of striations of period  $\mathcal{L}_p = \infty$ , can be excited in the system. In addition, there are systems in which an autosoliton is realized in the form of a solitary hot striation (Fig. 6c) only under the conditions  $A < A_d < A_c$ . There are also systems in which an autosoliton in the form of a solitary cold striation (Fig. 6c) can be excited only under the condition  $A > A'_d > A'_c$ . At the point  $A = A_d$  (or  $A = A'_d$ ), a hot (or cold) autosoliton divides (see Subsection 3.5 in Ref. 25). For such systems, the dependence  $\mathcal{L}_{\max}(A)$  is as shown in Figs 8b and 8c, respectively. For systems in which an autosoliton can be excited only under the conditions  $A < A_d$  and  $A > A'_d$  the  $\mathcal{L}_{\max}(A)$

dependence corresponds to that shown in Fig. 8d. The values  $A = A_d$  and  $A'_d$  and the corresponding values of the maximum possible width of hot and cold autosolitons are determined within  $\varepsilon \ll 1$  by Eqs. (3.37)–(3.39), respectively, in the review in Ref. 25.

As was stressed in the Introduction, a local breakdown leads to a dynamic restructuring of a DS; this restructuring is unrelated to the presence of fluctuations in the system. During a dynamic restructuring, the formation time of a new DS is determined by the time scales of the variation of the activator and the inhibitor and by the extent to which  $A$  exceeds the corresponding critical value  $A_d$ ,  $A'_d$ ,  $A_d^{(N)}$ , or  $A'_d^{(N)}$ . Fluctuations lead to simply a finite probability for the occurrence of a local breakdown, before these points are reached; it may also accelerate the initial stage of the development of local breakdown at a value of  $A$  greater than but very close to the corresponding critical value. This time evolution of the development of a local breakdown leading to the division of autosolitons and striations was observed in the model of an electron-hole plasma in Refs. 100, 104, and 109. The division of autosolitons and striations which is observed in numerical and experimental studies of composite superconductors<sup>19,97,142</sup> and of structures with a gas-discharge region (Figs. 5 in Ref. 87b) is apparently related to the local-breakdown effect which we have been discussing.

2.1.2. Local breakdown may occur not only at the center but also at the periphery, i.e., in the "tails," of an autosoliton.<sup>110</sup> The reason for this effect is that at values of  $A$  close to  $A_c$  the monotonic decay of  $\theta(x)$  and  $\eta(x)$  toward  $\theta_h$  and  $\eta_h$  at the periphery of the autosoliton may give way to an oscillatory decay.<sup>25</sup> The appearance of oscillations at the periphery of an autosoliton as  $A \rightarrow A_c$  can be linked with the circumstance that the tail of an autosoliton may be thought of as a reaction of the system to the local decrease in the activator caused by the autosoliton at the point with  $\theta = \theta_{\min}$  (Fig. 6d). In turn, the response of a homogeneous stable system to a small local irregularity in the parameters of the medium at values of  $A$  close to  $A_c$  consists of an oscillatory<sup>13</sup>  $\theta(x)$  distribution whose amplitude decays with distance from the irregularity.

As  $A$  approaches  $A_c$ , the amplitude of the most prominent of the maxima,  $\theta = \theta_1$ , in the oscillating distributions  $\theta(x)$  in the tails of the autosoliton becomes larger (Fig. 6d). At a certain value  $A = \bar{A}_c$ , close to  $A_c$ , at which the value of  $\theta_1$  at the points of this maximum exceed the value of  $\theta_0$  (Fig. 6b) by a certain critical value, a local breakdown occurs in

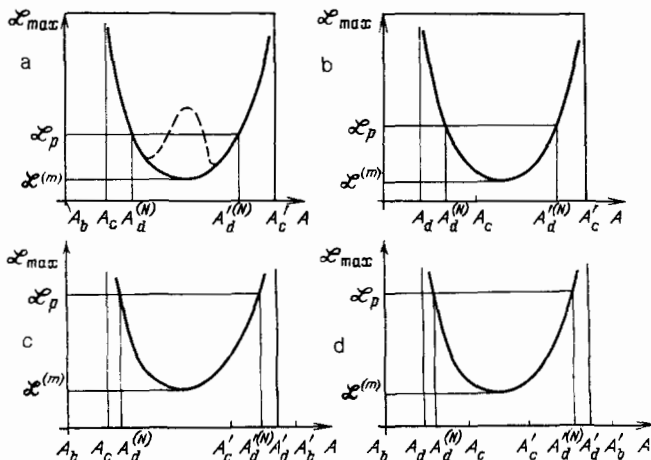


FIG. 8. Possible versions of the behavior of the maximum striation period  $\mathcal{L}_{\max}$  as a function of the excitation level  $A$  (Subsection 12.2 and footnote<sup>12</sup>).

these regions. In other words, there is an abrupt local increase in the activator (shown schematically by the arrows in Fig. 6, b and d) from  $\theta_1 \approx \theta_0$  to  $\theta \approx \theta'_d$ . The reason for the local breakdown is that as  $A \rightarrow A_c$  the value of  $\eta_h$  is close to  $\eta_0$ , and the local dependence  $\theta(\eta)$  is S-shaped (Fig. 6b). Consequently, the nearest two maxima in the oscillating distribution  $\theta(x)$  (Fig. 6d), which lie a distance  $\mathcal{L}_1$  from the center of the autosoliton, act as seeds for the abrupt appearance of striations. In turn, a local breakdown occurs in the tails of the striations, and new striations form.

A local breakdown can also occur in the tails of a cold autosoliton as  $A \rightarrow A'_c$ . Such a breakdown, i.e., a local decrease in the activator from  $\theta_1 \approx \theta'_0$  to  $\theta \approx \theta_d$  in an avalanche fashion, arises at the minima of the oscillatory distribution  $\theta(x)$  closest to the center of the cold autosoliton, at the periphery of the autosoliton (Fig. 7d). It occurs at a certain value  $A = \tilde{A}'_c$  which is close to  $A'_c$ , at which the value of  $\theta_1$  at these minima is smaller than  $\theta'_0$  by a certain critical amount (the local breakdown is shown schematically by the arrows in Fig. 7, b and d).

## 2.2. "Pumping" of activator between striations<sup>75,76</sup>

It follows from the theory of the stability of striations (Subsection 12.4) that at certain values  $A = A_p^{(N)}$  or  $A'_p^{(N)}$  a state in the form of  $N$  striations of period  $\mathcal{L}_p = \mathcal{L}/N$  (Fig. 9a) becomes unstable with respect to the growth of activator fluctuations  $\delta\theta \approx \delta\theta_{N/2,0}$  of doubled period. It follows from the form of the critical fluctuation (Fig. 9d) that the growth of this fluctuation leads to an increase in the width (or amplitude) of one striation and to a narrowing of a neighboring striation. In other words, it describes a pumping of activator between striations. As a result, the number of striations in the system may decrease by a factor of two (Fig. 10).<sup>109</sup>

An instability of the pumping type is realized at values  $A = A_p^{(N)} > A_b$  or  $A'_p^{(N)} < A'_b$ , i.e., before the points  $A = A_b$  and  $A'_b$ , which determine the stability boundary of the autosoliton (see Subsection 4.2 in Ref. 25). The reason for this result is that the growth of an activator fluctuation

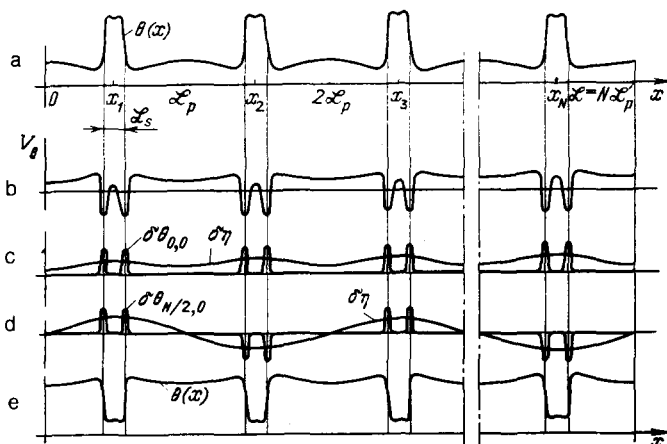


FIG. 9. Diagram used in analyzing the stability of periodic striations (a, e); b—the "potential"  $V_\theta$  (see Subsection 12.4); c, d—the critical functions (c)  $\delta\theta_{0,0}$  and (d)  $\delta\theta_{N/2,0}$  and the inhibitor perturbations  $\delta\eta$  which damp dangerous activator fluctuations  $\delta\theta \approx \delta\theta_{0,0}$ ,  $\delta\theta \approx \delta\theta_{N/2,0}$  in striations (a, e).

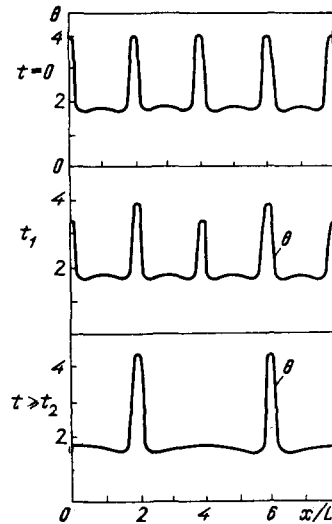


FIG. 10. Numerical simulation of the kinetics of the activator pumping (the "pumping" of carrier temperature) between striations in a "dense" electron-hole plasma<sup>109</sup> with  $t_1 = 20\tau_r$  and  $t_2 = 135\tau_r$ .

$\delta\theta \approx \delta\theta_{0,0}$ , which has a period  $\mathcal{L}_p$  and which is an even function of  $x$  with respect to the center of the striations (Fig. 9c), is suppressed by the fixed-sign change in the inhibitor (Fig. 9c) all the way to the point  $A = A_b$  (or  $A = A'_b$ ), where  $d\mathcal{L}_s/dA = \infty$  and  $d\eta_s/dA = \infty$ . The growth of a fluctuation  $\delta\theta \approx \delta\theta_{N/2,0}$  of period  $2\mathcal{L}_p$  is damped by a sign-varying change in the inhibitor,  $\delta\eta$ , of the same period (Fig. 9d). The damping effect of this change in the inhibitor is reduced by its diffusive spreading, which is more pronounced, the smaller the distance between striations,  $\mathcal{L}_p$ . It follows that with decreasing striation period the range of  $A$  in which the striations are stable decreases (Subsection 12.4).

The critical width of the striations of period  $\mathcal{L}_p < L$  (Subsection 12.4) at the point  $A = A_p^{(N)}$  is given approximately by<sup>79</sup>

$$\mathcal{L}_s(A_p^{(N)}) \equiv \mathcal{L}_c^{(N)} \sim l \ln \frac{L^2}{l \mathcal{L}_p}. \quad (2.1)$$

It follows from this picture of the striation instability that the period of the striations which are realized at a given value of  $A$  is limited from below by a certain  $\mathcal{L}_{\min}$ . Striations of period  $\mathcal{L}_p < \mathcal{L}_{\min}$  are unstable with respect to the growth of a fluctuation  $\delta\theta \approx \delta\theta_{N/2,0}$  (Fig. 9d), which describes a pumping of activator.

## 2.3. Corrugation of walls and granulation of striations<sup>77</sup>

Striations in 2D and 3D systems may lose their stability with respect to the growth of activator fluctuations  $\delta\theta(x,y,z)$  which are inhomogeneous in the plane of the walls of the striations, i.e., in regions in which  $\theta(x)$  varies sharply (Fig. 11a). A critical fluctuation  $\delta\theta = \delta\theta(x) \exp(ik_\perp r_\perp)$  (Fig. 11a) is localized near the striation walls, so its increase can lead to a corrugation of the striation walls in a 2D system (Fig. 11, c–e; in a 3D system, it can lead to the appearance of a cellular structure at the striation walls). Alternatively, it may lead to a breakup of the striations into smaller regions in the form of interacting autosolitons (Fig. 11b) with a shape

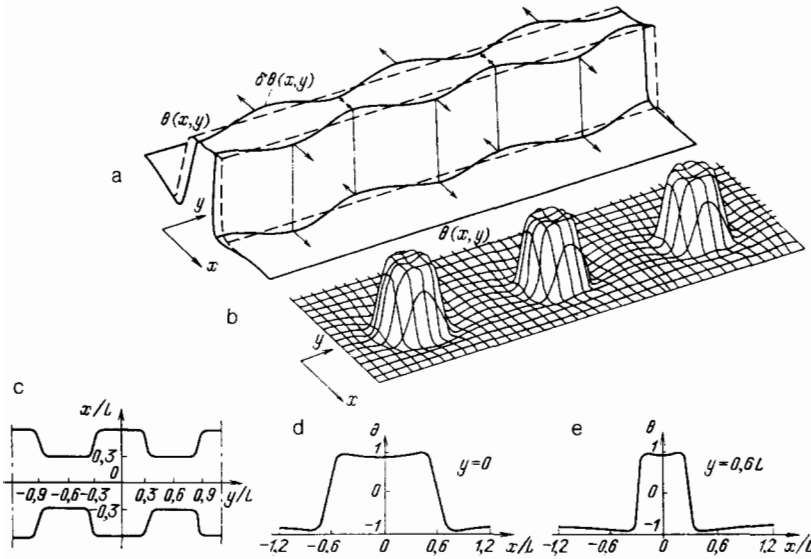


FIG. 11. Diagram used in explaining the "corrugation" and breakup of striations. a: Critical activator fluctuations  $\delta\theta(x, y)$ , localized at striation walls. The growth of these fluctuations (indicated schematically by the arrows) leads to (b) a breakup of striations and to the formation of a set of interacting autosolitons or (c) the formation of a striation with corrugated walls. d, e: Activator distributions in the cross sections of a striation (c),  $y = 0$  (d) and  $y = 0.6L$  (e) [these are the results of a numerical solution of Eqs. (1.1), (1.2), and (1.3) with  $A = 0.35$ ,  $\varepsilon = 0.033$ , and  $\alpha = 1$ , carried out by Gafichuk *et al.*].<sup>100</sup> The dashed lines in part a show the initial distribution  $\theta(x, y)$  in the striations.

approximating that of radially symmetric autosolitons (see Fig. 11 in Ref. 25). The critical striation widths in KN and KH systems can be estimated from expression (12.52) by setting  $\gamma = 0$  there. It follows from this criterion<sup>79</sup> that the striation instability condition is satisfied with respect to fluctuations with  $k_1 \sim (l/L_p)^{1/4}(lL)^{-1/2}$  when the width ( $\mathcal{L}_s$ ) of the hot striations (Fig. 6a) satisfies  $\mathcal{L}_s < \mathcal{L}_{bl}^{(N)}$  or  $\mathcal{L}_s > \mathcal{L}_{cl}^{(N)}$ , where<sup>79</sup>

$$\mathcal{L}_{bl}^{(N)} \equiv \mathcal{L}_s(A_{bl}^{(N)}) \sim l \ln \left[ \varepsilon^{-1} \left( \frac{\mathcal{L}_p}{l} \right)^{1/2} \right],$$

$$\mathcal{L}_{cl}^{(N)} \equiv \mathcal{L}_s(A_{cl}^{(N)}) \sim (lL)^{1/2} \left( \frac{l}{\mathcal{L}_p} \right)^{1/2}. \quad (2.2)$$

In other words, in the 2D and 3D cases the width of the stable striations is in the interval  $\mathcal{L}_{bl}^{(N)} < \mathcal{L}_s < \mathcal{L}_{cl}^{(N)}$ ; i.e., these striations are usually stable in a smaller interval  $[A_{bl}^{(N)}, A_{cl}^{(N)}]$  of values of  $A$  than in the 1D case (Subsection 3.1). Numerical studies show that the hot striations which shrink with decreasing  $A$  (with  $A = A_{bl}^{(N)}$ ) generally break up into smaller regions. As  $A$  increases (at the point  $A = A_{cl}^{(N)}$ ), there may be either a breakup (Fig. 11b) or a corrugation of striation walls (Fig. 11, c-d), depending on the parameters of the system. Striations with corrugated (or cellular) walls may be thought of as a metastable state.

### 3. SELF-ORGANIZATION SCENARIOS IN IDEALLY HOMOGENEOUS 1D SYSTEMS<sup>75,76</sup>

#### 3.1. Evolution of wide striations

It can be concluded from the results in Subsections 2.1 and 2.2 that a set of stable DSs in the form of striations with periods from  $\mathcal{L}_{max}$  to  $\mathcal{L}_{min}$  can exist in one-dimensional (1D) KN and KH systems of size  $\mathcal{L} \gg L$  at a given value of  $A$ .

The quantity  $\mathcal{L}_{max}$  determines the maximum possible striation period, i.e., the period above which the number of striations doubles as the result of a local breakdown at the center of striations or between striations (Subsection 2.1).

The quantity  $\mathcal{L}_{min}$  determines the minimum striation period, i.e., the period at which the striations lose their stability at the given value of  $A$  (Subsection 2.2). The value of

$\mathcal{L}_{min}$  is found from the formulas in §12. As was mentioned earlier, as  $A \rightarrow A_b$  or  $A'_b$  striations of finite period lose their stability, and all that remains stable is an autosoliton, i.e., a state which may be thought of as striations of period  $\mathcal{L}_p = \infty$ . It follows that the dependence  $\mathcal{L}_{min}(A)$  is qualitatively as shown in Fig. 12a.

The behavior of  $\mathcal{L}_{max}(A)$  (Fig. 8) and  $\mathcal{L}_{min}(A)$  (Fig. 12a) essentially also determine the various self-organization scenarios which operate in ideally homogeneous systems in the 1D case. It is also convenient to analyze the evolution of striations with varying  $A$  by using one of the bifurcation characteristics of a system: the dependence of the value of  $\eta = \eta_s$  at a striation wall on  $A$  (Fig. 12b), that of the striation width  $\mathcal{L}_s$  on  $A$ , etc.<sup>25</sup>

1) At the point  $A = A_c$ , the homogeneous state of the system stratifies with respect to the growth of fluctuations of period  $\mathcal{L}_0 = 2\pi k_0^{-1} \approx 2\pi(lL)^{1/2}$  (Subsections 1.1 and 1.2). As a result of the growth of such a fluctuation, i.e., a fluctuational restructuring of the homogeneous state, large-amplitude striations form abruptly in such systems (the jump  $0 \rightarrow 1$  in Fig. 12, a and b). The width of striations  $\mathcal{L}_s(A_c)$  of period  $\mathcal{L}_0$  depends strongly on the nonlinearity of the system. This width is determined by the formulas given in Subsection 12.1. The period of the striations which form is equal to  $\mathcal{L}_0$  if  $\mathcal{L}_0 > \mathcal{L}_{min}(A_c)$ , i.e., if their width  $\mathcal{L}_s(A_c)$  exceeds the critical width of stable striations,  $\mathcal{L}_{cl}^{(N)}$ , of period  $\mathcal{L}_0$ . An estimate of  $\mathcal{L}_{cl}^{(N)}$  can be found from (2.1) by setting  $\mathcal{L}_p = \mathcal{L}_0$  there.

In the opposite case,  $\mathcal{L}_0 < \mathcal{L}_{min}(A_c)$ , striations of period  $\mathcal{L}_0$  are unstable with respect to pumping, and striations of period  $\mathcal{L}_p > \mathcal{L}_0$  appear at the point  $A = A_c$ .

The hot striations which form in KN and KH systems at the point  $A = A_c$  as the excitation level is raised become broader (Fig. 12d) and transform into cold striations of the same period (Fig. 12e). At the point  $A = A'_p$ , the cold striations become unstable when their width  $\mathcal{L}_s$  (Fig. 12e) reaches the value  $\mathcal{L}_{cl}^{(N)}$ , which is equal in order of magnitude to the value given by (2.1) for the quantity  $\mathcal{L}_{cl}^{(N)}$ . This instability (of the pumping type) of cold striations (Fig. 12e) stems from the growth of a critical activator fluctuation

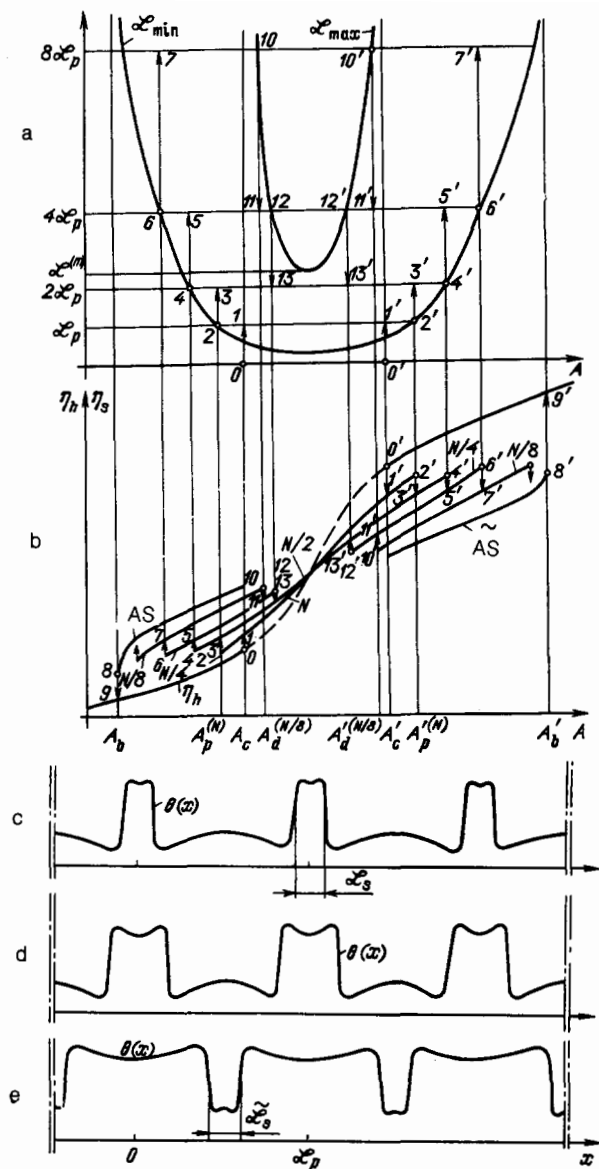


FIG. 12. Diagram used to explain the evolution of periodic striations. a, b— $L_{\min}$  and  $L_{\max}$  as functions of  $A$  (a) and the bifurcation characteristic  $\eta$ , as a function of  $A$  (b); c, e—activator distribution in hot striations (c, d) and cold striations (e). Curve labels  $N$ ,  $N/2$ ,  $N/4$ , and  $N/8$  in part b correspond to the number of striations of periods  $L_p$ ,  $2L_p$ ,  $4L_p$ , and  $8L_p$ , respectively, in the system;  $AS$  and  $\bar{AS}$  represent hot and cold autosolitons.

with a double period. As a result of the aperiodic growth of such a fluctuation, there may be an abrupt halving (the jump  $2' \rightarrow 3'$  in Fig. 12, a and b) of the number of cold striations. The kinetics of this effect has been examined in a numerical study of a model of a dense electron-hole semiconductor (see Fig. 22 in Ref. 109). [In certain systems, striations whose period is again equal to  $2L_p$  but which contain two (slightly distorted) asymmetric striations may arise at the point  $A = A_p^{(N)}$ .] With a further increase in  $A$ , as a result of a sequence of period-doubling bifurcations of this sort, there

are sequential abrupt decreases in the number of striations (jumps  $4' \rightarrow 5'$ ,  $6' \rightarrow 7'$ , ... , in Fig. 12, a and b). As a result, a cold autosoliton may arise spontaneously in the system at values of  $A$  near  $A_b'$ . This autosoliton abruptly disappears ( $8' \rightarrow 9'$  in Fig. 12b) at the point  $A = A_b'$ , at which we have  $dL_s/dA = d\eta_s/dA = \infty$  (Subsection 4.2 in Ref. 25).

2) Hot striations which form spontaneously at the point  $A = A_c$  shrink with decreasing  $A$  (Fig. 12c), and at a certain  $A = A_p^{(N)}$  they lose their stability with respect to a pumping of activator (Subsection 2.2). As a result, hot striations of a doubled period form abruptly in the system ( $2 \rightarrow 3$  in Fig. 12, a and b). The kinetics of this effect is shown by Fig. 10. As a result of a sequence of these period-doubling bifurcations ( $4 \rightarrow 5$ ,  $6 \rightarrow 7$ , ... , in Fig. 12, a and b), a hot autosoliton can form spontaneously in the system at values of  $A$  near  $A_b$ . This autosoliton abruptly disappears ( $8 \rightarrow 9$  in Fig. 12b) at the point  $A = A_b$ , where we have  $dL_s/dA = d\eta_s/dA = \infty$  (Ref. 25).

3) The hot striations of period  $L_p \gtrsim L$  which form with increasing  $A$ , at values of  $A$  near  $A_b$ , may undergo a spontaneous restructuring as a result of the local-breakdown effect discussed in Subsection 2.1. As a result of this dynamic restructuring, the number of striations in the system doubles sequentially and abruptly; i.e., the period of the striations decreases by a factor of two (jumps  $10 \rightarrow 11$ ,  $12 \rightarrow 13$  in Fig. 12, a and b).

The same conclusion applies to cold striations of period  $L_p \gtrsim L$  which form in accordance with scenario 1 near  $A = A_b'$ . In this case, the increase in the number of striations due to the local breakdown occurs with decreasing  $A$  (jumps  $10' \rightarrow 11'$ ,  $12' \rightarrow 13'$  in Fig. 12, a and b).

4) In systems with  $A_d < A_c$ , i.e., in the case of the situation in Fig. 8, b or d, the condition  $L_0 > L_{\max}(A_c)$  may hold. In this case, a local breakdown occurs during the formation of striations as a result of the growth of a critical fluctuation of period  $L_0$  in the regions with a high value of the activator which form as time elapses. This local breakdown leads to a breakup of the striations. As a result of this dynamic restructuring, striations of period  $L_p < L_0$  form. The subsequent evolution of these striations occurs in accordance with scenarios 1–3, outlined above.

### 3.2. Evolution of narrow peak striations

As was stressed in Subsection 1.5.2, narrow or wide peak striations can form in  $KA$  and  $KV$  systems (Fig. 4). The evolution of narrow peak striations (Fig. 13), like that of wide striations in  $KN$  and  $KH$  systems, is determined by local-breakdown effects and by the pumping of activator between striations, i.e., by the functional dependences  $L_{\max}(A)$  and  $L_{\min}(A)$  (Fig. 13c). A critical fluctuation  $\delta\theta \approx \delta\theta_{N/2,0}$  describing a pumping of activator in striations of period  $L_p$  (Fig. 13a) has a period  $2L_p$  and is localized near peaks (Fig. 13b). The growth rate calculated for this fluctuation without consideration of the damping effect of the change in the inhibitor, i.e., under the condition  $\delta\eta = 0$ , is approximately  $\lambda_0 \sim -1$ , as in the case of a narrow peak autosoliton.<sup>25</sup> According to the stability condition for periodic striations in (12.53), such striations are therefore stable when they have a large period and a large amplitude ( $\theta_{\max}$ ). The latter conclusion follows from the circumstance that the value of the coefficient  $\alpha_{0,0}^{(0)}$  (Ref. 25) in (12.53) increases

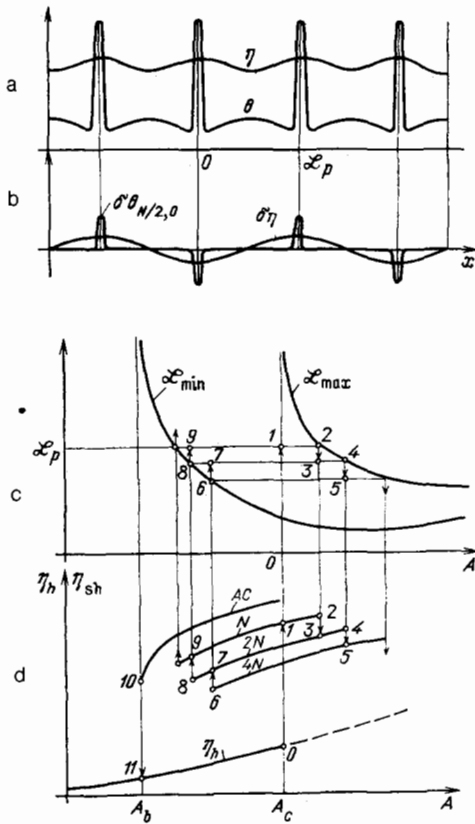
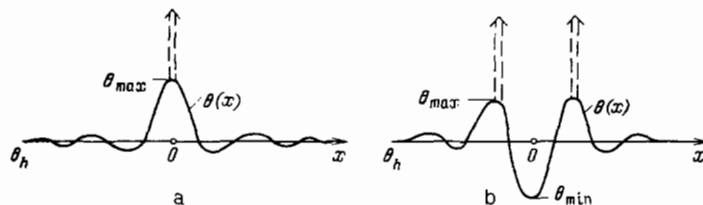


FIG. 13. a: Diagram used in explaining the evolution of narrow peak striations (a) in  $\Lambda$  and  $V$  systems. b: Critical activator fluctuations  $\delta\theta_{N/2,0}$  and inhibitor perturbations  $\delta\eta$  which damp the growth of the activator fluctuations. c: One possible dependence of  $\mathcal{L}_{\min}$  and  $\mathcal{L}_{\max}$  on  $A$ . d: Bifurcation characteristics, i.e., dependence of the inhibitor value at a striation peak,  $\eta = \eta_h$ , on the system excitation level  $A$ . The numbers  $N$ ,  $2N$ , and  $4N$  in part d correspond to the number of striations of periods  $\mathcal{L}_p$ ,  $\mathcal{L}_{p/2}$ ,  $\mathcal{L}_{p/4}$  respectively, in the system;  $AS$  represents a narrow peak autosoliton.

with  $\theta_{\max}$ . Let us examine some characteristic self-organization scenarios in 1D  $K\Lambda$  and  $KV$  systems.

1) During the stratification of a homogeneous state in a  $K\Lambda$  or  $KV$  system, peak striations form abruptly (jump 0  $\rightarrow$  1 in Fig. 13; see Subsection 1.5.2). Their period,  $\mathcal{L}_p$ , may be substantially greater than  $\mathcal{L}_0 = 2\pi k_0^{-1}$ . As  $\varepsilon = 1/L$  decreases, the striation amplitude  $\theta_{\max}$  increases. With increasing  $A$ , the amplitude of the peak striations increases, and at certain values  $A = A_d^{(N)}$ ,  $A_d^{(2N)}$ , ..., the number of striations sequentially and abruptly doubles (2  $\rightarrow$  3, 4  $\rightarrow$  5, ... in Fig. 13, c and d) as the result of a local breakdown between striations. In other words, the evolution of the striations with increasing excitation level of the system in  $\Lambda$  and  $V$  systems is usually determined by a dynamic, rather than



fluctuational, restructuring. At large values of  $A$  the number of striations may decrease abruptly as a result of a pumping of activator between closely spaced striations; alternatively, a turbulence arises in the system (§9).

2) As  $A$  decreases as a result of the pumping, i.e., as a result of the fluctuational restructuring, the number of narrow peaked striations sequentially and abruptly decreases at certain values  $A = A_p^{(4N)}$ ,  $A_p^{(2N)}$ , ... (6  $\rightarrow$  7, 8  $\rightarrow$  9, ... in Fig. 13, c and d). As  $A \rightarrow A_b$ , a narrow peaked autosoliton may arise spontaneously in the system. At the point  $A = A_b$ , where  $d\eta_{sh}/dA = \infty$ , the autosoliton abruptly disappears (10  $\rightarrow$  11 in Fig. 13d).<sup>25</sup>

3) In  $\Lambda$  and  $V$  systems with "degenerate" local-coupling curves (curves 1' in Fig. 2, b and d),<sup>25</sup> the number of peak striations may abruptly double with increasing  $A$  as the result of a local breakdown at the center of the peaks. This situation is realized,<sup>11,13</sup> for example, in the model of avalanche breakdown of a p-n junction discussed in Subsection 7.1.

In  $\Lambda$  and  $V$  systems, a turbulence may arise spontaneously; the mechanisms and scenarios for the formation of this turbulence are discussed in §9.

#### 4. SCENARIOS FOR SELF-ORGANIZATION IN REAL 1D SYSTEMS

Real systems always contain small inhomogeneities, which are capable in principle of altering the processes by which dissipative structures (DSs) form and evolve. Small-scale (local) irregularities of size  $d \lesssim (lL)^{1/2}$  and large-scale irregularities, of size  $d \gg (lL)^{1/2}$ , act in different way on the self-organization picture. Let us examine the most characteristic self-organization scenarios which play out in real systems.

##### 4.1. Spontaneous formation and evolution of autosolitons<sup>78,79</sup>

Self-organization in real systems may be determined by the spontaneous appearance of autosolitons near small local inhomogeneities and the subsequent evolution of these solitons. This spontaneous formation of autosolitons occurs when the excitation level of the system is below the critical value  $A = A_c$ . It leads to a dynamic restructuring of the initially nearly homogeneous state of the system.

4.1.1. As  $A$  increases or, more precisely, as  $A \rightarrow A_c$ , small local inhomogeneities are essentially nucleating regions of the spontaneous formation of autosolitons. The reason is that a local inhomogeneity causes corresponding perturbations of the activator and the inhibitor in its vicinity, and the amplitude,  $\Delta\theta_m = \theta_{\max} - \theta_h$ , increases as  $A \rightarrow A_0$ . The monotonic decay of  $\theta(x)$  and  $\eta(x)$  at the periphery of the

FIG. 14. Activator oscillations which arise in a stable system at values of  $A$  near  $A_c$ , near a small inhomogeneity which causes a local increase (a) or a decrease (b) in the activator.

inhomogeneity, toward the values  $\theta_h$  and  $\eta_h$  for the homogeneous state, gives way to an oscillatory decay<sup>13)</sup> with a period  $\mathcal{L}_0 = 2\pi k_0^{-1}$  (Fig. 14).

In the situation in Fig. 14a, at values of  $A$  close to  $A_c$  near an inhomogeneity, the value of the inhibitor at the center of an inhomogeneity,  $\eta_m \approx \eta_h$ , is close to  $\eta_0$ , while the value of the activator,  $\theta_{\max}$ , is close to  $\theta_0$ . We recall that the point  $\eta = \eta_0, \theta = \theta_0$  determines an extremum of the local-coupling curve, at which we have  $d\theta/d\eta = \infty$  (Fig. 6b). At a certain  $A = A_c^- < A_c$ , at which  $\theta_{\max}$  is greater than  $\theta_0$  by a certain critical amount, a local breakdown therefore occurs at the center of the inhomogeneity: an increase in the activator from  $\theta_{\max} \approx \theta_0$  to  $\theta \approx \theta'_d$  in an avalanche fashion (the local breakdown is shown schematically by the arrow in Figs. 14a and 6b). As a result of this local breakdown, an autosoliton arises spontaneously near the inhomogeneity. Figure 15 (Ref. 111) shows the kinetics of its formation in an electron-hole plasma (Subsection 8.2). The threshold for the spontaneous formation of an autosoliton, i.e., the value of  $A_c^-$ , may be quite different from the stratification point  $A = A_c$  of a homogeneous state of a system, even in cases in which the inhomogeneity amplitude  $a$  is small.

In the situation in Fig. 14b, the value of the activator at the center of the inhomogeneity is lowered. Consequently, and in contrast with the preceding case, a local breakdown does not occur at the center of the inhomogeneity. As we have already pointed out, as  $A \rightarrow A_c$  the decrease of  $\theta(x)$  toward the value  $\theta_h$  at the periphery of the inhomogeneity becomes oscillatory. The values of  $\theta = \theta_{\max}$  at the maxima of the oscillatory  $\theta(x)$  distribution (Fig. 14b) increase as  $A \rightarrow A_c$ . Consequently, at a certain  $A = A_c^-$ , at which the values of  $\theta_{\max}$  are greater than  $\theta_0$  by a certain critical amount, the conditions for the occurrence of a local breakdown become satisfied at the two maxima of the  $\theta(x)$  distribution nearest the center of the inhomogeneity. As a result of such local breakdowns, occurring in two spatially separated points (these breakdowns are shown schematically by the arrows in Fig. 14b), three different effects may occur, depending on the parameters of the inhomogeneity and those of the system:

- a) An autosoliton of complex shape, consisting of two striations, may form.
- b) An ordinary autosoliton may form as a solitary striation. It would arise because during the formation of a complex autosoliton one of the striations "perishes" as a result of the pumping (Subsection 2.2).

c) A sequence of striations may form and fill the entire system. These striations would form as the result of a multiple generation of two autosolitons near an inhomogeneity and the propagation of these solitons away from each other, on different sides of the inhomogeneity.

The local-breakdown effects which we have been discussing here, and which lead to the spontaneous formation of autosolitons near small inhomogeneities, are of the same nature as those which occur as  $A \rightarrow A_c$  in the oscillatory tail of an autosoliton (Subsection 2.1.2).

4.1.2. At parameter values of the system such that an autosoliton in the form of a solitary striation forms near a small inhomogeneity, the subsequent evolution of the autosoliton as  $A$  varies may occur in accordance with one of the following scenarios.

1) As  $A$  increases, there may be a sequential breakup of the autosoliton due to the local-breakdown effect at the center of the autosoliton which was discussed in Subsection 2.1.1. This situation occurs in systems with  $A_d < A_c$  (Fig. 8, b and d) when  $A$  exceeds the critical value  $A = A_d$ .

2) A local breakdown and a breakup of an autosoliton in systems with  $A_d < A_c$ , for which the dependence  $\mathcal{L}_{\max}(A)$  is the same as that shown in Fig. 8, b or d, can occur even during the spontaneous formation of an autosoliton near a small inhomogeneity at  $A = A_c^- > A_d$ . As a result of the sequential breakup of the newly formed autosolitons, the entire system becomes filled with striations (Fig. 16).

3) Another self-organization scenario occurs in systems in which the autosoliton does not break up before the value  $A = A_c$  (Fig. 8a), which corresponds to the point of the stratification of the homogeneous state of the system. In this case, a local breakdown occurs at the periphery of the autosoliton as  $A \rightarrow A_c$  (Subsection 2.1.2). Striations may form spontaneously, and they may be periodic, but their period  $\mathcal{L}_p \approx \mathcal{L}_1$  (Fig. 6d) may be quite different from that of a critical fluctuation,  $\mathcal{L}_0 = 2\pi_0^{-1}k \approx 2\pi(IL)^{1/2}$  (Subsection 1.5.1).

4) At a very small amplitude of a local inhomogeneity, a spontaneous formation of an autosoliton may occur at values of  $A$  extremely close to  $A_c$ . In this case the amplitude of the  $\theta(x)$  oscillation in the tail of the autosoliton which forms, i.e., the quantity  $\theta_1$  (Fig. 6d), is quite large. For this reason, there will be a sequential appearance of striations in the course of the formation of an autosoliton near a small inhomogeneity, as a result of local breakdowns in the tail of the autosoliton. These striations will fill the entire system.

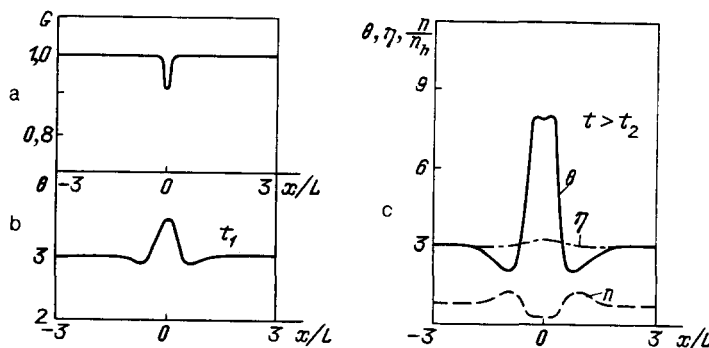


FIG. 15. Kinetics of the formation of a static autosoliton near a small inhomogeneity electron-hole plasma heated by an electric field (Subsection 8.2). a—Small static inhomogeneity in the carrier generation rate; b, c—distribution of the temperature  $\theta = T/T_i$ , the carrier density  $n/n_h$ , and the parameter  $\eta$  in an intermediate state ( $t = t_1$ ) and in an autosoliton ( $t > t_2$ ) (Ref. 111) ( $t_1 = 1.2\tau_r, t_2 = 5\tau_r$ ).



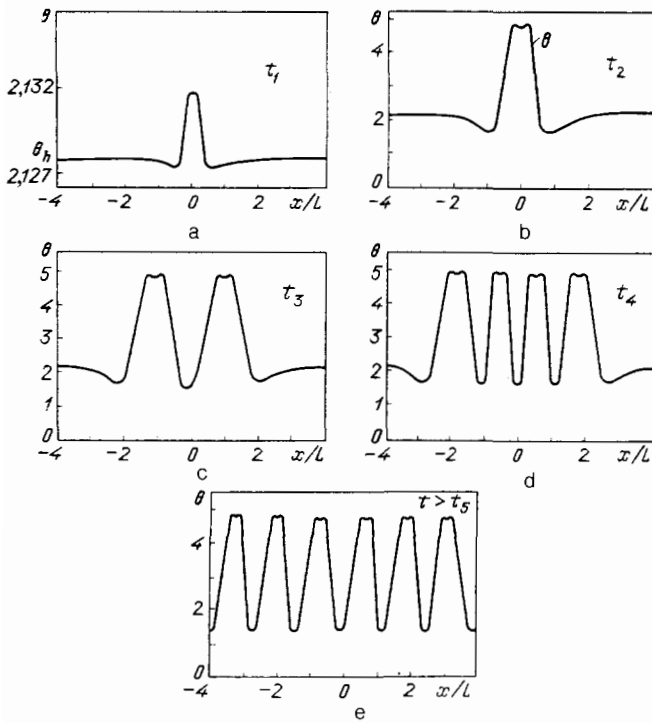


FIG. 16. Kinetics of the formation of periodic striations (e) which arise as a result of the breakup of an autosoliton (b, c) in the course of its spontaneous formation (a, b) near a small static inhomogeneity (with a relative amplitude  $a = 5 \cdot 10^{-3}$  and a width of  $0.2L$ ) at  $x = 0$  at  $t_1 = 0.5\tau_r$ ,  $t_2 = 2\tau_r$ ,  $t_3 = 5\tau_r$ ,  $t_4 = 6\tau_r$ ,  $t_5 = 20\tau_r$ . These are the results of a numerical simulation of a "dense" electron-hole plasma.<sup>109</sup>

The physics of the formation of these striations is similar to that described in Subsection 2.1.2.

5) In real systems, there are usually several local inhomogeneities of various amplitudes. As  $A$  varies, there can accordingly be a sequential formation of DSs near many inhomogeneities in accordance with scenarios 1–4.

6) If there are large-scale inhomogeneities in addition to the local inhomogeneities, the system could conceivably break up into several regions, each with its own value of  $A_c$ . In this case, at a value of  $A$  close to the smallest of these  $A_c$  values there will be a spontaneous formation of a DS in a corresponding region in accordance with one of scenarios 1–4 above. The formation of DSs in other regions of this system with increasing  $A$  may occur as a result of the "penetration" into neighboring regions of a DS which has formed or as a result of the formation of DSs in other regions of the system by one of scenarios 1–4.

As a result of the complex picture of self-organization corresponding to scenario 5 or 6, autosolitons or DSs of complex form may arise in real systems even without the participation of fluctuations. In the 1D case which we have been discussing, DSs may form as stochastically distributed asymmetric striations.

In KN and KH systems, the self-organization scenarios discussed above may also occur as  $A$  decreases, more precisely, as  $A \rightarrow A'_c$ , as a result of the formation of a cold autosoliton near a small local inhomogeneity. Such an inhomogeneity causes perturbations of the activator  $\theta(x)$  whose decay far from an inhomogeneity as  $A \rightarrow A'_c$  is oscillatory (Fig. 14),

as in the case  $A \rightarrow A_c$  (see the discussion above). In this case, a local breakdown leading to the formation of a cold autosoliton occurs in regions in which  $\theta(x)$  reaches its minimum value  $\theta_{\min}$ . Local breakdown occurs when  $\theta_{\min}$  is smaller than  $\theta'_0$  by a certain critical amount. This breakdown consists of a local decrease in the activator in an avalanche fashion from the value  $\theta_{\min} \approx \theta'_0$  to  $\theta \approx \theta_d$  (the local breakdown is shown schematically by the arrow in Fig. 7b). A local breakdown at the center of an inhomogeneity, followed by the formation of cold striations, which come to fill the entire system (scenario 4), occurs, for example, during a decrease in the heating level of a stable hot electron-hole plasma (Subsection 8.3). Figure 17 illustrates the kinetics of this breakdown.

#### 4.2. Evolution of striations<sup>78,79</sup>

The presence of small local inhomogeneities also has a substantial effect on the evolution of striations near points  $A = A_p^{(N)}$ , of period-doubling bifurcations, or points  $A = A_d^{(N)}$ , of striation-number doublings (Fig. 12, a and b). In this case the number of striations may either decrease or increase as  $A$  varies (as a result of a dynamic restructuring), not by a factor of two (§3) but (for example) by a single striation or several striations. A restructuring of the DS as a result of the appearance or disappearance of several new striations in individual fragments of a DS is characteristic of self-organization in real systems which contain small inhomogeneities. As a rule, the DS appears in the form of aperiodically distributed striations. In certain cases, the parameters of the striations away from such a fragment may vary in such a way that the DS becomes approximately periodic.

#### 4.3. Experimental results

The self-organization scenarios discussed above are observed in experimental studies of striations in rf gas discharges,<sup>146</sup> of the bright points in electron-hole plasmas in

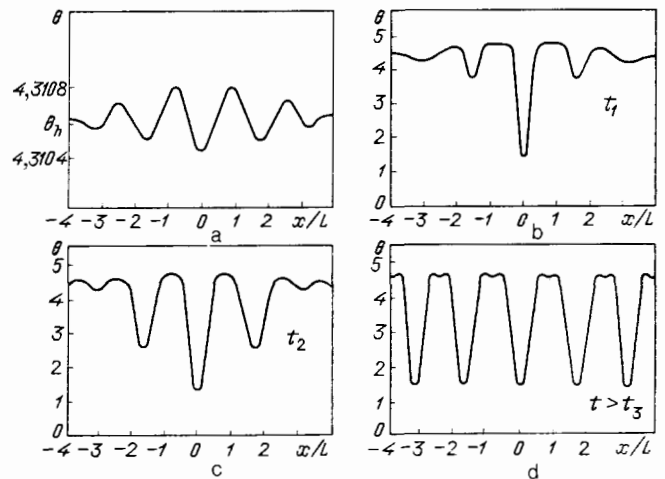


FIG. 17. Kinetics of the formation of periodic striations (d) which arise as the result of local breakdowns in the "tails" of a cold autosoliton (b, c) in the course of its formation near a small static inhomogeneity (with a relative amplitude  $a = 5 \cdot 10^{-4}$  and a width of  $0.16L$ ) at  $x = 0$ . Part a shows activator oscillations which decay with distance from the inhomogeneity  $t_1 = 1.2\tau_r$ ,  $t_2 = 1.7\tau_r$ ,  $t_3 = 3\tau_r$ . These are the results of a numerical simulation of a dense electron-hole plasma (Subsection 8.3) carried out in Ref. 100.

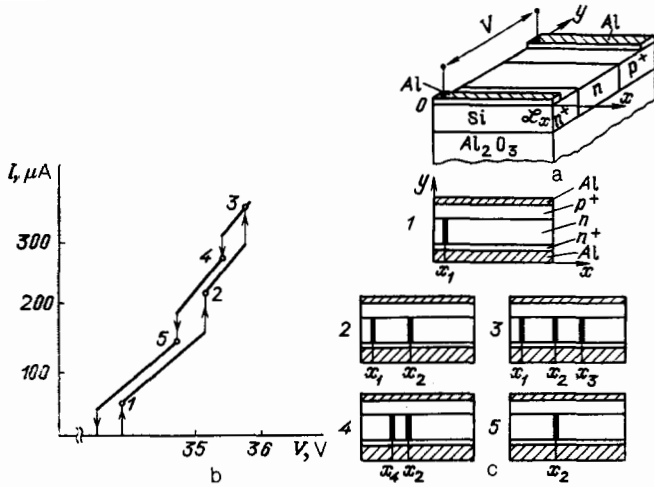


FIG. 18. Results of an experimental study of the evolution of striations (in the form of glowing current filaments) in a reverse-biased Si  $p^+ - n - n^+$  structure (a) (Ref. 35). Points 1-5 on the current-voltage characteristics  $I(V)$  of the sample (b) correlate with diagrams 1-5 of the arrangement of striations in the  $p^+ - n - n^+$  structure in the form of glowing current filaments (hatched regions) (c).  $\mathcal{L}_x = 15 \cdot 10^{-4}$  cm,  $x_1 = 10^{-4}$  cm,  $x_2 = 4 \cdot 10^{-4}$  cm,  $x_3 = 6 \cdot 10^{-4}$  cm,  $x_4 = 2.5 \cdot 10^{-4}$  cm.

GaAs (Ref. 31a), of the regions of metallic conductivity in composite superconductors,<sup>19,142</sup> of the glowing avalanche-current filaments in reverse-biased Si  $p^+ - n - n^+$  structures<sup>35</sup> (Fig. 18), and of the current filaments in structures with a gas-filled gap<sup>57,87</sup> and in electronic analogs of active systems<sup>87</sup> (Fig. 19). It can be seen from parts 1 of Figs. 18 and 19 that with increasing excitation level (with

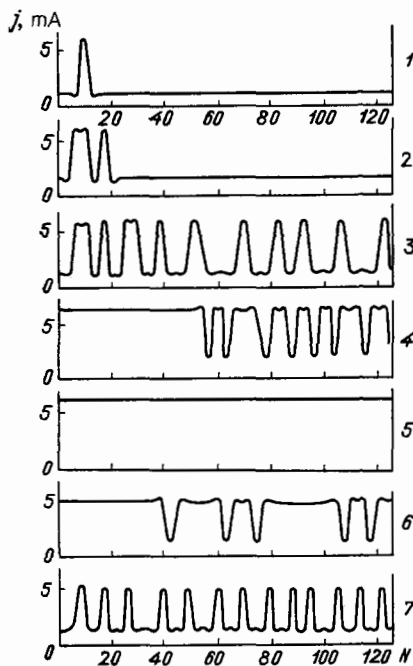


FIG. 19. Results of an experimental study of the evolution of striations (in the form of current filaments) in a discrete electronic analog of an active medium with diffusion<sup>87</sup> as the voltage across the structure is increased (distributions 1-5) or reduced (6, 7).

increasing voltage drop across the structure,  $V$ ) an autosoliton in the form of a single current filament initially forms, spontaneously, in the structure. With a further increase, the number of filaments increases (parts 2 and 3 of Figs. 18 and 19), and a DS in the form of periodically distributed current filaments forms in the system.

Experiments<sup>87</sup> also confirm other predictions of the theory of Refs. 76 and 79 (Subsection 3.1) regarding the evolution of striations. With increasing  $A \equiv V$ , the current filaments—i.e., the regions of a high activator value (“hot” striations)—expand, and the DS takes the form of narrow “cold” striations, i.e., regions of a low current (part 4 of Fig. 19). These striations then disappear abruptly and sequentially, in agreement with the results of Subsection 4.2. An approximately homogeneous state is established in the structure (part 5 of Fig. 19). If the voltage  $V$  is now reduced, filaments again begin to appear spontaneously in the structure, but now in the form of cold striations (part 6 of Fig. 19). With a further decrease in  $V$ , these striations expand, and DSs in the form of narrow hot striations again form in the structure. These formations are filaments of a high current density (part 7 of Fig. 19). They then disappear, sequentially and abruptly.

## 5. SELF-ORGANIZATION IN 2D AND 3D SYSTEMS

In K systems, self-organization is determined by three effects discussed in §2: local breakdown in certain regions of a DS, a pumping of activator between fragments of DSs, and a corrugation of the walls of striations or of more complex DSs.<sup>77,79</sup> The last of these effects may lead to a breakup of the striation walls or the surface layers DSs (regions of a rapid variation in the activator) into smaller regions or to the formation of a corrugated or cellular surface of the DS walls (Fig. 11).

### 5.1. Shape and evolution of dissipative structures in ideal homogeneous systems<sup>77,79</sup>

5.1.1. In 2D and 3D KN and KI systems, the point  $A = A_c$ , at which the homogeneous state of the system stratifies, is degenerate. By this we mean that numerous growing fluctuations, of various types, correspond to this point.<sup>3,6,12</sup> In this case there is thus the nontrivial question of just which type of DS forms in an ideally homogeneous system as its homogeneous state stratifies. The shape of the system plays an important role here.<sup>3,6,12</sup>

5.1.2. The simplest DS would consist of periodically distributed striations<sup>76,77</sup> (Figs. 6a and 7a). In 2D and 3D systems, striations of a given period  $\mathcal{L}_p$  usually exist in a narrower interval of  $A$  than in 1D systems. The reason is that as the striations either contract or expand they may become unstable with respect to a corrugation of their walls (Subsection 2.3). As a result, striations with corrugated walls may form (Fig. 11c), or the striations may break up into smaller regions (Fig. 11b). In the latter case, DSs consisting of a lattice of periodically arranged interacting autosolitons may form in the system; these autosolitons may be spots or blobs, i.e., regions of a high (or low) value of the activator. The distributions of the activator and of the inhibitor over a cross section passing through the center of these autosolitons are approximately the same as the  $\theta(x)$  and  $\eta(x)$  distributions in striations.<sup>77</sup>

The distance ( $R$ ) between interacting autosolitons is limited by the values  $R_{\min}$  and  $R_{\max}$ . As in the 1D case (§2), these limiting values can be found by analyzing the conditions for a pumping instability and for local breakdown.<sup>77-79</sup>

The evolution of a periodic 2D or 3D lattice of interacting autosolitons, like that of a periodic striations in 1D systems (§3), can be determined at a qualitative level from the behavior of  $R_{\min}$  and  $R_{\max}$  as functions of the excitation level  $A$ . All the self-organization scenarios discussed in Subsection 3.1 are realized in KN and KИ systems. In contrast with periodically distributed striations, however, the local breakdown in this case may occur not between nearest autosolitons but in the regions farthest from the centers of the autosolitons. The most closely spaced autosolitons are quicker to lose their stability with respect to the pumping of activator. In addition, as  $A$  varies, the autosolitons in KN and KИ systems may become unstable with respect to a corrugation of their walls. Let us take a look at this effect in the particular case of radially symmetric DSs.

5.1.3. In a radially symmetric system, radially symmetric DSs of large amplitude may form abruptly at  $A = A_c$ . In the 2D case, they would form as nested rings, and in the 3D case as (hollow) spheres.<sup>77</sup> The distributions  $\theta(\rho)$  and  $\eta(\rho)$  in these rings or spheres (see Fig. 11c in Ref. 25) are approximately the same as the distributions  $\theta(x)$  and  $\eta(x)$  in striations.

A fragment of a DS in the form of a ring (or sphere) with an inner radius  $\rho_{01} > L$  is stable at values of  $A$  such that its thickness  $\mathcal{L}_s = \rho_{02} - \rho_{01}$  lies in a region whose boundaries  $\mathcal{L}_{b1}$  and  $\mathcal{L}_{c1}$  can be estimated from (4.33) or (4.35) in Ref. 25. Outside this region, such a fragment of a DS would become unstable with respect to radially asymmetric fluctuations, which would lead to a corrugation of its walls (or to the formation of cellular structures at the surfaces of the DS walls) or to a breakup of the fragment into smaller spots (or blobs).

The ring (or sphere) may also undergo a restructuring as a result of the local-breakdown effects discussed in Subsection 2.1 in connection with striations.

Since the rings (or spheres) in the DS differ in radius and thus in thickness, their restructuring may occur at different values of  $A$ . In other words, the transformation of a radially symmetric DS upon a variation in  $A$  may occur as a result of an instability or local breakdown in one of its fragments. As a result, DSs of complicated form may arise even in radially symmetric systems.

5.1.4. Generalizing the results described above, one can conclude<sup>77</sup> that the inhibitor  $\eta(\mathbf{r})$  in a DS of complex shape varies smoothly in space with a length scale  $\sim L$ , and the  $\theta(\mathbf{r})$  distribution is a high-contrast pattern: In some regions (surface layers or the walls of DSs) the activator  $\theta$  varies sharply from the value  $\theta_{\min} \approx \theta_{s1}$  to the value  $\theta_{\max} \approx \theta_{s3}$  (Subsection 12.1) over a distance  $\sim l \ll L$ . In the regions of a smooth variation of  $\theta(\mathbf{r})$  and  $\eta(\mathbf{r})$ , i.e., between the walls of DSs, the values of  $\theta$  and  $\eta$  satisfy Eq. (1.29) with an accuracy to within  $\varepsilon \ll 1$ . More precisely, they correspond to local-coupling branch I or III (Fig. 2, a and c). In other words, between the walls of DSs the values are  $\theta < \theta_0$  or  $\theta > \theta_0'$  (Subsections 1.3 and 12.1). At these values of  $\theta$  we have a derivative  $q_0' > 0$ ; i.e., the state of the system is stable (Subsection 1.1). An unstable heated region with  $\theta_0 < \theta(\mathbf{r}) < \theta_0'$

and  $q_0' < 0$  is found only in thin surface layers (walls) of size  $\sim l$  in which  $\theta(\mathbf{r})$  varies sharply. The requirements on the form of stable DSs which have been formulated<sup>77</sup> are supported by the results of numerical calculations carried out in a series of studies.<sup>95</sup> As  $A$  varies, a DS undergoes a complex restructuring as a result of local breakdown in one of the fragments of the DS, as the result of a pumping instability or as the result of a corrugation of the walls of the DS.<sup>77</sup>

## 5.2. Evolution of narrow peaked DSs<sup>77,79,147</sup>

In 1D, ideally homogeneous KΛ and KV systems, narrow peak striations may form (Fig. 5). In the 2D and 3D cases, such striations, like a narrow 1D peak autosoliton (Subsection 5.2 in Ref. 25), are unstable with respect to breakup into smaller regions. The instability stems from a growth of an activator fluctuation which is localized near a striation peak and which is inhomogeneous along its surface. Also unstable with respect to breakup are radially symmetric rings (or spheres) or spots (or blobs) of any other type whose dimension in at least one direction is substantially greater than  $l$  (Ref. 77).

The only stable DSs are spots (blobs) with a size on the order of  $l$  which are separated from each other by a distance  $R$  such that  $R_{\max}(A) > R > R_{\min}$ , where  $R_{\min}$  is found from the condition for a pumping instability (Subsection 12.4), and  $R_{\max}$  is found from the condition for local breakdown (Subsection 12.2) between spots (or blobs).

The evolution of a periodic lattice of interacting narrow peak autosolitons is analogous to the evolution of periodic striations in 1D systems (Subsection 3.2). The evolution can be determined qualitatively from the behavior of  $R_{\min}$  and  $R_{\max}$  as a function of the excitation level of the system,  $A$  (but see the comment at the end of Subsection 5.1.2).

The variations in  $\theta$  and  $\eta$  in the cross section of the spots (or blobs) are approximately the same as the activator and inhibitor distributions in a narrow peak hot striation (Fig. 4a). These results explain the shape of DSs which Gierer and Meinhardt<sup>92,93</sup> have seen in a numerical study of the model of a KV system in (1.11).

## 5.3. Self-organization scenarios in real systems<sup>78,79</sup>

Small inhomogeneities in real systems raise the possibility that the self-organization in these systems may be determined by the spontaneous formation of autosolitons near certain local inhomogeneities.

5.3.1. Peak autosolitons<sup>25</sup> form as spots or blobs of a high value of the activator in KΛ and KV systems (Subsection 5.2). In this case the picture of the self-organization is a gradual filling of the system with peak autosolitons, which arise in accordance with the inhomogeneity field of the system or near an autosoliton that had been formed by one of scenarios 3–6 outlined in Subsection 4.1.2.

In 2D or 3D systems, there may be some qualitatively distinct features in scenarios 3 and 4 (in Subsection 4.1.2). The reason is that as  $A \rightarrow A_c$  a radially symmetric oscillatory activator distribution instead of oscillating tails forms at the periphery of the autosoliton (Fig. 6d). This oscillatory activator distribution is seen as a series of nested rings (or spheres). The amplitude of the activator oscillations in the rings (or spheres) decreases with distance from the center of the autosoliton. As has been noted in KΛ and KV systems,

peak DSs in a form of a ring (or sphere) are unstable.<sup>77</sup> The local breakdown in the oscillatory tail of an autosoliton (Subsection 2.1.2) therefore leads to a sharp increase in the activator in the ring nearest the center of the autosoliton in this case. During the formation of a region of a high activator value in the form of a narrow ring (or sphere), this region breaks up into small regions in the form of small-radius ( $\sim l$ ) peak autosolitons. Consequently, even a single slight inhomogeneity leads to the filling of the entire system with interacting peak autosolitons as  $A \rightarrow A_c$ .

5.3.2. In KN and KH systems, a radially symmetric autosoliton whose radius depends on the nonlinearities of the system forms near a small local inhomogeneity at values of  $A$  close to  $A_c$ . All the self-organization scenarios presented in Subsection 4.1.2 occur in this case. However, those scenarios have certain distinctive features in the 2D and 3D cases.

The reason for the distinctive features of scenarios 3 and 4 in Subsection 4.1.2 is that first one and then more rings (or spheres) can form in KN and KH systems near an autosoliton as  $A \rightarrow A_c$ , as the result of local breakdown in the radially symmetric tail of the autosoliton. In other words, a radially symmetric DS may arise spontaneously in a system which contains only a single local inhomogeneity. Such a state may prove to be unstable with respect to radially asymmetric fluctuations. Consequently, the spontaneous formation of an autosoliton near a small inhomogeneity may also lead to the appearance of DSs in the form of nested rings (or spheres) with a corrugated (or cellular) surface. Alternatively, the system may become filled with a multitude of interacting autosolitons, each with a shape approximating that of a radially symmetric autosoliton.

Distinctive features of scenarios 1 and 2 in Subsection 4.1.2 in 2D or 3D KN and KH systems with  $A_d < A_c$  are that the local breakdown at the center of the autosoliton in the form of a spot or blob may lead to a state in the form of a ring or sphere (Subsection 4.4 in Ref. 25). In turn, a local breakdown may occur in the ring (or sphere) and lead to the formation of at first two and then more nested rings (or spheres). However, another situation is also possible, because radially symmetric states may break up into smaller parts at the same (or a larger) value of  $A$ , as mentioned above. This breakup may occur either as the result of an instability in which the walls of the DS become corrugated (Subsection 2.3) or as the result of a dynamic restructuring in the course of which the wall of an expanding ring runs into one of the inhomogeneities.

#### 5.4. Self-completion of DSs during local excitation of a medium

A brief excitation of the medium in a local region can serve as an inhomogeneity which nucleates the abrupt appearance of an autosoliton.<sup>25</sup> All the self-organization scenarios presented in §4 and Subsection 5.3 are realized. In particular, after a brief local excitation of a medium during the formation of an autosoliton, periodic or more-complex DSs can arise. This DS formation process is called "self-completion."<sup>8,17,94,95</sup> Self-completion of DSs has been observed experimentally in studies of striations in gas discharges.<sup>14</sup> The formation of DSs as the result of self-completion has been examined in numerical studies of axiomatic models of active media<sup>92-95</sup> (see also Refs. 8, 10,

17, 19, 96, 100, 104, 105, 106, 109, 111, 113, and 142).

The formation of DSs as a result of self-completion is also linked with the effects discussed in §§2-5. In particular, the self-completion of a peak DS observed by Giere and Meinhardt<sup>92,93</sup> (see Fig. 10.3 in Haken's monograph<sup>5</sup>) in a numerical study of 2D model (1.11) is associated with a local breakdown at the periphery of a peak autosoliton (Subsection 5.3.1). This type of local breakdown leads to the formation of a narrow ring around the autosoliton. As a result of the instability of this ring with respect to radially asymmetric fluctuations,<sup>77</sup> it breaks up into smaller regions: small-radius peak autosolitons (Subsection 5.3.1). As a result of a chain of such processes, the entire system becomes filled with interacting peak autosolitons. A breakup of extended 2D regions of the DSs into smaller regions associated with corrugation of the walls of DSs is also observed in numerical studies of the formation of complex 2D DSs, which form in models of media with long-range coupling [see (1.31) and (1.32)].<sup>131,132</sup>

### 6. DISTINCTIVE FEATURES OF SELF-ORGANIZATION IN BISTABLE (FLIP-FLOP) SYSTEMS<sup>79</sup>

In bistable systems, the value of the inhibitor (and that of the activator) for the homogeneous state of the system is by definition a multivalued function of the excitation level  $A$  (Fig. 20). There exists an interval of values  $A'_c < A < A_c$  in which three homogeneous states ( $\eta_{h1}, \theta_{h1}; \eta_{h2}, \theta_{h2}; \eta_{h3}, \theta_{h3}$ ), are realized. Two of them are stable and correspond to respectively cold ( $\theta_{h1} < \theta_0$ ) and hot ( $\theta_{h3} > \theta'_0$ ) states of the system. This situation may be realized, for example, in semiconductors,<sup>148,149</sup> in semiconductor structures and gas-discharge structures,<sup>57,58,150</sup> in electron-hole and gaseous plasmas,<sup>48</sup> and in several chemical reactions.<sup>10,16</sup> In contrast

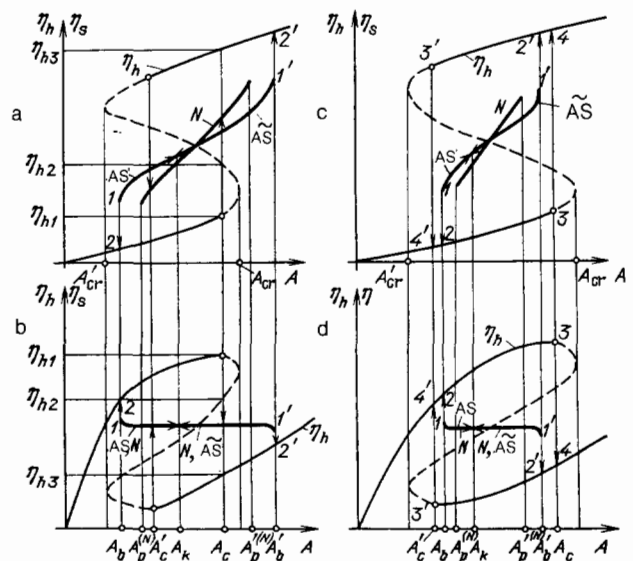


FIG. 20. Evolution of striations in bistable systems with  $A_b < A'_c, A'_b > A_c$  (a, b) and with  $A_b > A'_c, A'_b < A_c$  (c, d). a, c—Examples of bifurcation characteristics for KH systems with  $q'_A < 0, Q'_A = 0$ ; b, d—for N systems with  $q'_A = 0; Q'_A < 0$ . Curves  $N$  correspond to periodic striations, and curves  $AS$  and  $AS'$  to hot and cold autosolitons. The dashed lines correspond to unstable states.

with the monostable systems discussed in §§1–3, the relation  $A_c > A'_c$  holds in bistable systems (Fig. 20).

The theory set forth in §§1–5 also describes the shape and stability of DSs in bistable systems if condition (1.3) and  $q'_\eta Q'_\theta < 0$ , hold for them. These conditions also hold for monostable systems (Subsection 1.3). Self-organization has certain distinguishing features even in such bistable systems.

The nature of these features depends on the relationship between  $A'_c$  and  $A_b$  or that between  $A_c$  and  $A'_b$ , where  $A = A_b$  and  $A'_b$  are the points at which we have  $d\eta_s/dA = \infty$ . We recall that the values  $A_b$  and  $A'_b$  are the limiting values of the excitation level at which DSs can still be excited in a system (excited as a hot autosoliton in the case  $A = A_b$  or as a cold autosoliton  $A = A'_b$ ; Ref. 25).

Four different cases may be realized, depending on the parameter values of the system: a)  $A_b < A'_c$ ,  $A'_b > A_c$  (Fig. 20, a and b); b)  $A_b > A'_c$ ,  $A'_b < A_c$  (Fig. 20, c and d); c)  $A_b > A'_c$ ,  $A'_b > A_c$ ; d)  $A_b < A'_c$ ,  $A'_b < A_c$ .

In case a), the stratification of the homogeneous state of the system at the point  $A = A_c$  (or  $A = A'_c$ ) leads to the spontaneous formation of DSs-striations in the 1D case. The kinetics of their formation, their evolution, and the effect of small inhomogeneities are all the same as described in §§1–5 for KN and KI systems.

Since DSs are not realized in a system at  $A < A_b$  (or  $A > A'_b$ ), the stratification of the homogeneous state of the system at  $A = A_c$  (or at  $A = A'_c$ ) in case b) leads not to the formation of DSs but to an abrupt transition from an unstable homogeneous state to a stable state (jumps 3 → 4 and 3' → 4' in Fig. 20, c and d). As  $A \rightarrow A_c$  (or  $A \rightarrow A'_c$ ), small inhomogeneities lead to a local breakdown in this case and to the appearance of switching waves (Subsection 8.1 in Ref. 25), in which there is a switch from one homogeneous state to another.

In cases c) and d) the self-organization has some extremely nontrivial distinctive features. In case c), for example, as a cold system is heated (as  $A$  increases), DSs form abruptly at the point  $A = A_c$ . Their evolution is the same as described in §§3–5. As a hot system is cooled (as  $A$  is reduced), on the other hand, DSs do not form at the point  $A = A'_c$ ; instead there is an abrupt transition from a hot to a cold stable homogeneous state. In case d), on the contrary, DSs do not form at the point  $A = A_c$ , and the system goes abruptly from a cold to a hot stable homogeneous state. During the cooling of a hot system, on the other hand, DSs form spontaneously at the point  $A = A'_c$ . Their evolution is the same as described in §§3–5.

## 7. ACTIVE MEDIA WITH SPATIALLY SEPARATED REGIONS OF ACTIVATION AND INHIBITION

Among the various active distributed media with diffusion, there are, in addition to the systems of various types which are inhomogeneous over volume and which were listed in Subsection 1.1, some multilayer systems, which are homogeneous only over area or only over cross section. In such structures, the activation and inhibition processes may occur in spatially separate regions. The properties of DSs in such structures and thus the self-organization processes are again described by Eqs. (1.1) and (1.2) for the 2D and 1D cases.

Active media with spatially separate regions of activa-

tion and inhibition constitute an extremely broad class, which includes many active elements of semiconductor electronics. Such media are not only important but also convenient objects for an experimental study of the self-organization processes discussed in §§2–6. The reason is that it is possible in this case to vary independently the parameters of any of the layers making up the structure. Let us look at some examples of such media.

### 7.1. Growing filaments of avalanche current in p-n structures

The distribution of the avalanche current density  $j = env_d$  over the area of reverse-biased p-n and p-i-n structures is described by equations like (1.1) and (1.2) (Ref. 34):

$$\tau_n \frac{\partial n}{\partial t} = l^2 \Delta_{\perp} n + nv_i(n, V_i) \tau_n - n + G\tau_n, \quad (7.1)$$

$$\tau_v \frac{\partial V_i}{\partial t} = L^2 \Delta_{\perp} V_i - j\rho + V - V_i. \quad (7.2)$$

The first of these equations is the electron balance equation in (1.17), averaged over the thickness of the space-charge region of the p-n junction (Fig. 21a). In it,  $\tau_n = w/v_D$  is the transit time of the electron through the space-charge region, whose thickness is  $w$ ,  $v_D$  is the electron drift velocity,  $l = (D_e \tau_n)^{1/2}$ ,  $D_e$  is the electron diffusion coefficient, and  $G$  is the rate of thermal generation of carriers in the space-charge region. Equation (7.2) describes the distribution of the voltage drop  $V_i$  over the space-charge region of the p-n junction (Fig. 21a) associated with the spreading of the current over the quasineutral part of the structure. In this equation,  $\tau_v = C\rho$ ;  $V$  is the total voltage drop across the structure;  $C$  is the specific capacitance of the p-n junction;  $\rho = W/\sigma$ ;  $\sigma$  and  $W$  are the conductivity and thickness of the n-type (or p-type) region of the structure, which has a large value of  $\rho$ ; and  $L \approx W$ . In these structures, the inhibition process is associated with current spreading in the quasineutral p-type or n-type regions, which are distributed resistive layers (Fig. 21a), while the activation process occurs in the space-charge region of the p-n or p-i-n structure and is associated with the increasing dependence of  $v_i$  on  $n$  (Ref. 34).

In this case, the average electron density in the space-charge layer ( $\theta \equiv n$ ) plays the role of activator, while the voltage drop across the space-charge region ( $\eta \equiv V_i$ ) plays the role of inhibitor. The positive feedback through the activator is associated with the self-breeding of electrons,<sup>14)</sup> which is determined by the increasing dependence of the rate of impact ionization,  $v_i$ , averaged over the space-charge region, on the value of  $n$ . The damping role of the inhibitor stems from the circumstance that with  $V = \text{const}$  a uniform increase in  $n$ , i.e., in the current density  $j$ , is accompanied by a corresponding decrease in the value of  $V_i$  because of an increase in the voltage drop across the quasineutral regions of the structure. This effect leads in turn to a sharp decrease in the carrier density in the space-charge region, because of the strongly increasing dependence of the rate of carrier ionization,  $v_i$  on  $V_i$ . As a result, the current-voltage characteristic of this structure is single-valued (curve 3 in Fig. 21b). Nevertheless, a stratification of the uniform distribution of the avalanche current density occurs; i.e., the Turing stratifi-

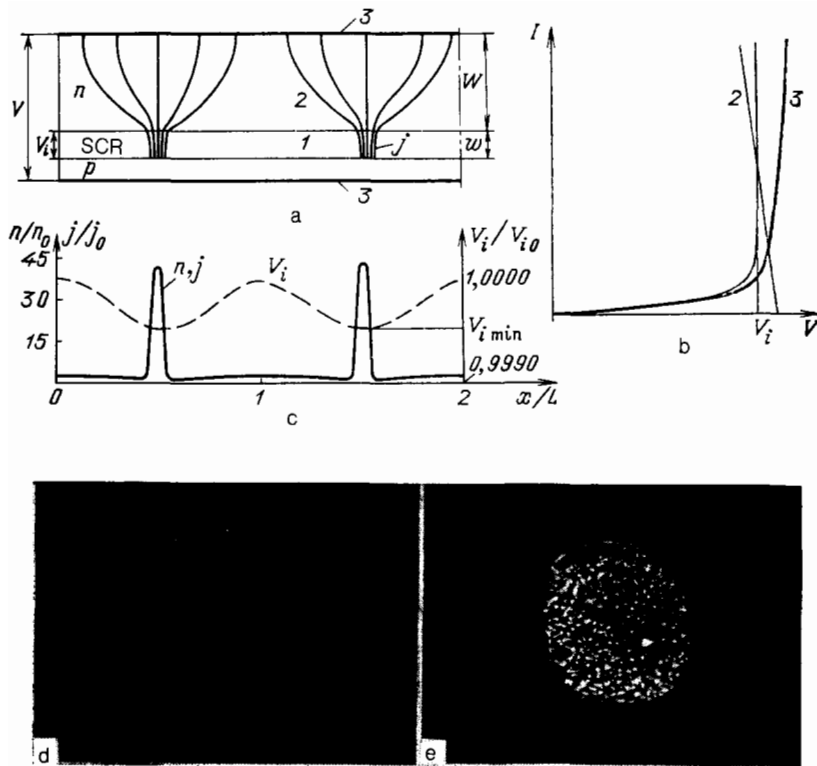


FIG. 21. Diagram used in explaining the formation of bright points during the stratification of a uniform avalanche breakdown of a p-n junction. a: Structure of the p-n junction. Thin solid lines—Schematic current lines within two periods of the peak dissipative structure; 1—active layer, or space-charge region (SCR), of the p-n junction; 2—resistive layer; 3—metal contacts. b: Current-voltage characteristic of the active layer,  $I(V_i)$  (curve between 2 and 3), load line determined by the conductance of the resistive layer (2), and resultant current-voltage characteristic of the overall structure (3) c: Results of numerical calculations<sup>113</sup> of the  $n, j$ , and  $V_i$  distributions. d, e: Photographs of the emission in the plane of the p-n junction<sup>34</sup> at currents respectively below and above the critical value.

cation condition, (1.10), holds.<sup>34</sup>

The reason for the stratification of the avalanche current density is that in real structures the current spreading length  $L$  is many orders of magnitude greater than  $l$ , the electron diffusion length during the transit of the electrons through the space-charge region. In other words, we have  $\varepsilon = l/L \ll 1$ . As a result, the stratification condition holds even if the dependence of  $v_i$  on  $n$  is weak. As a result of this stratification (whose physics was discussed in Refs. 34 and 113), regions of a high electron density and a high avalanche current form in the structures. This effect is a clear example of the formation of peak DSs in real physical systems (Fig. 21). The appearance of peak DSs in this case follows directly from the circumstance that the local-coupling curve (Subsection 1.3), i.e., the dependence  $V_i(n)$ , which is a consequence of Eq. (7.1) for the steady-state homogeneous case, is  $\Lambda$ -shaped. Experimentally, the formation of peak DSs is observed as the replacement of a glow of the p-n junction which is uniform over the area (Fig. 21d) by a high-contrast glow pattern in the form of bright points<sup>34</sup> (Fig. 21e) or filaments<sup>35</sup> (Fig. 18) against a dark background. The picture of the spontaneous appearance and evolution of such points on filaments agrees completely with that presented in §§4 and 5.

## 7.2. Multifilament states in a semiconductor film with a thermal instability

We consider a sandwich structure consisting of a thin semiconductor film (of thickness  $w$ ) on a considerably thicker resistive substrate. Metal electrodes are applied to them (Fig. 22a). An electric field  $E = V_i w^{-1}$  heats the electrons in the film. The distribution of the effective temperature of these electrons,  $T$ , is described by<sup>21,23</sup> Eq. (1.18), in which  $W_j = \sigma_e V_i^2 w^{-2}$ ,  $j_e = \kappa_e \nabla T$ , and  $\sigma_e$  and  $\kappa_e$  are the electrical and thermal conductivities of the electrons. In this case the electron temperature [more precisely, the quantity  $\theta = \int \kappa_e(T) dT$ ] serves as activator. It is easy to see that the second of conditions (1.3) is the same as the condition for the thermal instability of an electron gas.<sup>21</sup> The role of inhibitor is being played here by the voltage drop across the semiconductor film,  $V_i$ ; the distribution of this voltage drop over the film area is described by Eq. (7.2), in which  $j = \sigma_e V_i w^{-1}$ ;  $\rho = W/\sigma$ ;  $W$ ,  $\sigma$ , and  $\tau_V$  are respectively the thickness, conductivity, and Maxwellian dielectric relaxation time of the resistive layer;  $V$  is the voltage drop across the overall structure; and  $L \approx W$ .

The thermal instability in a semiconductor is usually studied with a lumped load resistance in the external circuit, in which case only an isolated current filament, whose prop-

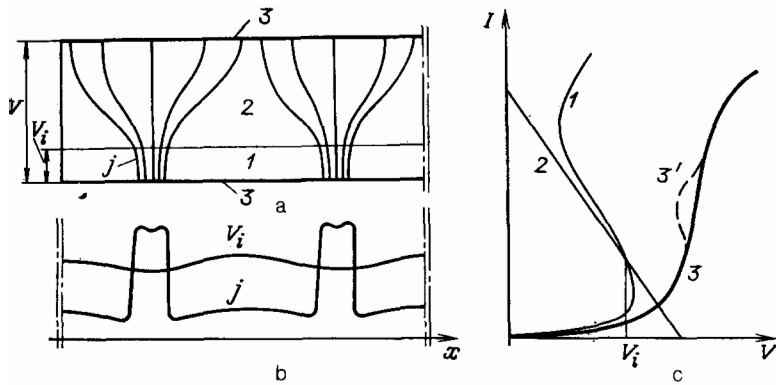


FIG. 22. Diagram used in explaining systems with spatially separate activation and inhibition regions. a: Diagram of the sandwich structure. 1—Active layer of thickness  $w$ ; 2—resistive layer (inhibition region) of thickness  $W$ ; 3—metal contacts. b: Distributions of the current density  $j$  and of the voltage drop across the active layer,  $V_i$ . c: S-shaped current-voltage characteristic of the active layer (curve 1), load line of the resistive layer (2), and possible resultant current-voltage characteristics of the overall structure (3 and 3').

erties depend on the size of the semiconductor plate, is stable.<sup>21,23,24</sup> In the sandwich structure which we are discussing here (Fig. 22a), in contrast, the current spreading in the resistive layer, i.e., the redistribution of the voltages among layers, results in the formation of stable multifilament states in which the distribution of the current density  $j = \sigma_e E$  is qualitatively the same as the distribution of the electron temperature  $T$  (Fig. 22b). The properties of the filaments which form do not depend on the dimensions of this system; they are determined by the parameter values of the layers, primarily the thickness of the resistive layer  $W$ , and the electron energy relaxation length in the film,  $l_e$ . The quantity  $W \approx L$  determines the distribution of the voltage  $V_i$ , i.e., of the inhibitor ( $\eta \equiv V_i$ ), according to (7.2), while  $l_e$  determines the distribution of  $T$ , i.e., of the activator.

In this case we thus have  $l \equiv l_e$ ,  $L \approx W$ ,  $\tau_\theta \equiv \tau_e$ ,  $\tau_\eta \equiv \tau_V$ , and  $A \equiv V$ . In semiconductors the conditions  $\epsilon = l/L \ll 1$  and  $\tau_e > \tau_V$  usually hold; i.e., this sandwich structure is a K system (Subsection 1.3) or, more precisely, a KN system. The latter conclusion follows from the circumstance that the local-coupling curve—in this case the dependence  $V_i(T)$ —is N-shaped under the conditions of the thermal instability,<sup>21</sup> as is easily verified. The shape of the DS and their evolution are therefore the same as those discussed in §§2–5 and 12 for KN systems.

Multifilament states also arise in a sandwich structure (Fig. 22a) in which the thin semiconductor film is heated. The distribution of the temperature  $T$  over the film area is described by the heat-conduction equation averaged over the film thickness  $w$ .

$$\tau_T \frac{\partial T}{\partial t} = l_T^2 \nabla_{\perp}^2 \left[ \frac{\kappa_l(T)}{\kappa_l(T_i)} \nabla_{\perp} T \right] + [W_j l_T^2 - (T - T_i) \kappa_l(T)] \kappa_l^{-1}(T_i), \quad (7.3)$$

where  $l_T$  and  $\tau_T = c \rho l_T^2 / \kappa_l(T_i)$  are a length scale and a time scale of the variations in  $T$ ;  $c$ ,  $\rho$ , and  $\kappa_l$  are respectively the specific heat, density, and thermal conductivity of the material;  $T_i$  is the temperature of the reservoir; and  $W_j = \sigma_e(T) V_i^2 w^{-2}$ . In this case, the lattice temperature is high in the regions in which the current density is high. These “hot spots” form in a film because the dependence of the film conductivity  $\sigma_e$  on the lattice temperature  $T$  is an ascending dependence, usually of a thermal-activation nature.

### 7.3. Hot spots in transistor structures

A structure of this sort (Fig. 23a) is a realistic model of an active distributed medium, which has been used as an example to analyze the current stratification and the shape of the DS which form in systems with a single-valued current-voltage characteristic.<sup>52,151</sup> In this structure (Fig. 23a), the temperature  $T$  of the structure serves as activator ( $\theta \equiv T$ ), the voltage drop across the forward-biased (emitter) p-n junction,  $V_E$ , serves as inhibitor ( $\eta \equiv V_E$ ), and the overall voltage drop across the structure,  $V$ , serves as the control parameter  $A$  ( $A \equiv V$ ). The  $T$  distribution in the structure is described by Eq. (7.3), in which the Joule heating power is

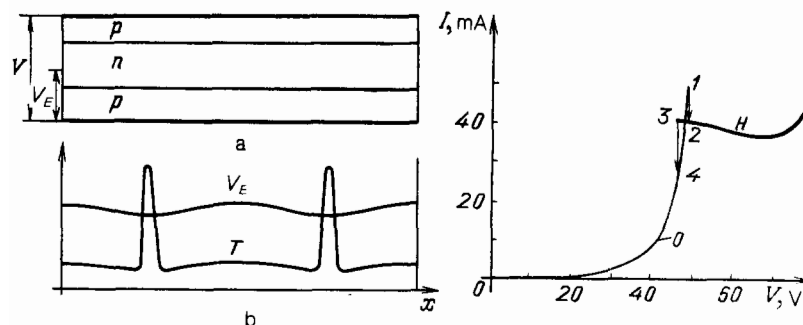


FIG. 23. “Hot spots” in a p-n-p transistor structure. a—Schematic diagram of the structure; b—distributions of the temperature and the voltage drop across the injection (emitter) p-n junction; c—experimental current-voltage characteristic,<sup>151</sup> on which region 0 corresponds to a uniform  $T$  distribution, while region H corresponds to a state with a hot spot. Jumps 1→2 and 3→4 in part c correspond to the formation and disappearance, respectively, of a hot spot.

$$W_j = jV_T^{-2}W = j_0 \exp\{(eV_E - E_g)T^{-1}\} V_T^{-2}W, \quad (7.4)$$

$E_g$  is the width of the band gap of the semiconductor,  $j_0 \exp(-E_g/T)$  is the saturation current of the reverse-biased emitter p-n junction, and  $W$  is the thickness of the crystal of the transistor structure. The distribution of  $V_E$  over the area of the structure is associated with the current spreading over the base of the structure (the n-type region in Fig. 23a). It is described by an equation like (7.2) (Ref. 52):

$$\tau_V \frac{\partial V_E}{\partial t} = L^2 \Delta_{\perp} V_E + V - V_E - j\rho_k(1 - \alpha_I M),$$

where  $\tau_V = C\rho_C$ ,  $L = (\sigma w\rho_C)^{1/2}$ ,  $\rho_C$  is the leakage resistivity of the collector p-n junction,  $w$  and  $\sigma$  are the thickness and conductivity of the base of the structure,  $C$  is the overall specific capacitance of the p-n junctions, and  $\alpha_I$  and  $M$  are the current transfer ratio and carrier breeding factor. As a rule, the quantity  $\rho_C$  is very large, while  $C$  is small, and the conditions  $L \gg l_T$  and  $\tau_V < \tau_T$  hold. These conditions are characteristic of K systems. According to (7.3) and (7.4), the local-coupling curve—in this case, the curve of  $V_E(T)$ —is  $\Lambda$ -shaped. The shape and evolution of the hot spots in transistor structures are therefore the same as those discussed in §§2–5 for KA systems, in which narrow peaked DSs form (Fig. 23b). Hot spots of this sort are also observed experimentally<sup>15)</sup> in transistors.<sup>15)</sup>

#### 7.4. Structures with "latent" S- or N-shaped current-voltage characteristic

7.4.1. It follows from the equations which describe the activation process in the structures discussed in Subsections 7.1–7.3 that the activation region has an S-shaped current-voltage characteristic. The resistive layer, i.e., the inhibition region (layer 2 in Fig. 22a), has a positive differential resistance, which may be greater in absolute value than the negative differential resistance of the activation region. As a result, the current-voltage characteristic of the overall structure corresponding to a uniform current distribution is single-valued.<sup>16)</sup> Sandwich structures of this sort are essentially media with a "latent" S-shaped current-voltage characteristic.<sup>52</sup> Among such media are numerous semiconductor structures,<sup>54,55,57</sup> gas-discharge structures,<sup>36,37</sup> and distributed electronic models of active media with diffusion<sup>17)</sup> (Refs. 57, 86, and 87).

The distribution of the inhibitor  $\eta \equiv V_i$  in these sandwich structures (Fig. 22a) is described by Eq. (7.2). If the

results of §§2–5 are to be used directly to analyze DSs and self-organization phenomena, it is necessary to express the current density in the layer with the S-shaped current-voltage characteristic unambiguously in terms of a parameter (playing the role of activator) whose distribution is described by an equation like (1.1), as in Subsections 7.1–7.3 (Refs. 34 and 52) and in Refs. 54, 55, and 57. This procedure has been carried out for complex semiconductor devices (injection diodes, avalanche transistors, and dynistors) in several papers, which are reviewed in Ref. 22.

7.4.2. One-dimensional DSs of various types may also arise in sandwich structures in which the resistive layer (region 2 in Fig. 24a) is connected in parallel with an active layer (region 1) with an N-shaped current-voltage characteristic (Fig. 24c). Striations can arise in such structures, as domains of a high electric field (Fig. 24b). The general results of §§2–6 can be used directly to describe the shape of such domains and self-organization effects. To do this, we need to express the electric field ( $E_N$ ) in the active layer with the N-shaped current-voltage characteristic in terms of some parameter  $\theta$  (which plays the role of activator), whose distributions are described by equations like (1.1). The role of inhibitor in such structures is played by the total current in the active layer,  $I_N$  ( $\eta \equiv I_N$ ). The equation describing the distribution  $I_N(x)$  can be found from the law of induction of the electric field for a closed circuit:

$$\oint E dl = \mathcal{E}_i,$$

where  $\mathcal{E}_i$  is the induced emf. Applying this equation to a small element of a thin sandwich structure, and taking its average over the thickness of the layers, we find

$$\tau_I \frac{\partial I_N}{\partial t} = L^2 \frac{\partial^2 I_N}{\partial x^2} - I_N + I - E_N(\theta) W \sigma b, \quad (7.5)$$

where  $\tau_I = W \sigma b \mathcal{L}_I$ ,  $L \approx W$ ,  $\mathcal{L}_I$  is the overall inductance per unit length of the layers, and  $\sigma$  and  $W$  are the conductivity and thickness of the resistive layer. The time and length scales of the variation of the inhibitor  $\eta \equiv I_N$  in this case are therefore  $\tau_\eta \equiv \tau_I$  and  $L \approx W$ , and the control parameter is  $A \equiv I$ .

Among structures with a latent N-shaped current-voltage characteristic are (for example) composite superconductors in which the active layer is a superconducting film, while the resistive layer is a film of a normal metal.<sup>19</sup> In such

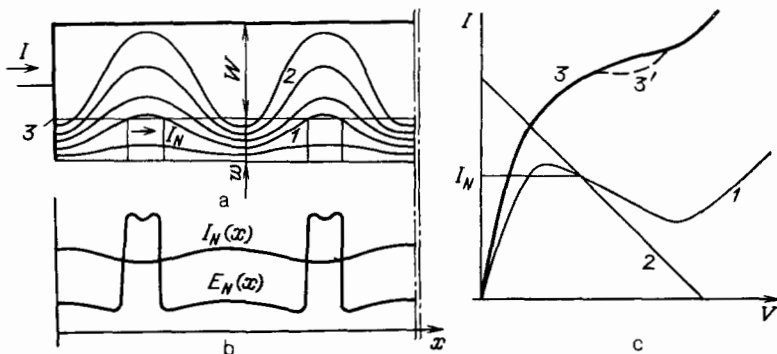


FIG. 24. Diagram used in explaining structures with a "latent" N-shaped current-voltage characteristic. a: Schematic diagram of the sandwich structure. 1—Active layer with N-shaped current-voltage characteristic; 2—resistive layer; 3—metal contact; solid lines—schematic current lines. b: Distributions of the electric field and the current in the active layer. c: N-shaped current-voltage characteristic of the active layer (curve 1), load line of the resistive layer (2), and possible types of resultant current-voltage characteristic of the structure (3 and 3').



sandwich structures, the film temperature plays the role of activator ( $\theta \equiv T$ ); its distribution along the structure is described by an equation like (7.3). The results of the experimental and theoretical studies of domains in composite superconductors which were carried out in Refs. 19 and 142 agree entirely with the general results of the theory of DSs as set forth in §§2–4 and 6 for KN systems.

7.4.3. A change in the number of current filaments (or of field domains) in these structures upon a variation in the parameters of the external circuit is accompanied by jumps in the current  $I$  (or in the voltage  $V$ ) on the current-voltage characteristic of the structure. These jumps are observed experimentally in studies of multifilament and multidomain states in various structures.<sup>19,31–38,57,86,87,142</sup> In ideally uniform monostable systems, the evolution of the current filaments (and of the field domains) is qualitatively independent of the magnitude of the active load resistance  $R_L$  (Ref. 18). There can be only an expansion of the range in which an autosoliton exists as an individual filament (or domain) which forms as a result of the evolution of multifilament (or multidomain) states (§§3 and 4). In a sample of size  $\mathcal{L} < L$  a current filament is stable if<sup>151,160</sup>

$$D(0)(1 + R_L Z^{-1}(0)) < 0, \quad (7.6)$$

and a field domain is stable if<sup>47,160</sup>

$$D(0)(R_L + Z(0)) < 0, \quad (7.7)$$

where  $Z(i\omega)$  is the impedance of the structure with the latent S or N-shaped current-voltage characteristic, respectively, and  $D(i\omega)$  is given by expression (4.9) in an earlier review.<sup>25</sup>

## 8. ACTIVE SYSTEMS WITH A "CROSS" DIFFUSION

In this section of the paper we discuss systems in which not only the stratification mechanism (Subsection 1.2) but also the properties of the DSs are determined by diffusion processes or, more precisely, by the sign of the cross diffusion coefficients  $D_{ij}$  with  $i \neq j$  in Eqs. (1.6) and by their behavior as functions of the quantities  $X_i$ . Among such systems are nonequilibrium gaseous and electron-hole plasmas, as

was mentioned back in Subsection 1.2. Thermodiffusion DSs, whose existence is determined by thermodiffusion, i.e., by the strong effect of the temperature distribution on the spatial distribution of the densities of electrons and holes (or ions), can form in these systems.<sup>75,76</sup>

### 8.1. Thermodiffusion DSs in electron-hole plasmas<sup>75,76</sup>

We consider an electron-hole plasma which is produced in a semiconductor film by light with a photon energy  $\hbar\omega$  greater than the band gap of the semiconductor,  $E_g$ , by an amount  $2\Delta = \hbar\omega - E_g$  (Fig. 25a). The absorption of such photons is accompanied by the formation of hot electrons and holes, which may be heated as a single system to an effective temperature  $T$  as a result of electron-electron collisions. The distributions of  $T$ , the electron density, and the hole density in a symmetric electron-hole plasma are described by Eqs. (1.26)–(1.28) with  $W_j = \Delta G$ . As was pointed out in Subsection 1.2, the instability which results in the stratification of the electron-hole plasma is aperiodic; i.e., its threshold is determined by the condition  $\gamma = 0$ . Another conclusion which essentially follows from this condition is that the left-hand sides of Eqs. (1.26) and (1.27), i.e., the nature of the time derivatives, usually do not affect the stability condition for DSs. Consequently, the conditions for the stability of thermodiffusion DSs (with  $\tau_c = \text{const}$ ) are usually the same as those studied in §12 for K systems, for which we also have  $\text{Im}\gamma = 0$  at the stability threshold.

It follows from (1.28) that the local-coupling curve is V-shaped or  $\bar{\text{H}}$ -shaped for  $\alpha + s > 0$ . This electron-hole plasma thus falls in the category of KV or  $\bar{\text{KH}}$  systems, for which the form of the DSs [the distributions  $\theta(\mathbf{r})$  and  $\eta(\mathbf{r})$ ] and their evolution were analyzed in §§2–5. The distribution of the density  $n(\mathbf{r})$  in thermodiffusion DSs can be reconstructed easily (Fig. 25, b and c) through the use of the relationship between  $\eta$ , on the one hand, and  $n$  and  $T$ , on the other, which follows from (1.25). Since  $D(T)$  is an increasing function of  $T$  in this case, it follows from (1.25) that the temperature and carrier density in thermodiffusion DSs vary out of phase. In other words, regions of a high temperature and of a low carrier density form in the electron-hole plasma (Fig. 25, b and c). We wish to stress that, despite the

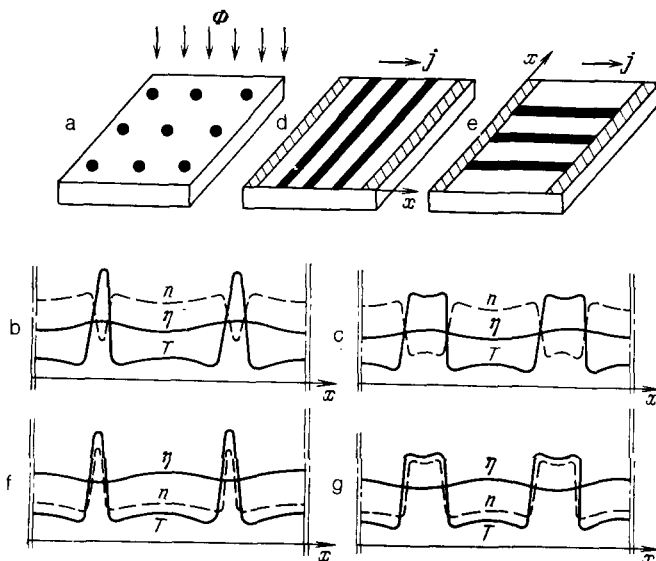


FIG. 25. Dissipative structures in systems with a "cross" diffusion. a, d, e—Schematic diagrams of local regions of (a) a high temperature of the electron-hole plasma, (d) transverse striations, and (e) longitudinal striations; b, c, f, g—distributions of the temperature  $T$  and the carrier density  $n$  in the striations realized in systems with (b, c) a positive and (f, g) a negative thermodiffusion.<sup>75,76</sup>

large diffusion length, the carrier density (like the temperature) varies sharply in regions of size  $l \ll L$ , i.e., the walls of the DSs (Fig. 25, b and c). The reason is that at the walls of the DSs the carrier diffusion flux  $\mathbf{j}_D = -D\nabla n$  is balanced by the thermodiffusion flux, which corresponds to the last term in (1.19).

### 8.2. Multidomain states in semiconductors with a single-valued current-voltage characteristic<sup>49</sup>

Let us consider the heating of intrinsic or photogenerated carriers in a static or rf field. Again in this case, the distributions of  $n$  and  $T$  are described by Eqs. (1.17) and (1.18), with the one difference that  $W_j = jE$  in (1.18) is the Joule power supplied to the electron-hole plasma. It follows from these equations that in the absence of a thermal instability, i.e., under the condition  $\alpha + s < 1$ , the current-voltage characteristic of the sample is single-valued. The homogeneous state of the plasma becomes unstable with respect to fluctuations with a wave vector  $\mathbf{k} \parallel \mathbf{E}$  (Refs. 49–51, 161, 162). The reason is that the presence of a field gives rise to a special direction. As a result of this instability, striations, i.e., electric field domains, form abruptly in the plasma, in a direction transverse with respect to the current lines<sup>49</sup> (Fig. 25d).

In such thermodiffusion striations, as in the formations discussed in Subsection 8.1,  $n$  and  $T$  vary out of phase (Fig. 25, b and c). The current density is a constant,  $j(x) = \text{const}$ , so the field  $E$  and the power  $W_j = j^2/\sigma = j^2(2e\mu n)^{-1}$  reach maxima in regions with a low carrier density (Fig. 25, b and c). As a result, the striation formation condition  $\alpha + s > -1$  is less stringent than in the case of an electron-hole plasma which is heated as a result of photogeneration (Subsection 8.1).

Under the condition  $\alpha + s > -1$ , the local-coupling curve for the variables in (1.25) which follows from the equation  $q = P - W_j = 0$  may be I/2- or V-shaped, depending on the value of  $T_i$  and the parameters of the electron-hole plasma.<sup>51</sup> This plasma thus falls in the category of a KI/2 or KV system, so the evolution of the multidomain states which occurs in it is the same as described in §§2–4.

### 8.3. Multifilament states in a “dense” electron-hole plasma<sup>48,51,100,104,109</sup>

In a dense electron-hole plasma, the carrier mobility  $\mu$  is determined by collisions of electrons and holes which are moving opposite to each other in the electric field. In this case we have  $\mu \propto T^{3/2}n^{-1}$  (Ref. 163); i.e., the conductivity  $\sigma = e\mu n$  of the electron-hole plasma is independent of its density. At low temperatures the carrier energy is usually dissipated on acoustic and optical phonons. In this case we have  $s < -1/2$ , and the current-voltage characteristic of the dense plasma is single-valued. Nevertheless, the homogeneous state of the plasma stratifies with respect to fluctuations with  $\mathbf{k} \perp \mathbf{E}$ , and multifilament states in the form of layers or cylinders directed parallel to the current lines form abruptly in the plasma<sup>48</sup> (Fig. 25e). The changes in the density and the temperature in these current filaments are out of phase (Fig. 25, b and c). They are described by equations like (1.17) and (1.18), with  $\mathbf{j}_c = -\mu_r e^{-1} \nabla_{\perp} P_c$  in the latter, where  $P_c = nT$  is the pressure of the electron-hole plasma, and  $\mu_r$  is the carrier mobility, which is determined by the

scattering of the carriers by defects and phonons.

The reason for the appearance of multifilament states parallel to the current lines in a dense electron-hole plasma is that in them we have  $E(\mathbf{r}_{\perp}) = \text{const}$ , and the Joule power is  $W_j = \sigma E^2 \propto T^{3/2}$ . As a result, the local-coupling curve corresponding to the equation  $q = P - W_j = 0$  is I-shaped or V-shaped<sup>104</sup> if we note that in this case we have  $\theta = T/T_i$  and  $\eta = P_c/T_i n_n$ . Consequently, the evolution of the multifilament states is the same as described for KA and KV systems in §§2–4.

A distinctive feature here is that a change in the number of filaments in the sample leads to numerous regions of hysteresis on the current-voltage characteristic. A current-voltage characteristic of this sort is observed during the stratification of electron-hole plasmas in thin GaAs films<sup>31</sup> and in GaAs transistor structures.<sup>164</sup> The evolution of the multifilament states upon a change in the voltage across the sample has been studied experimentally<sup>31</sup> and numerically.<sup>100,104,109</sup> The results agree with the results of the self-organization theory presented in §§2–5.

### 8.4. “Hot spots” in a semiconductor film

The DSs which form in systems with a “positive” thermodiffusion, in which the particle flux is directed out of a hot region into a cold one, were discussed in Subsections 8.1–8.3. In several systems, an increasing particle scattering cross section with increasing particle velocity may cause the thermodiffusion flux of particles to be directed out of a cold region into a hot one. A uniform particle distribution in such a system with a “negative” thermodiffusion may stratify, as was first pointed out in Refs. 59 and 60 for the particular cases of chemical reactions and a mixture of neutral gases. As a result of this stratification, DSs consisting of regions of a high temperature and a high particle density form in systems with a negative thermodiffusion<sup>75,51</sup> (Fig. 25, f and g).

Thermodiffusion DSs of this sort may arise spontaneously in a thin semiconductor film in which an electron-hole plasma is photoproduced in a uniform fashion.<sup>75</sup> At room temperature and at high carrier densities, the temperature of the plasma is essentially the same as the film temperature  $T$ . The distributions of  $T$  and of the carrier density  $n$  in the film are described by Eq. (7.3) and by the balance equation for the number of carriers, (1.17), averaged over the film thickness. It follows<sup>51,75</sup> that the bipolar diffusion length  $L$  characterizes the length scale of the variation in  $\eta = n\varphi^{-1}(T)$ , where  $\varphi(T)$  is an increasing function of  $T$ . As in Subsections 8.1–8.3, the role of activator is played in this case by the temperature ( $\theta \equiv T$ ), while the role of inhibitor is played by  $\eta$ . The equations for the form of the DSs in terms of the variables  $\theta$  and  $\eta$  are also analogous to (1.1) and (1.2). The properties of the DSs at  $L \gg l_T$  correspond to those discussed in §§1–6 for KN or KA systems.<sup>51</sup>

The reason for the existence of local regions of a high temperature (Fig. 25, f and g) is that the carrier density increases in these regions as a result of the negative thermodiffusion. On the other hand, the absorption of the electromagnetic radiation and the recombination of carriers occur more rapidly in a region of carrier buildup. The effect is to sustain the high temperature in local regions of the film;<sup>75</sup> this high temperature may be above the melting point of the

semiconductor and may cause a spotty damage to the film. This effect<sup>165</sup> is apparently also pertinent to a spotty melting of the surface of a semiconductor which has been observed experimentally<sup>166-168</sup> during uniform pulsed exposure to light at a power well below that sufficient to melt a surface layer of the semiconductor.

### 8.5. Dissipative structures in chemical reactions with a "cross" diffusion

Thermodiffusion DSs, including autosolitons, may also arise in nonisothermal chemical reactions, as a result of the dissipation or absorption of heat.

In principle, the stratification of the uniform distribution of chemical substances can also occur when a chemical reaction proceeds under isothermal conditions. Such a stratification may be associated with an entrainment of one chemical substance by the other.<sup>116</sup> In this case the fluxes of chemical substances can be described by<sup>8b,17,116</sup>

$$j_1 = -D_{11}\nabla n_1 - D_{12}\nabla n_2, \quad j_2 = -D_{21}\nabla n_1 - D_{22}\nabla n_2, \quad (8.1)$$

where  $n_1$  and  $n_2$  are the densities of the chemical substances, and the diffusion coefficients  $D_{ij}$  depend on  $n_1$  and  $n_2$ . In this case the matrix of coefficients  $D_{ij}$  in Eqs. (1.16) contains off-diagonal terms, which describe a nonlinear "cross" diffusion of the two chemical substances. It follows from linear stratification theory<sup>116</sup> that the densities of the substances,  $n_1$  and  $n_2$ , may vary either in phase or out of phase spatially, depending on the signs of the cross-diffusion coefficients  $D_{12}$  and  $D_{21}$ .

The form and properties of the DSs in isothermal chemical reactions with a cross diffusion can be determined by exploiting their analogy with thermodiffusion DSs (Subsections 8.1-8.4). Specifically, if we formally replace  $n$  by  $n_1$ , and  $T$  by  $n_2$ , in Eqs. (1.19) and (1.20), these equations assume the form of expressions (8.1). It follows from this analogy that, in systems in which  $n_1$  and  $n_2$  vary out of phase, DSs with the form shown in Fig. 25b or Fig. 25c may arise, depending on the nature of the nonlinearities in this system, if  $n$  is replaced by  $n_1$ , and  $T$  by  $n_2$ , in these figures. In systems in which  $n_1$  and  $n_2$  vary in phase, the DSs shown in Fig. 25,  $f$  or  $g$ , are realized, where  $n \equiv n_1$  and  $T \equiv n_2$ .

## 9. TURBULENCE IN ACTIVE DISTRIBUTED MEDIA

A turbulence, i.e., nonuniform oscillations which are random in time and space, is observed in many systems with convective flows, in particular, various hydrodynamic flows (see, for example, Refs. 1 and 74). A turbulence is also observed in systems without convective flows.<sup>7,8,10</sup> A turbulence can arise even in K systems, in which there are no convective flows and in which there furthermore can be no uniform self-oscillations, pulsating DSs, or autowaves (Table II). Let us discuss the mechanisms for the formation of such a turbulence.

### 9.1. Conditions for the occurrence of, and scenarios for the development of, turbulence<sup>80-83</sup>

The minimum distance ( $\mathcal{L}_{\min}$ ) and the maximum distance ( $\mathcal{L}_{\max}$ ) between striations (spots or blobs) are determined by effects which are completely different in nature (§2). Periodically arranged striations (or spots or blobs) of

period  $\mathcal{L}_p < \mathcal{L}_{\min}$  are unstable because of a pumping effect (Subsection 2.2). Because of the local-breakdown effect (Subsection 2.1), a state in which the distance between striations is  $\mathcal{L}_p > \mathcal{L}_{\max}$  does not occur. In KA and KV systems, the quantities  $\mathcal{L}_{\min}$  and  $\mathcal{L}_{\max}$  may be comparable in magnitude,<sup>81</sup> and the following condition may hold in certain of these systems:<sup>80,81</sup>

$$\mathcal{L}_{\max}(A) < \mathcal{L}_{\min}(A), \quad (9.1)$$

Under this condition, all static DSs are unstable. Since we have  $\alpha = \tau_\theta/\tau_\eta > 1$  (Subsection 1.3) in K systems, stationary states in the form of uniform oscillations or pulsating DSs cannot arise<sup>80</sup> (§11). Furthermore, autowaves cannot arise.<sup>25</sup> Under the condition  $A > A_c$ , a homogeneous state of the system is also unstable (Subsections 1.1 and 1.2). Consequently, when condition (9.1) holds a turbulence may arise spontaneously in an ideally homogeneous system at values  $A > A_c$ . The turbulence here is a time-varying state in the form of autosolitons (striations, spots, or blobs) which appear and disappear at random.

The mechanism for the onset of turbulence in this case can be summarized as follows: Neighboring striations (or spots or blobs)—interacting autosolitons—separated by a distance less than  $\mathcal{L}_{\min}$  are unstable by virtue of the pumping effect (Subsection 2.2). As a result of this instability, the number of autosolitons in the system should decrease, and the distance between them should increase. Under condition (9.1), such autosolitons should break up as a result of the local breakdown effect even as they are forming (Subsection 2.1). Since the breakup and instability processes of two neighboring autosolitons can occur in an uncorrelated fashion in well-separated spatial regions, the effect is the onset of turbulence.

Another mechanism for the onset of turbulence can be summarized as follows: At the center of peak DSs which arise spontaneously in KA and KV systems (Subsection 1.5), the condition<sup>82,83</sup>

$$\left. \frac{\partial Q}{\partial \eta} \right|_{\theta=\theta_{\max}, \eta=\eta_{sh}} < 0, \quad (9.2)$$

may hold, where  $\theta_{\max}$  and  $\eta_{sh}$  are the values of the activator and the inhibitor at the center of the peak of the DS. Inequality (9.2) is the opposite of the condition  $Q'_\eta > 0$  which was used in §§1-6 [see (1.3)] and which corresponds to the presence of a negative feedback through the inhibitor in the system (Subsection 1.1). In other words, condition (9.2) means that during the formation of peak striations (or spots or blobs) the negative feedback through the inhibitor gives way to a positive feedback at the center. This result may in turn cause a change in  $\eta$  such that a striation (or spot or blob) is annihilated. Since this process may occur in an uncorrelated fashion at well-separated spatial points, a turbulence may arise in the system (Subsection 9.2).

It follows from these mechanisms for the onset of turbulence<sup>80-83</sup> that the formation of oscillations which are random in time and space is determined by the complex behavior of the autosolitons, which is associated in a fundamental way with effects of the interaction of these autosolitons. The picture of the turbulence is essentially one of a random appearance and disappearance of autosolitons at various spatial points.<sup>79</sup> Similar ideas have recently been used to explain

the picture of turbulence which arises in liquid flows at Reynolds numbers near the critical level.<sup>74</sup>

Following from the mechanisms outlined above are these scenarios for the onset of turbulence:

1) Condition (9.1) or (9.2) may hold even at the point  $A = A_c$ . In this case, a turbulence may arise at  $A = A_c$  as a result of a stratification of the homogeneous state of the system.

2) Stable DSs (striations, spots, or blobs) form spontaneously in the system at  $A = A_c$ . As  $A$  increases, condition (9.1) or (9.2) becomes satisfied at a certain  $A > A_c$ , and a turbulence arises spontaneously in the system.

3) Stable static DSs form spontaneously at  $A = A_c$ . As  $A$  increases, the number of striations (or spots or blobs) increases sequentially as a result of local breakdown between striations (Subsection 3.2), and condition (9.1) or (9.2) holds only at sufficiently large values of  $A$ , at which a turbulence arises.

4) In real systems, a turbulence can also arise at  $A < A_c$  as the result of a spontaneous formation of an autosoliton near a small local irregularity and its breakup into first two and then more striations (scenario 2 in Subsection 4.1). The reason is that the striations which form in the course of the breakup process may be unstable.

Experimentally, a turbulence has been observed in a gas discharge in the form of striations which appear and disappear at random.<sup>14</sup> Their turbulence is apparently due to the satisfaction of condition (9.1) (Ref. 46b).

## 9.2. Turbulence in an electron-hole plasma

Turbulence condition (9.2) can be satisfied in a heated electron-hole plasma. Numerical studies show that oscillations which are irregular in space and time do indeed arise.<sup>82,83</sup>

The reason why condition (9.2) can be satisfied in an electron-hole plasma is that peak striations may form in which the carrier temperature at the center is so high that interband impact ionization of carriers must be taken into account.<sup>98,170</sup> In this case the carrier generation rate  $G$  in (1.17) can be written in the form  $G = G_0 + n\nu_i(T)$  where  $G_0 = \text{const}$ , and  $\nu_i$  is the rate of impact ionization, which increases exponentially with increasing  $T$ . In this case, expression (1.28) for the function  $Q$  should be replaced by

$$Q = \eta\theta^{-1-\alpha}(1 - \nu_i(\theta)\tau_r) - 1. \quad (9.3)$$

From (9.3) we see that at the center of a striation, where  $\theta = \theta_{\text{max}}$ , we have  $Q'_\eta < 0$ , in which case we have  $\nu_i(\theta_{\text{max}})\tau_r > 1$ . Numerical studies show that a turbulence arises in an electron-hole plasma when the quantity  $\nu_i(\theta_{\text{max}})\tau_r$  is considerably greater than unity. Depending on the parameters of the plasma, all the scenarios for the onset of turbulence described above may be realized.<sup>82,83</sup>

## 10. SYSTEMS WITH CONVECTIVE FLOWS

It follows from a qualitative theory<sup>46</sup> that in a system with convective flows the shape of static striations is distorted, and these striations may be carried off at a velocity proportional to the magnitude of the flows.<sup>19)</sup> These results explain the shape observed experimentally for moving striations in a gas discharge.<sup>169</sup> This shape has also been studied in numerical<sup>170,111</sup> and experimental<sup>84</sup> studies of

thermodiffusion striations in an electron-hole plasma heated by a static electric field. The evolution of moving striations as the current is varied is also determined by a local breakdown (Subsection 2.1) and a pumping instability (Subsection 2.2).<sup>170</sup>

Boundaries and small irregularities in systems with convective flows may change the picture of self-organization more substantially than as described in Subsection 4.1. For example, an autosoliton which forms spontaneously near a small irregularity or the boundary of a sample may detach from this irregularity and give rise to a sequence of moving striations.<sup>51,98,111</sup> This effect has been observed experimentally<sup>84</sup> and in numerical calculations.<sup>111</sup> Asymmetric static striations with an amplitude and a width which vary along the sample can form throughout the sample or in some part of it. These effects are observed experimentally in low-temperature gaseous plasmas<sup>171</sup> and semiconductor plasmas.<sup>84</sup>

## 11. SPONTANEOUS FORMATION AND EVOLUTION OF PULSATING DSs AND AUTOWAVES

In this section of the paper we will discuss self-organization in  $K\Omega$  and  $\Omega$  systems (Subsection 1.3). Falling in these categories are systems with a uniformly generated combustible substance,<sup>25</sup> a degenerate electron-hole plasma which is heated in the course of Auger recombination,<sup>149</sup> Belousov-Zhabotinskii models of chemical reactions,<sup>7,8,10,11,16,17</sup> models for various types of excitable and neuristor media, in particular, the Fitz-Hugh-Nagumo model,<sup>7,8,16,17,121b,122-124</sup> and certain models of neuron networks whose  $\Omega$  and  $K\Omega$  systems are structures with a latent S-shaped or N-shaped current-voltage characteristic, in which (in contrast with the cases discussed in §7) it is necessary to choose the parameters of the layers in such a way that the inhibition process is slower (see, for example, Ref. 158).

Before we take up the particular features of the evolution of DSs and autowaves (Subsections 11.3-11.6), we wish to point out some characteristic properties of these inhomogeneous states in  $\Omega$  systems (Subsection 11.1) and  $K\Omega$  systems (Subsection 11.2).

### 11.1.

Static and pulsating DSs are not realized in  $\Omega$  systems (Table II). Traveling autosolitons (pulses) and more-complex autowaves—spiral, coiled, ring, etc.—can form in them (see, for example, Refs. 7, 8, 11, 16, 17, and 121-124). The properties of traveling autosolitons and other autowaves in  $\Omega N$  (and  $\Omega H$ ) systems have been studied in extreme detail in models of the Fitz-Hugh-Nagumo type (see, for example, Refs. 8, 11b, 16, 17, 121b, 122, and 124), i.e., in models which are described by Eqs. (1.1) and (1.2) with  $L = 0$  ( $\varepsilon = \infty$ ),  $\alpha = \tau_\theta/\tau_\eta \ll 1$ . Research on these models has shown that (a) a traveling one-dimensional autosoliton (pulse) is stable over a fairly wide range of  $A$ , from some  $A = A_v$ , at which its width  $\mathcal{L}_s$  and its velocity  $v$  are at a minimum ( $v = v_{\text{min}} \sim \alpha^{1/2}/\tau_\theta$ ; Ref. 122b), up to a critical value  $A = A_c$  (Subsections 1.1 and 1.3), at which the width and velocity of the autosoliton reach maxima  $v = v_{\text{max}} \sim 1/\tau_\theta$ ; (b) colliding traveling autosolitons (pulses) annihilate<sup>7,8,11,16,17,123,124</sup>; and (c) a one-dimensional traveling autosoliton is stable in a two-dimensional system. These properties of traveling autosolitons (pulses)

determine the basic properties of the more-complex autowaves which are realized in  $\Omega$  systems.<sup>7,8,10,11,16,17,121-124</sup>

### 11.2.

In  $K\Omega$  systems, not only autowaves but also static and pulsed DSs can arise (Table I). A theory of autowaves and DSs in  $K\Omega$  systems was derived in Refs. 80 and 172.

Autowaves in  $K\Omega$  systems have properties which may be fundamentally different from those of the autowaves which are realized in  $\Omega$  systems (Subsection 11.1). In  $K\Omega$  systems, traveling autosolitons and other autowaves may not annihilate in the course of collisions. The reason is that the condition  $\varepsilon \ll 1$ , i.e.,  $L \gg l$ , means that a "diffusion precursor," a refractory region of the order of  $L$  in size,<sup>25,172</sup> forms ahead of the traveling autosoliton. Consequently, two autosolitons which are traveling opposite to each other interact at distances much greater than the size of the front of the autosoliton ( $\sim l$ ). As a result of this interaction, the autosolitons slow down, and instead of annihilating they may be repelled from each other or may convert into static or pulsating DSs.<sup>25,115</sup> The formation of static DSs in collisions of traveling autosolitons is observed in numerical studies of various models of active media,<sup>107,131,132</sup> including models of the type in (1.31) and (1.32) with  $\alpha \ll 1$ .

In two-dimensional and three-dimensional  $K\Omega N$  and  $K\Omega H$  systems (Table I), a one-dimensional traveling autosoliton, spiral autowaves, and other autowaves may be unstable with respect to a "corrugation" of their walls, i.e., with respect to the effect which was discussed in Subsection 2.3 in connection with static striations. This effect may result in the breakup of autowaves into smaller regions. As a result, autowaves of a new type or a turbulence may arise in the system.

The properties of autowaves, static DSs, and pulsating DSs in  $K\Omega$  systems depend primarily on the relations among the parameters which determine the range and speed of the inhibition process in comparison with the activation. In systems described by equations like (1.1) and (1.2), the region of existence and the properties of autowaves, pulsating DSs, and static DSs are determined by the value of the ratio  $\alpha/\varepsilon \equiv (\tau_\theta/\tau_\eta)(l/L)^{-1}$  (Ref. 172; see also Fig. 8 in the review in Ref. 25).

It follows from the qualitative procedure for the construction of traveling autosolitons in systems with  $\varepsilon = l/L \ll 1$  (Refs. 25, 77, 160) that the condition for the existence of autowaves in  $K\Omega N$  ( $K\Omega H$ ) systems reduces to<sup>172</sup>

$$\alpha/\varepsilon < b_c,$$

i.e.,

$$L/\tau_\eta < b_c l/\tau_\theta. \quad (11.1)$$

Here  $b_c$  is of the order of unity and is determined by the nonlinearities of the system, i.e., by the functions  $q(\theta, \eta)$  and  $Q(\theta, \eta)$  in (1.1) and (1.2). (For the piecewise-linear model of an active medium discussed in Subsection 8.1 of the review in Ref. 25, for example, we have  $b_c \approx 2^{-3/2}$ .)

With increasing value of the ratio  $\alpha/\varepsilon$  or, more precisely, with increasing value of the inhibitor diffusion length  $L$ , the region in which a traveling autosoliton exists, i.e., the region  $(A_v, A_c)$ , shrinks. The value of  $v_{\min}$  increases, while

$v_{\max}$  decreases. As the ratio  $\alpha/\varepsilon$  tends toward the threshold  $b_c$  [see (11.1)], a traveling autosoliton can be excited only at values of  $A$  close to  $A_c$ . With decreasing value of the ratio  $\alpha/\varepsilon$ , the boundary of the region in which a traveling autosoliton exists, i.e., the quantity  $A = A_v$ , becomes progressively more different from  $A_c$ . At  $\alpha < \varepsilon^4$  (Ref. 172), the velocity of the autosoliton at the point  $A = A_v$  reaches its minimum possible value  $v_{\min} \sim \alpha^{1/2} l/\tau_\theta$ .

In  $K\Omega N$  and  $K\Omega H$  systems with

$$\varepsilon^2 \ll \alpha < \varepsilon \ll 1 \quad (11.2)$$

there exists a certain range of excitation levels in which static DSs are stable.<sup>80,172</sup> At the boundaries of this range, static DSs lose their stability with respect to pulsations; i.e., fluctuations which oscillate in time at a certain frequency  $\omega_c$  grow (Subsection 12.4).

### 11.3.

In homogeneous  $K\Omega N$  and  $K\Omega H$  systems which satisfy condition (11.2), static autosolitons, striations, and other DSs may convert spontaneously into pulsed DSs or autowaves as the deviation of the system from equilibrium,  $A$ , varies. A pulsating autosoliton may arise as  $A$  is either increased or reduced, when the width of a static autosoliton becomes respectively greater than or less than a critical value  $\mathcal{L}_\omega$  or  $\mathcal{L}_{b\omega}$ . These critical values are calculated in Subsection 6.2 of Ref. 25. It follows from the stability of a static autosoliton<sup>172</sup> that a traveling autosoliton may arise at values of  $A$  close to  $A_\omega$ , at which the width of a static autosoliton is  $\mathcal{L}_s = \mathcal{L}_\omega$ .

### 11.4.

In narrow-ring systems, autowaves in the form of an isolated traveling autosoliton or a sequence of traveling autosolitons (striations) of various periods may be excited at a given excitation level  $A$ . As  $A$  varies, the number of these autosolitons may change abruptly as the result of a local breakdown and a pumping of activator between striations, as discussed in Subsections 2.1 and 2.2 for static autosolitons (striations).

### 11.5.

At values of  $A$  close to  $A_c$ , a traveling autosoliton acquires an oscillatory tail in the form of repeating regions of excitation and refractoriness.<sup>102b</sup> As in the case of a static autosoliton (Subsection 2.1.2), a local breakdown may occur in the tail of a traveling autosoliton, with the result that new traveling autosolitons continually arise behind a traveling autosoliton. The local breakdown which occurs in the tail of a traveling autosoliton can explain the existence of a steady-state guiding center (a source of outgoing autowaves) in ideally homogeneous  $K\Omega$  systems.<sup>102b</sup>

### 11.6.

Local irregularities in real  $K\Omega$  systems may, depending on their parameter values, lead to the spontaneous formation of static, pulsating, or traveling autowaves. The smaller the irregularity, the closer the corresponding critical value  $A$  is to  $A_c$ . Even small local irregularities may nucleate the spontaneous formation of a guiding center through the effect discussed in Subsection 11.5. The spontaneous formation of

various types of autowaves (spiral autowaves and guiding centers) near local irregularities or boundaries of a system has been observed in, for example, experiments on Belousov-Zhabotinskiĭ reactions.<sup>10,16</sup>

## 12. PARAMETERS AND STABILITY OF PERIODIC STRIATIONS

### 12.1. Development of the shape of striations<sup>75-77</sup>

To analyze the shape and parameters of striations of period  $\mathcal{L}_p \gtrsim L$  in N and H systems, we note that solutions of Eqs. (1.1) and (1.2) in the form of periodic striations, as in the case of autosolitons (Subsection 3.2 in Ref. 25), can be described within  $\varepsilon = l/L \ll 1$  as successive combinations of regions of sharp and smooth distributions.

The sharp distributions satisfy the equation

$$l^2 \frac{d^2\theta}{dx^2} + \frac{dU_\theta}{d\theta} = 0, \quad U_\theta = - \int^\theta q(\theta, \eta, A) d\theta, \quad (12.1)$$

where  $\eta = \text{const}$ . The smooth distributions satisfy the equation

$$L^2 \frac{d^2\eta}{dx^2} + \frac{dU_\eta}{d\eta} = 0, \quad U_\eta = - \int^\eta Q(\theta(\eta), \eta, A) d\eta. \quad (12.2)$$

The length scale of the variation of the activator in sharp distributions is  $l$ , while that in smooth distributions is  $L$ . The function  $\theta(\eta)$  in (12.2) is one of the single-valued functional dependences  $\theta_I(\eta)$ ,  $\theta_{II}(\eta)$ ,  $\theta_{III}(\eta)$  determined by Eq. (1.29); i.e., the function  $\theta(\eta)$  corresponds to branch I, II, or III of a local-coupling curve (Fig. 2, a and c). Branch I corresponds to values  $\theta < \theta_0$ , II to values  $\theta_0 < \theta < \theta'_0$ , and III to values  $\theta > \theta'_0$ . In other words, the potential  $U_\eta$  in (12.2) consists of three independent branches, I, II, and III (Ref. 25).

It can be seen from (12.1) and (12.2) that the smooth and sharp distributions may be thought of as trajectories of particles with coordinates  $\theta$  and  $\eta$ , respectively, which are moving with the "time"  $x$  in the potentials  $U_\theta$  and  $U_\eta$  in (12.1) and (12.2), respectively. The form of the latter is determined unambiguously<sup>25</sup> by the local-coupling curve (Fig. 26). In order to construct periodic striations, it is necessary to join the fragments of sharp and smooth distributions and the corresponding branches of potentials in a self-consistent way. Making use of the symmetry of the periodic striations, we can describe them by simply considering a fragment of size  $\mathcal{L}_p/2$  ( $0 < x < \mathcal{L}_p/2$ ) at whose boundaries we have  $d\theta/dx = d\eta/dx = 0$  (Fig. 26d). The procedure for constructing  $\theta(x)$  and  $\eta(x)$  in this fragment is analogous to the procedure for constructing autosolitons which is described in detail in Subsection 3.2 of Ref. 25.

It follows from the shape of the local-coupling curve (Fig. 26) in N and H systems that  $U_\theta$  in (12.1) has the form of a potential well bounded by the points  $\theta_1$  and  $\theta_3$  [which correspond to branches I and III, respectively, of the single-valued  $\theta(\eta)$  dependence]. At these points, the potential  $U_\theta$  has maxima. It follows from this form of potential  $U_\theta$  that Eq. (12.1) has periodic and solitary solutions  $\theta(x)$ . The latter correspond to the highest particle trajectories in potential  $U_\theta$ , i.e., to the separatrices of Eq. (12.1) which close at the

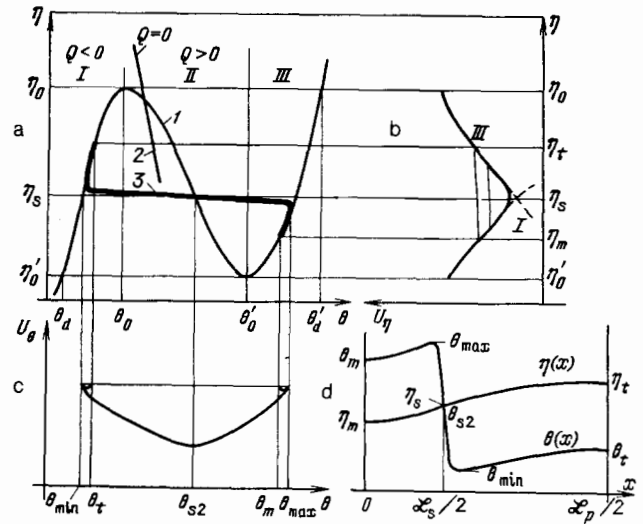


FIG. 26. Diagram used in the construction of periodic striations in N systems. a: 1—Local-coupling curve; 2—state-equation curve; 3—actual  $\eta(\theta)$  dependence in the striations (d). b: The actual potential  $U_\eta$  and "particle" trajectories in it corresponding to a distribution  $\eta(x)$  in the striations (d). c: The actual potential  $U_\theta$ , the highest trajectory of a particle in which corresponds to distribution  $\theta(x)$  in the striations (d).

saddle points  $\theta_1$  or  $\theta_3$ . At a certain value  $\eta = \eta_s$ , the maxima of  $U_\theta$  at the point  $\theta_1 = \theta_{s1}$  and  $\theta_3 = \theta_{s3}$  coincide; i.e., the conditions

$$\int_{\theta_{s1}}^{\theta_{s3}} q(\theta, \eta_s, A) d\theta = 0, \quad q(\theta_{si}, \eta_s, A) = 0 \quad (i = 1, 2, 3), \quad (12.3)$$

hold. These conditions determine the values of  $\eta_s$ ,  $\theta_{s1}$ , and  $\theta_{s3}$ . The highest particle trajectory in a potential  $U_\theta$  of this sort describes the activator distribution  $\theta(x) = \theta_{sh}(x)$  at the walls of striations, i.e., in regions with a size of the order of  $l$  in which  $\theta$  varies from  $\theta_{\min} = \theta_{s1}$  to  $\theta_{\max} = \theta_{s3}$ . Here we have  $\theta_{s1} < \theta_0$ ; i.e., this value belongs to branch I of the local coupling curve. We also have  $\theta_{s3} > \theta_0$ ; i.e., this value belongs to branch III of the local-coupling curve (Fig. 26a). A sharp distribution  $\theta_{sh}(x)$  thus joins the solutions  $\eta(x)$  of Eq. (12.2) corresponding to branches I and III of the potential  $U_\eta$ , i.e., to the  $\theta_I(\eta)$  and  $\theta_{III}(\eta)$  curves. It follows that in order to construct the potential  $U_\eta$  it is necessary to arrange its branches I and III in such a way that they intersect at the point  $\eta = \eta_s$  (Fig. 26b).

In monostable systems, the potential  $U_\eta$  has a unique extremum, which corresponds to the point  $\eta = \eta_h$ ,  $\theta = \theta_h$ , which in turn corresponds to a homogeneous state of the system.<sup>25</sup> This homogeneous state stratifies (Subsections 1.1 and 1.2) when the point  $\theta = \theta_h$  and  $\eta = \eta_h$  lies on branch II of the single-valued  $\theta(\eta)$  curve, on which we have  $q'_\theta < 0$  (Ref. 25). In the region in which the homogeneous state of the system is unstable, i.e., in the region  $A_c < A < A'_c$  (Subsections 1.1–1.3), branches I and III of the potential  $U_\eta$  have no extremum. From the sign of  $Q$  we can determine the slope of the branches<sup>25</sup> (Fig. 26b).

The various trajectories of a particle in the actual poten-

tial  $U_\eta$  (Fig. 26b) corresponding to a given "energy" of the particle determine the inhibitor distributions  $\eta(x)$  in the periodic striations. According to (1.29), they describe smooth distributions of the activator,  $\theta(x)$ , away from the walls of the striations. These smooth  $\theta(x)$  distributions join in a natural way<sup>25</sup> at the point  $\eta = \eta_s$  with the sharp distribution  $\theta(x) = \theta_{sh}(x)$ , which describes the variation of the activator in the walls of the striations.<sup>76,77</sup> There are a number of such trajectories which correspond to the same potential  $U_\eta$  (Fig. 26b). It follows that under the condition  $A = \text{const}$  there are a number of states in the form of striations of various periods in the distributed system.

Equations which determine the characteristic parameters of the striations of a given period  $\mathcal{L}_p$ , i.e., the quantities  $\mathcal{L}_s$ ,  $\eta_t$ ,  $\theta_t$ ,  $\eta_m$ , and  $\theta_m$  (Fig. 26d), can be found by integrating Eq. (12.2) under the boundary conditions

$$\left. \frac{d\eta_I}{dx} \right|_{x=\mathcal{L}_p/2} = 0, \quad \eta_I\left(\frac{\mathcal{L}_s}{2}\right) = \eta_{III}\left(\frac{\mathcal{L}_s}{2}\right) = \eta_s, \quad \left. \frac{d\eta_{III}}{dx} \right|_{x=0} = 0 \quad (12.4)$$

and by making use of the smoothness of the function  $\eta(x)$  at the point  $x = \mathcal{L}_s/2$  (i.e., the condition  $d\eta_I/dx|_{x=\mathcal{L}_s/2} = d\eta_{III}/dx|_{x=\mathcal{L}_s/2}$ ). As a result we find<sup>79</sup>

$$\begin{aligned} \mathcal{L}_p &= \mathcal{L}_s + \sqrt{2}L \int_{\eta_s}^{\eta_t} \left( \int_{\eta_s}^{\eta} Q_I d\eta \right)^{-1/2} d\eta, \\ \mathcal{L}_s &= \sqrt{2}L \int_{\eta_m}^{\eta_s} \left( \int_{\eta_m}^{\eta} Q_{III} d\eta \right)^{-1/2} d\eta, \\ \int_{\eta_s}^{\eta_t} Q_I d\eta + \int_{\eta_m}^{\eta_s} Q_{III} d\eta &= 0, \\ q(\theta_m, \eta_m, A) &= q(\theta_t, \eta_t, A) = 0. \end{aligned} \quad (12.5)$$

The functions  $Q_{I,III} \equiv Q(\theta_{I,III}(\eta), \eta, A)$ ,  $\theta_{I,III}(\eta)$ ,  $\eta_{I,III}(x)$ , and  $\theta_{I,III}(x)$  correspond to values of  $\eta$  and  $\theta$  which in turn correspond to branches I and III of the single-valued  $\theta(\eta)$  curve on the local-coupling curve (Fig. 26a). The functions  $\eta_{I,III}(x)$  and  $\theta_{I,III}(x)$  describe the inhibitor and activator distributions away from striation walls.

Generalizing the results above,<sup>76,77</sup> we can write the distributions  $\theta(x)$  and  $\eta(x)$  in a wide striation, of size  $\mathcal{L}_s \gg 1$ , as follows, where we are making use of the symmetry of the striation with respect to the point  $x = 0$  (Figs. 6a and 26d):<sup>79</sup>

$$\begin{aligned} \theta(x) &= \theta_{sh}(x) + \theta_{III}(x) - \theta_{s3}, \quad 0 \leq x \leq \frac{\mathcal{L}_s}{2}, \\ &= \theta_{sh}(x) + \theta_I(x) - \theta_{s1}, \quad \frac{\mathcal{L}_s}{2} \leq x \leq \frac{\mathcal{L}_p}{2}, \\ \eta(x) &= \eta_{III}(x), \quad 0 \leq x \leq \frac{\mathcal{L}_s}{2}, \\ &= \eta_I(x), \quad \frac{\mathcal{L}_s}{2} \leq x \leq \frac{\mathcal{L}_p}{2}, \end{aligned} \quad (12.6)$$

where  $\theta_{sh}(x)$  is a sharp distribution corresponding to a striation wall. This sharp distribution corresponds to the separatrix of Eq. (12.1) at  $\eta = \eta_s$ , which runs from one saddle

point,  $\theta_{s3} = \theta_{\max}$ , to the other,  $\theta_{s1} = \theta_{\min}$ .

Equations (12.3), (12.5), and (12.6), which follow from the qualitative theory of DSs,<sup>75-77</sup> determine the basic parameters of striations to within  $\varepsilon \ll 1$ . This conclusion can be substantiated with the help of the asymptotic theory,<sup>79</sup> which is based on the idea that the activator varies sharply over a short distance  $\sim l \ll L$  in the walls of striations, so these walls may be thought of as boundary layers. The presence of such boundary layers makes it possible to apply to the analysis of striations the ideas of the theory of singular perturbations which have been developed in other problems involving boundary layers.<sup>173-175</sup> For example, one can verify that Eqs. (1.1) and (1.2) for stationary states reduce<sup>176,177</sup> within  $\varepsilon \ll 1$  to equations for sharp and smooth distributions according to the qualitative theory of differential equations.<sup>26</sup> To construct the shape of striations in accordance with the qualitative theory presented above from a set of sharp and smooth distributions, however, it is necessary to construct a solution which satisfies certain integral conditions [see expression (11) in Ref. 77] and boundary conditions. An asymptotic theory of striations of this sort was derived in Ref. 79 (a theory is presented in Subsection 3.3 of Ref. 25 for the case of autosolitons).

## 12.2. Conditions for local breakdown in striations<sup>75,76,78</sup>

In systems whose homogeneous state  $\theta = \theta_h$  and  $\eta = \eta_h$  is unstable, there naturally cannot be states in the form of one or several autosolitons, i.e., solitary states at whose periphery we find  $\theta \rightarrow \theta_h$  and  $\eta \rightarrow \eta_h$  (Ref. 25). In other words, at excitation levels  $A_c < A < A'_c$  the striation period  $\mathcal{L}_p$  has an upper limit  $\mathcal{L}_{\max}$ , whose value becomes infinite as  $A \rightarrow A_c$  (or as  $A \rightarrow A'_c$ ) (Fig. 8a). At a given value of  $A$ , the quantity  $\mathcal{L}_{\max}$  is the period of the striations in which the distribution  $\eta(x)$  corresponds to the highest trajectory of the particle in the potential  $U_\eta$  (Fig. 26b). Two situations may be realized in the range  $A_c < A < A'_c$ .

The first is shown in Fig. 27a. It occurs if

$$U_\eta(\eta'_0) - U_\eta(\eta_s) = \int_{\eta'_0}^{\eta_s} Q_{III} d\eta > U_\eta(\eta_0) - U_\eta(\eta_s) = \int_{\eta_0}^{\eta_s} Q_I d\eta. \quad (12.7)$$

Under inequality (12.7), the  $A$  dependence of the maximum striation period  $\mathcal{L}_p = \mathcal{L}_{\max}$  is given by<sup>12</sup> (12.5), in which it is necessary to set  $\eta_t = \eta_0$  and  $\theta_t = \theta_0$ :

$$\begin{aligned} \mathcal{L}_{\max} &= \mathcal{L}_m + \sqrt{2}L \int_{\eta_s}^{\eta_0} \left( \int_{\eta_0}^{\eta} Q_I d\eta \right)^{-1/2} d\eta, \\ \mathcal{L}_m &= \sqrt{2}L \int_{\eta_m}^{\eta_s} \left( \int_{\eta_m}^{\eta} Q_{III} d\eta \right)^{-1/2} d\eta, \\ \int_{\eta_0}^{\eta_s} Q_I d\eta + \int_{\eta_m}^{\eta_s} Q_{III} d\eta &= 0, \quad q(\theta_m, \eta_m, A) = 0. \end{aligned} \quad (12.8a)$$

Here  $\mathcal{L}_s = \mathcal{L}_m$  is the critical width of the hot region of striations.

The second situation is illustrated in Fig. 27b. It occurs if, as  $A$  is increased, condition (12.7) reverses at a certain value of  $A$ . In this case the dependence  $\mathcal{L}_{\max}(A)$  is determined by (12.5), in which we must set  $\eta_m = \eta'_0$ , and  $\theta_m = \theta'_0$ :

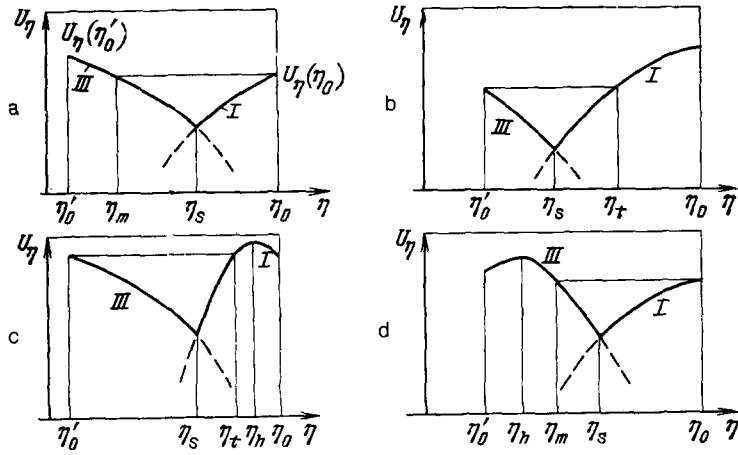


FIG. 27. The potentials  $U_\eta$  for smooth distributions and the highest trajectories of the "particle" in them which correspond to striations of period  $\mathcal{L}_p = \mathcal{L}_{\max}$ . a, b  $A_c < A < A'_c$ ; c— $A_d < A < A'_c$ ; d— $A'_c < A < A'_d$ .

$$\mathcal{L}_{\max} = \mathcal{L}_m + \sqrt{2}L \int_{\eta_s}^{\eta_t} \left( \int_{\eta_t}^{\eta} Q_{II} d\eta \right)^{-1/2} d\eta,$$

$$\mathcal{L}_m = \sqrt{2}L \int_{\eta_0}^{\eta_s} \left( \int_{\eta_0}^{\eta} Q_{III} d\eta \right)^{-1/2} d\eta, \quad (12.8b)$$

$$\int_{\eta_s}^{\eta_t} Q_{II} d\eta + \int_{\eta_0}^{\eta_s} Q_{III} d\eta = 0, \quad q(\theta_t, \eta_t, A) = 0.$$

It follows from the qualitative  $A$  dependence of  $\mathcal{L}_{\max}$  (Fig. 8a) that  $N$  striations of period  $\mathcal{L}_p = \mathcal{L}/N$  exist in a system of size  $\mathcal{L}$  in a certain interval of  $A$  values. At the boundaries of this interval,  $A = A_d^{(N)}$  and  $A = A'_d^{(N)}$  (Fig. 8a), the number of striations increases abruptly as the result of a local breakdown (Subsection 2.1.1). For striations of a given period  $\mathcal{L}_p$ , the critical values  $A = A_d^{(N)}$ ,  $A = A'_d^{(N)}$  (Fig. 8a) are determined from Eq. (12.8a) or (12.8b) if we set  $\mathcal{L}_{\max} = \mathcal{L}_p$  in them.

In certain systems there may be a situation in which the local breakdown at the center of an isolated striation (autosoliton) occurs at  $A < A_c$ . In such systems, a single autosoliton can be excited only under the conditions  $A < A_d < A_c$  [the value of  $A_d$  is given by (3.37) in Ref. 25]. It follows that in the limit  $A \rightarrow A_d$  the maximum striation period becomes infinite:  $\mathcal{L}_p = \mathcal{L}_{\max} \rightarrow \infty$  (Fig. 8b). Under the condition  $A > A_d$  but with  $A < A_c$ , the situation shown in Fig. 27c occurs, in which case we have

$$U_\eta(\eta_h) - U_\eta(\eta_s) > U_\eta(\eta_0') - U_\eta(\eta_s).$$

In this case the quantity  $\mathcal{L}_p = \mathcal{L}_{\max}(A)$  is given by (12.8b). It follows from Fig. 8b that at  $A > A_d^{(N)}$  a local breakdown occurs at the center of hot striations (Fig. 7a).

In systems in which a breakup of cold autosolitons occurs<sup>25</sup> at  $A > A'_c$ , the  $A$  dependence of the maximum striation period  $\mathcal{L}_p = \mathcal{L}_{\max}$  is qualitatively as shown in Fig. 8c. The critical value  $A = A'_d$ , at which the local breakdown occurs in a cold autosoliton, is determined by Eq. (3.39) in Ref. 25. Under the condition  $A < A'_d$  but with  $A > A'_c$ , we have the situation shown in Fig. 27d. In this case the quantity  $\mathcal{L}_p = \mathcal{L}_{\max}(A)$  is determined by (12.8a). It follows from Fig. 8c that under the condition  $A < A'_d^{(N)}$  a local

breakdown occurs at the center of cold striations (Fig. 6a).

In principle, there can be systems in which there is a breakdown of both hot and cold autosolitons. In such systems, the maximum striation period becomes infinite,  $\mathcal{L}_p = \mathcal{L}_{\max} \rightarrow \infty$  not as  $A \rightarrow A_c$  and  $A'_c$  but as  $A \rightarrow A_d$  and  $A'_d$ . In other words, the dependence  $\mathcal{L}_{\max}(A)$  is qualitatively as shown in Fig. 8d.

In  $\mathbb{H}$  systems the quantity  $\mathcal{L}_p = \mathcal{L}_{\max}$  is also determined by Eq. (12.8a) or (12.8b).

### 12.3. Striations of small period<sup>172</sup>

To analyze the shape of the striations of period  $\mathcal{L}_p \ll L$ , it is convenient to rewrite Eqs. (1.1) and (1.2) for the steady-state case in the form

$$\frac{d^2\theta}{dx^2} - q(\theta, \eta, A) = 0, \quad \varepsilon^{-2} \frac{d^2\eta}{dx^2} - Q(\theta, \eta, A) = 0, \quad (12.9)$$

where  $x$  is expressed in units of  $l$ . We seek solutions of Eqs. (12.9) in the form

$$\eta = \eta^{(0)} + \varepsilon^2 \eta^{(2)} + \dots, \quad \theta = \theta^{(0)} + \varepsilon^2 \theta^{(2)} + \dots \quad (12.10)$$

Substituting (12.10) into (12.9), we find equations for the zeroth approximation,

$$\frac{d^2\theta^{(0)}}{dx^2} - q(\theta^{(0)}, \eta^{(0)}, A) = 0, \quad (12.11)$$

$$\frac{d^2\eta^{(0)}}{dx^2} = 0, \quad (12.12)$$

and for the first approximation,

$$\frac{d^2\theta^{(1)}}{dx^2} - q'_\theta(\theta^{(0)}, \eta^{(0)}, A) \theta^{(1)} = q'_\eta(\theta^{(0)}, \eta^{(0)}, A) \eta^{(1)}, \quad (12.13)$$

$$\frac{d^2\eta^{(1)}}{dx^2} = Q(\theta^{(0)}, \eta^{(0)}, A). \quad (12.14)$$

At the boundaries of the period of the striations, we have  $d\eta/dx = d\theta/dx = 0$ ; i.e., according to (12.10), at  $x = \pm (\mathcal{L}_p/2) + n\mathcal{L}_p$  ( $n = 0, 1, 2, \dots$ ) we have

$$\frac{d\eta^{(0)}}{dx} = \frac{d\theta^{(0)}}{dx} = 0, \quad \frac{d\eta^{(1)}}{dx} = \frac{d\theta^{(1)}}{dx} = 0. \quad (12.15)$$



It follows from (12.12) and (12.15) that we have  $\eta^{(0)} = \text{const}$ . The condition under which problem (12.14), (12.15) has a solution reduces to the condition that its right-hand side be orthogonal to the solution of the homogeneous problem (with a zero right-hand side) which is the adjoint of problem (12.14), (12.15) (the Fredholm theorem<sup>178</sup>). Since this homogeneous problem has a solution  $\eta^{(1)} = \text{const}$ , the condition under which problem (12.14), (12.15) can be solved reduces to

$$\int_{-\mathcal{L}_p/2}^{\mathcal{L}_p/2} Q(\theta^{(0)}(x), \eta^{(0)}, A) dx = 0. \quad (12.16)$$

Equation (12.11) with  $\eta^{(0)} = \text{const}$ , along with condition (12.16), completely determines the function  $\theta^{(0)}(x)$  and the quantity  $\eta^{(0)}$ , i.e., the activator and inhibitor distributions in the zeroth approximation in  $\varepsilon^2$ . This problem was analyzed in Ref. 160 and is discussed in the review in Ref. 25. It follows from this analysis that the distribution  $\theta^{(0)}(x)$  is determined substantially by the shape of the local-coupling curve (Fig. 2).

Since the local-coupling curve is V-,  $\Lambda$ -,  $\mathbb{H}$ -, or N-shaped, Eq. (12.11) has periodic solutions.<sup>25</sup> Striation distributions  $\theta^{(0)}(x)$ , i.e., layers of high and low values of the activator, are potentially stable in N and  $\mathbb{H}$  systems.<sup>25</sup> The size of the striation walls, in which  $\theta^{(0)}(x)$  varies sharply from  $\theta_{\min}$  to  $\theta_{\max}$ , is of the order of  $l$  (the dashed curves in Fig. 28a). In wide striations of size  $\mathcal{L}_s \gg l$ , we have  $\theta_{\min} = \theta_{s1}$  and  $\theta_{\max} = \theta_{s3}$ , and the quantity  $\eta^{(0)} = \eta_s$  is found from conditions (12.3). The striation size  $\mathcal{L}_s$  is found from Eq. (12.16) (Refs. 79 and 160).

In N systems at  $\eta^{(0)} > \eta_s$  there are  $\theta^{(0)}(x)$  distributions in the form of narrow hot striations (the dashed curves in Fig. 28b), while at  $\eta^{(0)} < \eta_s$  there are narrow cold striations (Fig. 28c).

In  $\mathbb{H}$  systems, narrow hot striations are realized at  $\eta^{(0)} < \eta_s$ , and narrow cold striations at  $\eta^{(0)} > \eta_s$  (Refs. 25 and 160).

Differentiating Eq. (12.11) with respect to  $x$ , we find

$$\frac{d^2}{dx^2} \frac{d\theta^{(0)}}{dx} - q'_\theta(\theta^{(0)}, \eta^{(0)}, A) \frac{d\theta^{(0)}}{dx} = 0. \quad (12.17)$$

A comparison of (12.17) with (12.13) shows that the function  $\theta^{(1)}(x) \propto d\theta^{(0)}/dx$  is a solution of self-adjoint equation (12.13) with a zero right-hand side. Since  $\theta^{(0)}(x)$  tends toward a constant value ( $\theta_{\min}$  or  $\theta_{\max}$ ) exponentially rapidly away from the striation walls, the derivative

$d\theta^{(1)}/dx \propto d^2\theta^{(0)}/dx^2$  is close to zero with an exponential accuracy at the points  $x = \pm \mathcal{L}_p/2$  (Fig. 28a; see also Subsection 3.1 in Ref. 25). In other words, it satisfies boundary conditions (12.15). It follows that the condition under which problem (12.13), (12.15) has a solution reduces to

$$\int_{-\mathcal{L}_p/2}^{\mathcal{L}_p/2} \eta^{(1)}(x) q'_\eta(\theta^{(0)}(x), \eta^{(0)}, A) \frac{d\theta^{(0)}}{dx} dx = 0. \quad (12.18)$$

Since the function  $\theta^{(0)}(x)$  is an even function with respect to the point  $x = 0$  in the striations (Fig. 28a), while  $d\theta^{(0)}/dx$  is odd, it follows from (12.18) that  $\eta^{(1)}(x)$  is an even function. At the center of a striation we have  $\theta^{(0)} = \theta_{s3}$ , and  $\eta^{(0)} = \eta_s$ . In N systems we have  $Q(\theta_{s3}, \eta_s, A) > 0$ , and in  $\mathbb{H}$  systems  $Q < 0$  (Subsection 3.1 in Ref. 25). It thus follows from (12.14) that the function  $\eta^{(1)}(x)$  has a minimum at the center of the striations in N systems (Fig. 28a), while it has a maximum there in  $\mathbb{H}$  systems. It follows from an analysis of (12.13) that in both N and  $\mathbb{H}$  systems the function  $\theta^{(1)}(x)$  has a minimum at the center of the striations, while it has a maximum at the boundaries of a period (at the points  $x = \pm \mathcal{L}_p/2 + n\mathcal{L}_p$ ;  $n = 0, 1, \dots$ ) (Fig. 28a). The same result follows from the procedure for the construction of striations as described in Subsection 12.1.

#### 12.4. Stability of striations<sup>75,76,160</sup>

To study the stability of the striations, we linearize Eqs. (1.1) and (1.2) around a solution in the form of striations of period  $\mathcal{L}_p$ , with respect to fluctuations of the type

$$\delta\theta(\mathbf{r}, t) = \delta\theta(x) \exp(i\mathbf{k}_\perp \mathbf{r}_\perp - \gamma t),$$

$$\delta\eta(\mathbf{r}, t) = \delta\eta(x) \exp(i\mathbf{k}_\perp \mathbf{r}_\perp - \gamma t). \quad (12.19)$$

here  $k_\perp^2 = k_y^2 + k_z^2$ ;  $k_y = 2\pi n_1/\mathcal{L}_y$ ,  $k_z = 2\pi n_2/\mathcal{L}_z$ ,  $n_{1,2} = 0, \pm, \dots$ ; and  $\mathcal{L}_y$  and  $\mathcal{L}_z$  are the sizes of the system along the  $y$  and  $z$  directions. As a result we find the system of equations

$$(\hat{H}_\theta - \gamma + k_\perp^2) \delta\theta = -q'_\theta \delta\eta,$$

$$\hat{H}_\theta = -\frac{d^2}{dx^2} + V_\theta, \quad V_\theta = q'_\theta(\theta(x), \eta(x), A), \quad (12.20)$$

$$(\hat{H}_\eta - \alpha^{-1}\gamma + \varepsilon^{-2}k_\perp^2) \delta\eta = -Q'_\theta \delta\theta,$$

$$\hat{H}_\eta = -\varepsilon^{-2} \frac{d^2}{dx^2} + V_\eta, \quad V_\eta = Q'_\eta(\theta(x), \eta(x), A), \quad (12.21)$$

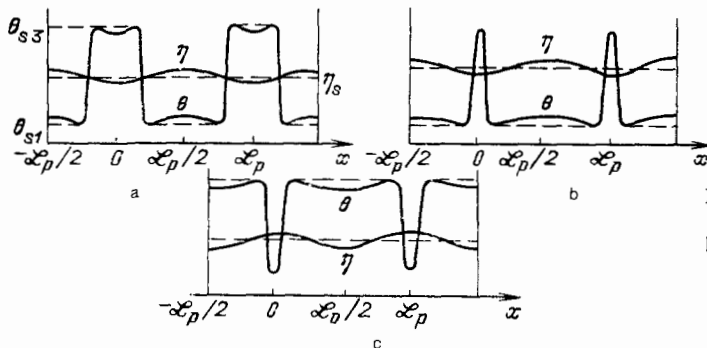


FIG. 28. Periodic striations of period  $\mathcal{L}_p \ll L$ . a—Wide striations ( $\mathcal{L}_s \gg l$ ); b—narrow hot striations; c—narrow cold striations. Dashed lines: Distributions of  $\theta$  and  $\eta$  in the limit  $L \rightarrow \infty$ .

in which lengths and times are expressed in units of  $l$  and  $\tau_\theta$ , respectively. In an extended system of size  $\mathcal{L} \gg L$ , we can use cyclic boundary conditions for fluctuations  $\delta\theta(x)$  and  $\delta\eta(x)$ :

$$\delta\theta(0) = \delta\theta(\mathcal{L}), \quad \left. \frac{d\delta\theta}{dx} \right|_0 = \left. \frac{d\delta\theta}{dx} \right|_{\mathcal{L}}, \quad (12.22)$$

$$\delta\eta(0) = \delta\eta(\mathcal{L}), \quad \left. \frac{d\delta\eta}{dx} \right|_0 = \left. \frac{d\delta\eta}{dx} \right|_{\mathcal{L}}.$$

It can be seen from (12.19) that this state is unstable if  $\text{Re}\gamma < 0$ .

12.4.1 To analyze  $\gamma$ , we consider the auxiliary problem

$$\begin{aligned} \hat{H}_\theta \delta\theta_n &= \lambda_n \delta\theta_n, \\ \delta\theta_n(0) &= \delta\theta_n(\mathcal{L}), \quad \left. \frac{d\delta\theta_n}{dx} \right|_0 = \left. \frac{d\delta\theta_n}{dx} \right|_{\mathcal{L}}, \end{aligned} \quad (12.23)$$

whose eigenfunctions  $\delta\theta_n(x)$  are normalized. It can be seen from (12.20) and (12.23) that the eigenfunctions  $\delta\theta_n$  and the eigenvalues  $\lambda_n$  describe activator fluctuations with  $\delta\eta = 0$ .

For striations of period  $\mathcal{L}_p$  (Fig. 9a), the potential  $V_\theta$  (Fig. 9b) in the operator  $\hat{H}_\theta$  is a periodic repetition of the potential for an individual striation ( $0 < x < \mathcal{L}_p$ ; Fig. 9). It follows from the construction of a striation (Subsection 12.1), that the form of the latter is similar to that discussed for an autosoliton in Subsection 4.2 of Ref. 25.

For an isolated striation the potential  $V_\theta = q'_\theta$  consists of two narrow wells (of size  $\sim l$ ) with  $\min V_\theta < 0$  which are localized near the striation walls, i.e., which are at a distance  $\mathcal{L}_s$  from each other. Outside these wells we have  $V_\theta = q'_\theta \sim 1$  ( $0 < x < \mathcal{L}_p$ ; Fig. 9b). In the  $\lambda_n$  spectrum of problem (12.23) for an isolated striation, as for an autosoliton,<sup>25</sup> only the values  $\lambda_0$  and  $\lambda_1$  are less than 0. They correspond to functions  $\delta\theta_0$  and  $\delta\theta_1$  which are localized at striation walls and which are similar in form to the corresponding functions for an autosoliton (see Fig. 60 in Ref. 25). Away from the striation walls, the functions  $\delta\theta_0$  and  $\delta\theta_1$  fall off exponentially with a length scale  $\sim l$ . The estimates of  $\lambda_0$  and  $\lambda_1$  for an isolated striation and for an autosoliton are the same, i.e., are<sup>25,79,172</sup>

$$\lambda_0 \sim -\frac{e\mathcal{L}_s}{L} \exp\left(-\frac{\mathcal{L}_s}{l}\right), \quad \lambda_1 \sim -\frac{e\mathcal{L}_s}{L}. \quad (12.24)$$

Since the functions  $\delta\theta_0$  and  $\delta\theta_1$  for an isolated striation are very localized, to find the eigenfunctions  $\delta\theta_n$  and the eigenvalues  $\lambda_n$  of problem (12.23) for periodically arranged striations (Fig. 9) one can use the perturbation theory which is called the "approximation of tightly bound electrons" in solid-state theory.<sup>179</sup> When that approach is taken, the eigenfunctions  $\delta\theta_n$  of the periodic potential  $V_\theta$  (Fig. 9b), which are localized at the striation walls, can be written in the form

$$\delta\theta_n \equiv \delta\theta_{s,t}(x) = \sum_{p=1}^N \exp(ik_s x_p) \delta\theta_t(x - x_p) \quad (t = 0, 1), \quad (12.25)$$

where  $k_s = 2\pi s/N\mathcal{L}_p$  [ $s = 0, \pm 1, \dots, \pm(N/2 - 1), N/2$ ];  $N = \mathcal{L}/\mathcal{L}_p$  is the number of hot striations in the system;  $\delta\theta_t(x - x_p)$  are the eigenfunctions for an isolated

hot striation, which are localized near the walls of this striation; and  $x_p = p\mathcal{L}_p - \mathcal{L}_p/2$  is the coordinate of the center of striation  $p$ . The functions  $\delta\theta_{s,t}(x)$  and  $\delta\theta_t(x - x_p)$  are orthonormal:

$$\langle \delta\theta_{s,t} | \delta\theta_{s',t'} \rangle \equiv \frac{1}{V} \int_V \delta\theta_{s,t} \delta\theta_{s',t'}^* dr = \delta_{ss'} \delta_{tt'}, \quad N \langle \delta\theta_t | \delta\theta_{t'} \rangle = \delta_{tt'}, \quad (12.26)$$

where  $V$  is the volume of the system, and  $\delta_{ss'}$  and  $\delta_{tt'}$  are Kronecker deltas. The functions  $\delta\theta_t(x - x_p)$  for different striations, i.e., which correspond to different values of  $p$  (Fig. 9a), overlap to an exponentially small extent. The discrete eigenvalues  $\lambda_0$  and  $\lambda_1$  for an isolated striation thus undergo an  $N$ -fold splitting in the case of  $N$  striations, into narrow bands of width  $\Delta\lambda_t \sim \exp(-\mathcal{L}_p/l) \ll 1$ . In other words, the eigenvalues are given with exponential accuracy by

$$\lambda_n \equiv \lambda_{n,t} \approx \lambda_t \quad (t = 0, 1) \quad (12.24).$$

12.4.2. We first consider the stability of striations of a small period  $\mathcal{L}_p \ll L$ . For such striations, solutions of problem (12.20)–(12.22) can be sought in series form:

$$\delta\theta = \delta\theta^{(0)} + \varepsilon^2 \delta\theta^{(2)} + \dots, \quad \delta\eta = \delta\eta^{(0)} + \varepsilon^2 \delta\eta^{(2)} + \dots,$$

$$\gamma = \gamma^{(0)} + \varepsilon^2 \gamma^{(2)} + \dots \quad (12.27)$$

Substituting (12.10) and (12.27) into (12.20)–(12.22), and assuming  $\varepsilon^2 \ll \alpha, 1$ , we find the equations of the zeroth approximation,

$$(\hat{H}_\theta^{(0)} - \gamma^{(0)} + k_\perp^2) \delta\theta^{(0)} = -q'_\eta \delta\eta^{(0)}, \quad (12.28)$$

$$\begin{aligned} \hat{H}_\theta^{(0)} &= -\frac{d^2}{dx^2} + V_\theta^{(0)}, \quad V_\theta^{(0)} = q'_\theta, \\ -\frac{d^2 \delta\eta^{(0)}}{dx^2} + k_\perp^2 \delta\eta^{(0)} &= 0, \end{aligned} \quad (12.29)$$

and those of the first approximation,

$$(\hat{H}_\theta^{(0)} - \gamma^{(0)} + k_\perp^2) \delta\theta^{(1)} = -q'_\eta \delta\eta^{(1)} - (\psi - \gamma^{(1)}) \delta\theta^{(0)} - \varphi \delta\eta^{(0)}, \quad (12.30)$$

$$\begin{aligned} \psi &= q''_{\theta 0} \theta^{(1)} + q''_{\theta 1} \eta^{(1)}, \quad \varphi = q''_{\eta 0} \theta^{(1)} + q''_{\eta 1} \eta^{(1)}, \\ -\frac{d^2 \delta\eta^{(1)}}{dx^2} + k_\perp^2 \delta\eta^{(1)} &= -Q'_\theta \delta\theta^{(0)} - (Q'_\eta - \alpha^{-1} \gamma^{(0)}) \delta\eta^{(0)}. \end{aligned} \quad (12.31)$$

Here  $q'_\theta \equiv q'_\theta(\theta^{(0)}, \eta^{(0)}, A)$ , etc., and the functions  $\delta\eta^{(i)}$  and  $\delta\theta^{(i)}$  ( $i = 0, 1$ ) satisfy the cyclic boundary conditions

$$\begin{aligned} \delta\theta^{(i)}(0) &= \delta\theta^{(i)}(\mathcal{L}), \quad \left. \frac{d\delta\theta^{(i)}}{dx} \right|_0 = \left. \frac{d\delta\theta^{(i)}}{dx} \right|_{\mathcal{L}}, \\ \delta\eta^{(i)}(0) &= \delta\eta^{(i)}(\mathcal{L}), \quad \left. \frac{d\delta\eta^{(i)}}{dx} \right|_0 = \left. \frac{d\delta\eta^{(i)}}{dx} \right|_{\mathcal{L}} \quad (i = 0, 1). \end{aligned} \quad (12.32)$$

It follows from (12.29) and (12.32) that we have  $\delta\eta^{(0)} = 0$  for  $k_\perp \neq 0$  and  $\delta\eta^{(0)} = \text{const}$  for  $k_\perp = 0$ .

From the condition under which problem (12.31), (12.32) has a solution with  $k_{\perp} = 0$  (the Fredholm theorem) we find

$$\delta\eta^{(0)} = - \langle Q'_{\theta} \delta\theta^{(0)} \rangle (\mu_0 - \alpha^{-1}\gamma^{(0)})^{-1}, \quad (12.33)$$

where  $\mu_0 = \langle Q'_{\eta} \rangle$ , and  $\langle \dots \rangle$  means (as above) an average of the function over the volume of the system.

It follows from (12.28) and (12.33) that problem (12.20)–(12.22) corresponds in the zeroth approximation in  $\varepsilon^2$  to the case  $L = \infty$ ; i.e., it is the same as the problem studied in Refs. 80 and 160 (Subsections 4.1 and 6.1 in Ref. 25).

**12.4.2-1.** We first consider the stability of striations with respect to fluctuations (12.19) with  $k_{\perp} = 0$ . Among the fluctuations  $\delta\theta^{(0)}$  for which  $\delta\eta^{(0)} \neq 0$  the most dangerous is a fluctuation  $\delta\theta^{(0)} \approx \delta\theta_{0,0}$ , which has no nodes (Fig. 9c).

In  $k\Omega$  systems (Subsection 1.3) with  $\varepsilon^2 \ll \alpha \ll 1$ , the condition<sup>80</sup>

$$\lambda_0 + \alpha\mu_0 < 0 \quad (12.34)$$

may hold. This is the condition for the appearance of pulsating striations, i.e., for the growth of fluctuations  $\delta\theta^{(0)} \approx \delta\theta_{0,0}$  with some special frequency  $\omega_c$ . It follows from (12.34) and (12.24) of the present paper and from Eq. (6.2) of Ref. 25 that the frequency  $\omega_c$  and the critical width of a striation of period  $\mathcal{L}_p$  at the threshold for the appearance of pulsations are given approximately by

$$\begin{aligned} \mathcal{L}_s(A_{bw}) &= \mathcal{L}_{bw} \sim l \ln(\alpha\mu_0)^{-1}, \\ \omega_c &= (\tau_{\theta}\tau_{\eta})^{-1/2} \left( \frac{l}{\mathcal{L}_p} \right)^{1/2}. \end{aligned} \quad (12.35)$$

In  $K$  systems (Subsection 1.3), condition (12.34) does not hold, according to (12.24), because of the conditions  $\alpha > 1$  and  $\varepsilon \ll 1$ , and a dangerous fluctuation  $\delta\theta^{(0)} \approx \delta\theta_{0,0}$  does not grow up to the point  $A = A_b^{(N)}$ , at which we have  $d\eta_s/dA = \infty$ . The width of the striations is

$$\mathcal{L}_s(A_b^{(N)}) \equiv \mathcal{L}_b^{(N)} \sim l \ln(\mathcal{L}_p/l)$$

(Subsection 4.1 in Ref. 25). Periodic striations lose their stability before they reach the point  $A = A_b^{(N)}$ , when their width is  $\mathcal{L}_s > \mathcal{L}_b^{(N)}$ .

The reason is that for striations there are fluctuations in the  $\delta\theta^{(0)}$  spectrum such that the condition  $\delta\eta^{(0)} = 0$  holds. For such fluctuations, our initial problem, (12.20)–(12.22), and the auxiliary problem (12.23) discussed above are precisely the same in the zeroth approximation in  $\varepsilon^2$ ; i.e., we have  $\delta\theta^{(0)} = \delta\theta_n^{(0)}$  and  $\gamma^{(0)} = \lambda_n^{(0)}$ . The fluctuations which are the most dangerous,  $\delta\theta_n^{(0)} = \delta\theta_{s,t}^{(0)}$ , are described by (12.25) or, more precisely,

$$\begin{aligned} \delta\theta_{s,t}^{(0)}(x) &= \sum_{p=1}^N \exp(ik_s x_p) \delta\theta_t^{(0)}(x - x_p), \\ s &= \pm 1, \dots, \pm \left( \frac{N}{2} - 1 \right), \frac{N}{2}; \quad t = 0, 1. \end{aligned} \quad (12.36)$$

For fluctuations  $\delta\theta^{(0)} = \delta\theta_{s,t}^{(0)}$  we have<sup>25</sup>  $\gamma^{(0)} = \lambda_n^{(0)} \equiv \lambda_{s,t}^{(0)} \sim -\exp(-\mathcal{L}_s/l)$  and  $\delta\eta^{(0)} = 0$ . The latter assertion can be verified by substituting the function  $\delta\theta^{(0)} = \delta\theta_{s,t}^{(0)}$  from (12.36) into (12.33) and by making use of the properties of the functions  $\delta\theta_t^{(0)}(x - x_p)$  (Subsection 12.4.1).

In the next approximation in  $\varepsilon^2$ , the value of  $\gamma$  corresponding to the dangerous fluctuations  $\delta\theta^{(0)} = \delta\theta_{s,t}^{(0)}$  in (12.36) can be found from the condition under which problem (12.30), (12.32) has a solution (the Fredholm theorem). For this purpose we note that the functions  $\delta\theta^{(0)*} = \delta\theta_{s,t}^{(0)*}$ , which are the conjugates of (12.36), constitute the solution of the problem which is adjoint of problem (12.30), (12.32) with a zero right-hand side in (12.30). It follows from the condition under which problem (12.30), (12.32) has a solution that

$$\gamma^{(1)} = \langle \psi \delta\theta_{s,t}^{(0)} \delta\theta_{s,t}^{(0)*} \rangle + \langle q'_{\eta} \delta\eta^{(1)} \delta\theta_{s,t}^{(0)*} \rangle. \quad (12.37)$$

In deriving (12.37), we made use of the circumstance that the functions  $\delta\theta_{s,t}^{(0)}$  are orthonormal:

$$\langle \delta\theta_{s,t}^{(0)} \delta\theta_{s',t'}^{(0)*} \rangle = \delta_{ss'}.$$

An expression for  $\delta\eta^{(1)}(x)$  can be found from (12.31) and (12.32). With  $k_{\perp} = 0$  and  $\delta\eta^{(0)} = 0$ , this expression is

$$\delta\eta^{(1)}(x) = - \langle \Gamma(x, x') Q'_{\theta} \delta\theta^{(0)} \rangle, \quad (12.38a)$$

where

$$\begin{aligned} \Gamma(x, x') &= \sum_{m=-\infty}^{\infty} k_m^{-2} \exp[ik_m(x - x')], \\ k_m &= \frac{2\pi m}{N\mathcal{L}_p} \quad (m = 0, \pm 1, \dots), \quad N = \frac{\mathcal{L}}{\mathcal{L}_p}. \end{aligned} \quad (12.38b)$$

Substituting (12.38) into (12.37), and noting that we have  $\langle Q'_{\theta} \delta\theta^{(0)} \rangle = 0$ , i.e.,  $\delta\eta^{(0)} = 0$ , for the fluctuations under consideration here,  $\delta\theta^{(0)} = \delta\theta_{s,t}^{(0)}$  [see (12.36)], we find

$$\begin{aligned} \gamma &= \gamma^{(0)} + \varepsilon^2 \gamma^{(1)} \\ &= \lambda_{s,t} + \tilde{a}_{s,t} \varepsilon^2 k_s^{-2} \left( s = \pm 1, \dots, \pm \left( \frac{N}{2} - 1 \right), \frac{N}{2}; \quad t = 0, 1 \right), \end{aligned} \quad (12.39)$$

where  $k_s = 2\pi s/N\mathcal{L}_p$ ,

$$\begin{aligned} \tilde{a}_{s,t} &= - \mathcal{L}_p^{-2} \int_{-\mathcal{L}_p/2}^{\mathcal{L}_p/2} \exp(ik_s x) q'_{\eta} \delta\theta_t^{(0)*}(x) dx \int_{-\mathcal{L}_p/2}^{\mathcal{L}_p/2} \\ &\quad \times \exp(-ik_s x) Q'_{\theta} \delta\theta_t^{(0)}(x) dx, \end{aligned} \quad (12.40)$$

and

$$\lambda_{s,t} = \lambda_{s,t}^{(0)} + \varepsilon^2 \langle \psi \delta\theta_{s,t}^{(0)} \delta\theta_{s,t}^{(0)*} \rangle \approx \lambda_t \quad (t = 0, 1), \quad (12.41)$$

Here the  $\lambda_t$  are the eigenvalues of auxiliary problem (12.23), estimates of which are given in (12.24). In deriving (12.39) we also made use of the periodicity conditions of the functions  $q'_{\eta}(x)$ , and  $Q'_{\theta}(x)$  the equation<sup>179</sup>

$$N^{-1} \sum_{p=1}^N \exp[ix_p(k_s - k_m)] = \delta_{sm}, \quad (12.42)$$

and the normalization conditions on the functions  $\delta\theta_t^{(0)}$ ,

$$N \langle \delta\theta_t^{(0)} \delta\theta_t^{(0)*} \rangle = 1 \quad (t = 0, 1). \quad (12.43)$$

For the systems under consideration here we have

$q'_\eta Q'_\theta < 0$  (Subsection 2.2 in Ref. 25), so the coefficients  $\tilde{a}_{s,t}$  are greater than 0. It follows from (12.39) that the striation instability condition ( $\gamma < 0$ ) can be satisfied most easily for  $s = s_{\max} = N/2$  and that the most dangerous<sup>20)</sup> fluctuation is  $\delta\theta^{(0)} = \delta\theta_{N/2,0}^{(0)}$  with a period  $2\mathcal{L}_p$  (Fig. 9d).

The threshold for the growth of such a fluctuation reduces to the following condition according to (12.39) and (12.40):

$$\lambda_0 + \frac{\tilde{a}_0 \mathcal{L}_p^2}{\pi^2 L^2} = 0. \quad (12.44)$$

Here we have made use of the circumstance that we have  $\tilde{a}_{s,0} \approx \tilde{a}_{0,0} \equiv \tilde{a}_0$ , i.e., that these coefficients depend only weakly on the index  $s$ . The reason for this circumstance is that the functions  $\delta\theta_i^{(0)}$  in (12.36) are highly localized in a region of size  $\sim l \ll \mathcal{L}_p$ . Making use of this circumstance and also the normalization condition for the functions  $\delta\theta_i^{(0)}$ , i.e., (12.43), we find  $\tilde{a}_0 \sim l/\mathcal{L}_p$  from (12.40). Using the estimate (12.24), we find from (12.44) that at the threshold for the loss of stability of the striations their critical width is  $\mathcal{L}_c^{(N)} = \mathcal{L}_s(A_p^{(N)}) > \mathcal{L}_p^{(N)} \sim l \ln(\mathcal{L}_p/l)$ , and for  $\mathcal{L}_p < L$  the quantity  $\mathcal{L}_c^{(N)}$  is given approximately by (2.1). The minimum period of the stable striations,  $\mathcal{L}_{\min}$  (Subsection 2.2), is given by (12.5) if we set  $\mathcal{L}_p = \mathcal{L}_{\min}$  and  $\mathcal{L}_s = \mathcal{L}_c^{(N)}$  [see (2.1)] there.

Striations of period  $\mathcal{L}_p \gg L$  are weakly interacting autosolitons, so they lose their stability at a value of  $A$  close to  $A_b$ , i.e., near the point with<sup>25)</sup>  $d\mathcal{L}_s/dA = d\eta_s/dA = \infty$ . Their critical width is essentially the same as the width of an autosoliton,  $\mathcal{L}_b \sim l \ln(L/l)$ , at the critical point  $A = A_b$  (Ref. 25).

12.4.2-2. In the two-dimensional or three-dimensional case, in an analysis of the conditions for the growth of fluctuations in (12.19) with  $k_\perp \neq 0$ , the factor  $k_m^{-2}$  in (12.38b) must be replaced by  $(k_m^2 + k_\perp^2)^{-1}$ , and we must make use of the relation  $\gamma^{(0)} = \lambda_n^{(0)} + k_\perp^2$ , as follows from analysis of Eqs. (12.28)–(12.31). In other words, instead of (12.39) we find

$$\gamma = \lambda_{s,t} + k_\perp^2 + \tilde{a}_{s,t} \varepsilon^2 (k_s^2 + k_\perp^2)^{-1} \times \left( s = 0, \pm 1, \dots, \pm \left( \frac{N}{2} - 1 \right), \frac{N}{2}; t = 0, 1 \right). \quad (12.45)$$

The condition  $\mathcal{L}_s < \mathcal{L}_{b1}^{(N)}$  for the instability of striations with respect to a corrugation of their walls, discussed in Subsection 2.3, follows from (12.45). We wish to stress that for striations of period  $\mathcal{L}_p < L(I/L)^{1/3}$  the condition  $\mathcal{L}_s < \mathcal{L}_{b1}^{(N)}$  is more restrictive than the condition  $\mathcal{L}_s < \mathcal{L}_c^{(N)}$  for the instability of striations due to a pumping effect (Subsection 2.2).

12.4.3. To analyze the stability of striations of arbitrary period, including  $\mathcal{L}_p \gtrsim L$ , we consider the auxiliary problem

$$\hat{H}_\eta \delta\eta_k = \mu_k \delta\eta_k, \quad \delta\eta_k(0) = \delta\eta_k(\mathcal{L}), \quad \left. \frac{d\delta\eta_k}{dx} \right|_0 = \left. \frac{d\delta\eta_k}{dx} \right|_{\mathcal{L}}, \quad (12.46)$$

in which the operator  $\hat{H}_\eta$  is given in (12.21), and the functions  $\delta\eta_k$  are orthonormal:

$$\langle \delta\eta_k \delta\eta_{k'} \rangle = \delta_{kk'}. \quad (12.47)$$

In the "Hamiltonian"  $\hat{H}_\eta$  the "potential" satisfies  $V_\eta = Q'_\eta > 0$ , so all the eigenvalues satisfy  $\mu_k > 0$ . Their values increase with increasing  $k$  according to the oscillation theorem. Making use of the periodicity of the potential  $V_\eta$ , we can write the eigenfunctions  $\delta\eta_k$  in the form of Bloch functions:<sup>179)</sup>

$$\delta\eta_k \equiv \delta\eta_{\beta,\nu}(x) = u_{\beta,\nu}(x) \exp(ik_\beta x), \quad (12.48)$$

where  $u_{\beta,\nu}(x)$  are Bloch factors with a period  $\mathcal{L}_p$ , and

$$k_\beta = \frac{2\pi\beta}{N\mathcal{L}_p}, \quad \beta = 0, \pm 1, \dots, \pm \left( \frac{N}{2} - 1 \right), \frac{N}{2}; \quad \nu = 0, 1, \dots$$

It follows from the analysis in Subsections 12.4.1 and 12.4.2 that among the eigenfunctions  $\delta\theta(x)$  of problem (12.20)–(12.22) the fluctuations  $\delta\theta \approx \delta\theta_{s,t}$  [see (12.25)] are "dangerous." For them, as we have already noted, the condition  $\lambda_{s,t} \approx \lambda_t < 0$  holds. The growth of such fluctuations of the activator can be suppressed through appropriate changes in the inhibitor; it follows from (12.21) that these appropriate changes are<sup>7)</sup>

$$\delta\eta(x) = - \langle \Gamma(x, x', \gamma) Q'_\theta \delta\theta_{s,t} \rangle = - \sum_{\beta,\nu} \delta\eta_{\beta,\nu}(x) \langle \delta\eta_{\beta,\nu}^* Q'_\theta \delta\theta_{s,t} \rangle (\mu_{\beta,\nu} + \varepsilon^{-2} k_\perp^2 - \alpha^{-1} \gamma)^{-1}, \quad (12.49)$$

where  $\Gamma(x, x', \gamma)$  is the Green's function of problem (12.21), (12.22) with a zero right-hand side in (12.21). [In (12.49), the function  $\Gamma(x, x', \gamma)$  is expressed in terms of the eigenfunctions  $\delta\eta_k \equiv \delta\eta_{\beta,\nu}(x)$  and the eigenvalues  $\mu_k \equiv \mu_{\beta,\nu}$  of auxiliary problem (12.46).] We substitute (12.49) into (12.20) with the function  $\delta\theta = \delta\theta_{s,t}$  from (12.25), multiply the resulting equation from the left by  $\delta\theta_{s,t}^*$ , and take an average of the result over  $V$ . Using (12.42) and the condition for the periodicity of the functions  $u_{\beta,\nu}(x)$ , we thus find equations for estimating the critical values of  $\gamma$  (Ref. 80):

$$\Phi_{s,t}(\gamma) = \lambda_t + k_\perp^2 - \gamma + \sum_{\nu=0}^{\infty} a_{s,t}^{(\nu)} \mu_{s,\nu} (\mu_{s,\nu} + \varepsilon^{-2} k_\perp^2 - \alpha^{-1} \gamma)^{-1} = 0. \quad (12.50)$$

The coefficients here are

$$a_{s,t}^{(\nu)} = - \mu_{s,\nu}^{-1} \mathcal{L}_p^{-2} \int_{-\mathcal{L}_p/2}^{\mathcal{L}_p/2} u_{s,\nu}(x) \exp(ik_s x) q'_\eta \delta\theta_t^*(x) dx \times \int_{-\mathcal{L}_p/2}^{\mathcal{L}_p/2} u_{s,\nu}^*(x) \exp(-ik_s x) Q'_\theta \delta\theta_t(x) dx > 0, \quad s = 0, \pm 1, \dots, \pm \left( \frac{N}{2} - 1 \right), \frac{N}{2}; \quad t = 0, 1. \quad (12.51)$$

12.4.4. Condition (12.34) does not hold in K systems. In this case it follows from an analysis of Eqs. (12.50) similar to the analysis in Subsections 4.2 and 6.2 of Ref. 25 (in a study of the stability of autosolitons) that the value of  $\gamma$  near the striation stability threshold is<sup>75,77)</sup>

$$\gamma = \lambda_t + k_{\perp}^2 + \sum_{\nu=0}^{\infty} a_{s,t}^{(\nu)} \mu_{s,\nu} (\mu_{s,\nu} + \varepsilon^{-2} k_{\perp}^2)^{-1}. \quad (12.52)$$

Noting that the values of  $\mu_{s,\nu}$  increase with increasing index  $\nu$ , we need consider only the first term in the sum in (12.52), and we can use  $a_{0,0}^{(0)} \mu_{0,0} \approx \tilde{a}_0 \sim l / \mathcal{L}_p$  in estimating the critical parameters of the striations.

In this case, (12.52) gives us the critical values which we presented in Subsection 2.3 for the quantity  $k_{\perp}$  and the striation width, (2.2), at points at which the striations lose stability with respect to the growth of a fluctuation

$$\delta\theta \approx \delta\theta_{0,0}(x) \exp(i\mathbf{k}_{\perp} \mathbf{r}_{\perp}).$$

The condition for the instability of hot striations (Fig. 9a) with respect to activator pumping follows from expression (12.52) when we set  $k_{\perp} = 0$  and  $t = 0$  in it:<sup>75,78</sup>

$$\lambda_0 + a_{0,0}^{(0)} \mu_{0,0}^{-1} < 0 \quad \left( s = 0, \pm 1, \dots, \pm \left( \frac{N}{2} - 1 \right), \frac{N}{2} \right). \quad (12.53)$$

Since  $\mu_{s,0}$  increases with increasing  $s$ , the fluctuation  $\delta\theta \approx \delta\theta_{\mu_{s,0}}(x)$  with  $s = s_{\max} = N/2$  is the most dangerous. It follows from (12.24) and (12.53) that the critical width of the striations at the point of instability (the instability is an activator-pumping instability) is

$$\mathcal{L}_s (A_p^{(N)}) \equiv \mathcal{L}_c^{(N)} \sim l \ln [\mu_{N/2,0} (a_{0,0}^{(0)} \mu_{0,0})^{-1}]. \quad (12.54)$$

Let us estimate the value of  $\mu_{N/2,0}$  for striations of period  $\mathcal{L}_p \ll L$ . In this case, a solution of problem (12.46) can be sought in series form:

$$\delta\eta_k = \delta\eta_k^{(0)} + \varepsilon^2 \delta\eta_k^{(1)} + \dots, \quad \mu_k = \varepsilon^{-2} \tilde{\mu}_k^{(0)} + \tilde{\mu}_k^{(1)} + \dots \quad (12.55)$$

Substituting (12.55) into (12.46), we find, in the zeroth approximation,

$$-\frac{d^2 \delta\eta_k^{(0)}}{dx^2} = \tilde{\mu}_k^{(0)} \delta\eta_k^{(0)}, \quad \delta\eta_k^{(0)}(0) = \delta\eta_k^{(0)}(\mathcal{L}), \quad \left. \frac{d\delta\eta_k^{(0)}}{dx} \right|_0 = \left. \frac{d\delta\eta_k^{(0)}}{dx} \right|_{\mathcal{L}}. \quad (12.56)$$

Problem (12.56) has solutions  $\delta\eta_k^{(0)}(x) = \exp(2\pi i k x / N \mathcal{L}_p)$ ,  $\tilde{\mu}_k^{(0)} = (2\pi k / N \mathcal{L}_p)^2$ ,  $k = 0, \pm 1, \dots$ . Consequently, for  $\mathcal{L}_p \ll L$  we have  $\mu_{N/2,0} \approx \varepsilon^{-2} \mu_{N/2}^{(0)} = \pi^2 L^2 / \mathcal{L}_p^2$ . Since we have  $a_{0,0}^{(0)} \mu_{0,0} \approx \tilde{a}_0 \sim l / \mathcal{L}_p$ , we find Eq. (2.1) from (12.54). Equation (2.1) was derived above from condition (12.44).

12.4.5. In  $K\Omega$  systems, a fluctuation  $\delta\theta \approx \delta\theta_{0,0}(x) \cos(\omega_c t)$  with  $\omega_c \neq 0$  may be a growing fluctuation, as follows from an analysis of Eqs. (12.50) by the procedure in Subsection 6.2 of Ref. 25. The striation pulsation frequency  $\omega_c$  is given by (12.35), and the condition for the appearance of pulsating striations reduces to (12.34). It follows from (12.34) and (12.24) that the width of striations which are stable with respect to pulsations, like the width of autosolitons,<sup>25</sup> lies in the interval  $\mathcal{L}_{b\omega} < \mathcal{L}_s < \mathcal{L}_\omega$ , where  $\mathcal{L}_{b\omega}$  is given by (12.35), and  $\mathcal{L}_\omega \sim L \mu_{0,0}(\alpha/\varepsilon)$ .

## CONCLUSION

The results presented in this review make it possible to analyze the picture of self-organization as not only the excitation level of the system but also other of its parameters are varied. For example, as the length of the system decreases, and  $\mathcal{L}$  reaches the value  $N \mathcal{L}_{\min}(A)$ , the number of striations,  $N$ , decreases abruptly as a result of a pumping instability (Subsection 2.2). Conversely, as the size of the system,  $\mathcal{L}$  (in semiconductors and gases, the distance between electrodes), increases, the striation period increases, and at a certain critical length  $\mathcal{L} = N \mathcal{L}_{\max}(A)$  a local breakdown occurs at the center of striations or between them (Subsection 2.1). This dynamic restructuring increases the number of striations.

These results are important for biology, e.g., in the analysis of embryos and morphogenesis, i.e., changes in the shape of a fetus or an organism as it grows. Models of the types in (1.11) and (1.12) are frequently used to describe such processes; fluctuations are assigned a governing role in them.<sup>3,5,6,8,12</sup> In addition, as we have seen, the self-organization phenomena which occur as a system grows usually result from a dynamic restructuring (Subsection 2.1). Fluctuations may thus not play an important role in the selection of the type of dissipative structure which forms.<sup>78,115</sup>

In real systems, i.e., experimentally, the picture of self-organization is determined by the inhomogeneities of the systems. Small local inhomogeneities serve as nucleating regions for the abrupt appearance of autosolitons, whose subsequent evolution determines the self-organization process (§4 and Subsection 5.3).

We wish to stress that in most cases the spontaneous formation and the evolution of dissipative structures occur in monostable systems, i.e., in systems whose external parameters depend on the excitation level in a single-valued fashion, even linearly. The formation of filaments or domains of an electric field is generally unrelated to the shape of the current-voltage characteristic of the system. For example, multifilament and multidomain states may arise in a monostable electron-hole plasma with a single-valued current-voltage characteristic (§8). A gas discharge has an S-shaped current-voltage characteristic, and striations (electric field domains) form in it.<sup>45,46b</sup> In a transistor structure, in contrast, current filaments form, and the current-voltage characteristic may be N-shaped (Subsection 7.3). The local breakdown effect (Subsection 2.1.1) is directly related to the monostable nature of a system, since only striations of finite width can form in such systems. The realization of wide striations of large period essentially implies the existence of two stable homogeneous states in the system; i.e., such striations are possible only in bistable systems (§6).

We also wish to stress that the picture of self-organization, in particular, the appearance of turbulence (§9), does not depend on the nature of the system, i.e., on the particular mechanisms which determine the activation and inhibition processes. The picture is determined primarily by the nature of the nonlinearity of the system, more precisely, the local-coupling curve, and by the response time and range of the activator in comparison with those of the inhibitor (Subsection 1.3). By experimentally studying the properties of dissipative structures in complex chemical and biological systems, one can thus draw conclusions about the qualitative

form of the local-coupling curve and of other parameters of a mathematical model which can be used to describe the observed picture of self-organization. On the other hand, by studying specific physical systems for which the equations describing dissipative structures can be derived correctly [e.g., an electron-hole plasma (Subsections 8.1–8.3) or semiconductor structures, which are the most convenient for experimental studies (§8)], one can draw conclusion about the self-organization scenarios which apply to systems differing in nature, including chemical and biological systems.

*Basic notation*

DS—dissipative structure;

AS—autosoliton;

$\theta$ —value of activator;

$\eta$ —value of inhibitor;

$\theta_h$  and  $\eta_h$ —values of activator and inhibitor in homogeneous medium;

$l$  and  $\tau_\theta$ —length scale and time scale of the variation of the activator;

$L$  and  $\tau_\eta$ —length scale and time scale of the variation of the inhibitor;

$\varepsilon = l/L$ ;

$\alpha = \tau_\theta/\tau_\eta$ ;

$A$ —excitation level of the system (a control or bifurcation parameter);

$A_c$  and  $A'_c$ —critical values of  $A$ , which are the lower and upper limits on the region of instability of the homogeneous state of the medium;

$A_b$  ( $A'_b$ )—the limiting value of  $A$ , below (above) which static autosolitons and other dissipative structures do not occur;

$A_p^{(N)}$  ( $A'_p^{(N)}$ )—the value of  $A$  at which  $N$  “hot” (“cold”) striations of period  $\mathcal{L}_p$  in a system of size  $\mathcal{L} = N\mathcal{L}_p$  lose their stability as the result of “pumping” effect;

$A_d$  ( $A'_d$ ) or  $A_d^{(N)}$  ( $A'_d^{(N)}$ )—values of  $A$  at which a local breakdown occurs at the center of a hot (cold) autosoliton or at the center of hot (cold) periodic striations;

$\mathcal{L}_p$ —period of striations;

$\mathcal{L}_s$  ( $\mathcal{L}'_s$ )—width of hot (cold) striations and autosolitons;

$\mathcal{L}_{\min}$ —minimum possible striation period;

$\mathcal{L}_{\max}$ —maximum possible striation period;

$K$ ,  $\Omega$ ,  $K\Omega$ ,  $KN$  systems (and other systems) are explained in Table I.

<sup>1)</sup> In general, the term “dissipative structure” proposed by Prigogine is sometimes applied not only to spatially inhomogeneous states but also to homogeneous self-oscillations which may arise spontaneously in distributed media.<sup>3,10,16</sup> A study of the various types of self-oscillations,<sup>26</sup> including stochastic ones,<sup>27–29</sup> is an independent problem, which is not discussed in the present review.

<sup>2)</sup> In its general meaning, “self-organization” is a change in the nature of the ordering of a nonequilibrium system upon a change in the excitation level of the system. For this reason, self-organization processes are also called “nonequilibrium” or “kinetic phase transitions.”<sup>3–6</sup> Criteria for the degree of ordering in the course of self-organization processes have been proposed by Klimontovich.<sup>30</sup> As a rule, dissipative structures are a macroscopically inhomogeneous state and can thus be also thought of as incommensurate phase transitions in nonequilibrium systems. Questions concerning the analogies between and differences between equilibrium and nonequilibrium phase transitions, critical phenomena near nonequilibrium phase transitions, and statistical approaches to the analysis of self-organization phenomena constitute an independent problem, which is not discussed in the present review.

<sup>3)</sup> For this reason, such media are also called “activator-inhibitor sys-

tems” in the English language literature. In systems in which there is no inhibition process, an instability leads to either an unbounded growth of the activator in a certain region of the system or an abrupt transition of the system from one homogeneous state to another. The first of these processes occurs, for example, upon the breakdown of a dielectric or during an explosion which starts at a specific point.<sup>20</sup> A theory for such time-varying processes (sharpening regimes) is offered in Ref. 42. The second of these processes occurs, for example, in semiconductors, gases, and other systems which have an S-shaped current-voltage characteristic. When there is an external circuit, the voltage drop across the structure plays the role of a uniformly varying inhibitor, so an isolated filament<sup>21–24</sup> forms in systems with an S-shaped current-voltage characteristic. Such a filament is the simplest sort of dissipative structure.

<sup>4)</sup> Conditions for the instability of three-component active systems are discussed in Refs. 114, 8, and 17.

<sup>5)</sup> Under neutral boundary conditions in a one-dimensional system of size  $\mathcal{L}$ , we would have  $k = k_m = \pi m/\mathcal{L}$ , where  $m = 0, 1, \dots$ . For this reason, the stratification is realized with respect to fluctuations with a wave number  $k = k_{m_0}$  which may be close to the value of  $k_0$  given by (1.9) (Ref. 3). The discrete nature of the values of  $k$ , however, is essentially unseen in the picture of self-organization in distributed systems of size  $\mathcal{L} \gg k_0^{-1}$  which is discussed below.

<sup>6)</sup> Expressions (1.11)–(1.13) are written in a form in which the lengths  $l$  and  $L$  are essentially independent of the control parameter  $A$ , i.e., are length scales of the variation of the activator and the inhibitor.

<sup>7)</sup> Incorporating the difference between the parameters of the electrons and the holes essentially leads to only a simple renormalization of the coefficients (the electron diffusion coefficient is replaced by a bipolar diffusion coefficient, and so forth).<sup>75,76</sup>

<sup>8)</sup> This stratification condition is far less restrictive than the condition for the thermal instability in unipolar semiconductors;<sup>21</sup>  $\alpha + s > 1$ . The reason is that in an electron-hole plasma inhomogeneous quasineutral distributions of the carrier density may form because the holes as well as the electrons have a mobility.

<sup>9)</sup> In a certain region of stability of the homogeneous state of  $\Omega$  systems, traveling autosolitons and other, more-complex autowaves can be excited by a brief external perturbation. The properties of these solitons have been discussed in many places (e.g., Refs. 7, 8, 10–11, 17, and 121–124).

<sup>10)</sup> This conclusion essentially follows from the theory of current filaments and field domains in semiconductors which have S- and N-shaped current-voltage characteristics. Specifically, the stratification of the homogeneous state of a semiconductor is realized with respect to the longest-wavelength mode, with  $k = \pi/\mathcal{L}$  ( $\mathcal{L}$  is the size of the system). The stable state (a filament or domain) which forms is a step. The transition region of this step has a size  $l \ll \mathcal{L}$  (Refs. 21–24). All modes, including the shortest-wavelength mode, with  $k = \pi/l$ —which is highly damped at the critical point—participate in the formation of this step.

<sup>11)</sup> In certain systems, states in the form of stable striations do not occur, and a turbulence may arise upon the stratification of the homogeneous state (§9).

<sup>12)</sup> Corresponding to a given value of  $\mathcal{L}_{\max}$  there may be several values of  $A$ . In other words, the  $\mathcal{L}_{\max}(A)$  dependence can in principle have several minima (see the dashed line in Fig. 8a). This comment applies to all the curves in Fig. 8.

<sup>13)</sup> The appearance of oscillatory distributions  $\theta(x)$  and  $\eta(x)$  (Ref. 143) near an inhomogeneity as  $A \rightarrow A_c$  essentially follows from the form of the spatial-correlation function of the fluctuations near the point of the stratification ( $A = A_c$ ) analyzed by Nitzan *et al.*<sup>144</sup> and also from the form of the Green’s function of this inhomogeneous problem as  $A \rightarrow A_c$  (Ref. 145).

<sup>14)</sup> The formation of striations in a gas discharge is also associated with a self-breeding of electrons as the result of an increasing dependence of the rate of electron impact ionization,  $\nu_i$ , on the electron density  $n$  (Ref. 14). In this case, however (in contrast with the systems which are being discussed in this section), the activation and inhibition processes occur in the same volume of the gas-discharge tube.

<sup>15)</sup> In transistors, because of the special base electrode, the condition  $L \gg \mathcal{L}$  usually holds ( $\mathcal{L}$  is the linear size of the structure), and only a single “hot spot” forms. Hot spots were first observed experimentally in Ref. 152. They were subsequently explained at a qualitative level in Refs. 153 and 154. A nonlinear theory of hot spots in transistors was derived in Ref. 151. In particular, it was shown there that the current-voltage characteristic of the transistor may be N-shaped upon current filamentation (Fig. 23c).

<sup>16)</sup> Dissipative structures can also arise in bistable sandwich structures whose current-voltage characteristics remain S-shaped, despite the presence of an inhibition region. The distinctive features of self-organization phenomena for bistable structures of this sort are discussed in §6.

- <sup>17)</sup> Structures with a "latent" S-shaped current-voltage characteristic are also being studied as electronic models of neuristors (Refs. 156–158, for example), in which traveling autosolitons can be excited. The parameters of such structures correspond to  $\Omega$  systems (Subsection 1.3).
- <sup>18)</sup> The evolution of dissipative structures may change significantly if the external circuit has a complex impedance.<sup>80</sup>
- <sup>19)</sup> Terms proportional to  $\nabla\theta$  and  $\nabla\eta$  arise in equations like (1.1) and (1.2) (see, for example, Refs. 14 and 46).
- <sup>20)</sup> This assertion is valid for hot striations (Fig. 9a) of width  $L_s < L_p/2$ . In the opposite case, i.e., in the case of cold striations (Fig. 9e), a fluctuation  $\delta\theta^{(0)} = \delta\theta_{N/2,1}^{(0)}$  is the most dangerous. This fluctuation describes an increase in the width of a cold region in one striation and a narrowing of a cold region in a neighboring striation. In other words, the growth of a fluctuation of this sort leads to a pumping of activator between cold striations.
- 
- <sup>1</sup> L. D. Landau and E. M. Lifshitz, *Hydrodynamics* [in Russian], Nauka, M., 3rd revised ed., 1986. [Engl. transl. of earlier ed. Fluid Mechanics, Pergamon Press, Oxford, 1959].
- <sup>2</sup> a) D. D. Joseph, *Stability of Fluid Motions*, Springer-Verlag, N.Y., 1976 [Russ. transl. Mir, M., 1981]; b) G. Z. Gershuni, E. M. Zhukhovitskiĭ, and A. A. Nepomnyashchii, *Stability of Convective Flows* [in Russian], Nauka, M., 1989.
- <sup>3</sup> G. Nicolis and I. Prigogine, *Self-Organization in Non-Equilibrium Systems*, Wiley, N.Y., 1977 [Russ. transl. Mir, M., 1979].
- <sup>4</sup> W. Ebeling, *Structure Formation in Irreversible Processes* [in German], Teubner, Leipzig, 1976 [Russ. transl. Mir, M., 1979].
- <sup>5</sup> H. Haken, *Introduction to Synergetics*, Springer-Verlag, N.Y., 1977 [Russ. transl. Mir, M., 1980].
- <sup>6</sup> H. Haken, *Advanced Synergetics: Instability Hierarchies of Self-Organizing Systems and Devices*, Springer-Verlag, N. Y., 1983 [Russ. transl. Mir, M., 1985].
- <sup>7</sup> a) N. Wiener and A. Rosenbluth, *Arch. Inct. Cardiol. Mech.* **16**, 205 (1946); b) L. S. Polak and A. S. Mikhaĭlov, *Self-Organization in Non-equilibrium Physicochemical Systems* [in Russian], Nauka, M., 1983.
- <sup>8</sup> a) V. A. Vasil'ev, Yu. M. Romanovskii, and V. G. Yakhno, *Usp. Fiz. Nauk* **128**, 625 (1979) [Sov. Phys. Usp. **22**, 615 (1979)]; b) V. A. Vasil'ev, Yu. M. Romanovskii, and V. G. Yakhno, *Autowave Processes* [in Russian], Nauka, M., 1987.
- <sup>9</sup> A. V. Gaponov-Grekhov and M. I. Rabinovich, in *Nonlinear Waves: Structures and Bifurcations* [in Russian], Nauka, M., 1987, p. 7.
- <sup>10</sup> A. M. Zhabotinskiĭ, *Concentration Oscillations* [in Russian], Nauka, M., 1974.
- <sup>11</sup> a) Yu. M. Romanovskii, N. V. Stepanova, and D. S. Chernavskii, *Mathematical Modeling in Biophysics* [in Russian], Nauka, M., 1975; b) Yu. M. Romanovskii, N. V. Stepanova, and D. S. Chernavskii, *Mathematical Biophysics* [in Russian], Nauka, M., 1984.
- <sup>12</sup> B. N. Belintsev, *Usp. Fiz. Nauk* **141**, 55 (1983) [Sov. Phys. Usp. **26**, 775 (1983)].
- <sup>13</sup> G. I. Sivashinsky, *Ann. Rev. Fluid Mech.* **15**, 179 (1983).
- <sup>14</sup> a) A. V. Nedospasov, *Usp. Fiz. Nauk* **94**, 439 (1968) [Sov. Phys. Usp. **11**, 174 (1968)]; A. V. Nedospasov and V. D. Khait, *Oscillations and Instabilities of Low-Temperature Plasmas* [in Russian], Nauka, M., 1979; b) L. Pekárek, *Usp. Fiz. Nauk* **94**, 463 (1968) [Sov. Phys. Usp. **11**, 188 (1968)].
- <sup>15</sup> B. B. Kadomtsev, in *Nonlinear Waves: Structures and Bifurcations* [in Russian], Nauka, M., 1987, p. 45.
- <sup>16</sup> R. J. Field and M. Burger, (Eds.) *Oscillations and Traveling Waves in Chemical Systems*, Wiley, N.Y., 1984 [Russ. transl. Mir, M., 1988].
- <sup>17</sup> V. A. Vasilev, Yu. M. Romanovskii, D. S. Chernavskii, and V. G. Yakhno, *Autowave Processes in Kinetic Systems*, Veb Deutscher Verlag der Wissenschaften, Berlin, 1987.
- <sup>18</sup> P. S. Landa, *Self-Oscillations in Distributed Systems* [in Russian], Nauka, M., 1983.
- <sup>19</sup> A. V. Gurevich and R. G. Mints, *Thermal Autowaves in Normal Metals and Superconductors* [in Russian], IVT Akad. Nauk SSSR, M., 1987.
- <sup>20</sup> A. G. Merzhanov and E. N. Rumanov, *Usp. Fiz. Nauk* **151**, 553 (1987) [Sov. Phys. Usp. **30**, 293 (1987)].
- <sup>21</sup> A. V. Volkov and Sh. M. Kogan, *Usp. Fiz. Nauk* **96**, 633 (1968) [Sov. Phys. Usp. **11**, 881 (1968)].
- <sup>22</sup> V. V. Osipov and V. A. Kholodnov, *Mikroelektronika* **2**, 529 (1973).
- <sup>23</sup> V. L. Bonch-Bruевич, I. P. Zvyagin, and A. G. Mironov, *Domain Electrical Instability in Semiconductors* [in Russian], Nauka, M., 1972.
- <sup>24</sup> E. Schöll, *Nonequilibrium Phase Transitions in Semiconductors* (Vol. 35, Springer Series in Synergetics), Springer-Verlag, N.Y., 1987.
- <sup>25</sup> B. S. Kerner and V. V. Osipov, *Usp. Fiz. Nauk* **157**, 201 (1989) [Sov. Phys. Usp. **32**, 101 (1989)].
- <sup>26</sup> A. A. Andronov, A. A. Vitt, and S. E. Khaikin, *Theory of Oscillators*, Addison-Wesley, Reading, Mass., 1966 [Russ. original, Fizmatgiz, M., 1959].
- <sup>27</sup> A. V. Gaponov-Grekhov and M. I. Rabinovich, *Usp. Fiz. Nauk* **128**, 579 (1979) [Sov. Phys. Usp. **22**, 590 (1979)].
- <sup>28</sup> M. I. Rabinovich and D. M. Trubetskov, *Introduction to the Theory of Oscillations and Waves* [in Russian], Nauka, M., 1984.
- <sup>29</sup> G. I. Zaslavskii and R. Z. Sagdeev, *Introduction to Nonlinear Physics* [in Russian], Nauka, M., 1988.
- <sup>30</sup> Yu. L. Klimontovich, *Usp. Fiz. Nauk* **158**, 59 (1989) [Sov. Phys. Usp. **32**, 416 (1989)].
- <sup>31</sup> a) B. S. Kerner and V. F. Sinkevich, *Pis'ma Zh. Eksp. Teor. Fiz.* **36**, 359 (1982) [JETP Lett. **36**, 436 (1982)]; b) B. S. Kerner, V. V. Osipov, M. T. Romanko, and V. F. Sinkevich, *Pis'ma Zh. Eksp. Teor. Fiz.* **44**, 77 (1986) [JETP Lett. **44**, 97 (1986)]; V. A. Bashchenko, B. S. Kerner, V. V. Osipov, and V. F. Sinkevich, *Fiz. Tekh. Poluprovodn.* **23**, 1378 (1989) [Sov. Phys. Semicond. **23**, 857 (1989)].
- <sup>32</sup> K. M. Mayer, J. Parisi, and R. P. Huebener, *Z. Phys. Kl. B* **71**, 171 (1988).
- <sup>33</sup> a) D. Jäger, H. Baumann, and R. Symanczyk, *Phys. Lett. A* **117**, 141 (1986); b) A. V. Gorbatyuk, I. A. Liničuk, and A. V. Svirin, *Pis'ma Zh. Tekh. Fiz.* **15**, 42 (1989) [Sov. Tech. Phys. Lett. **15**, 224 (1989)].
- <sup>34</sup> B. S. Kerner, D. P. Litvin, and V. I. Sankin, *Pis'ma Zh. Tekh. Fiz.* **13**, 819 (1987) [Sov. Tech. Phys. Lett. **13**, 342 (1987)].
- <sup>35</sup> V. A. Vashenko, B. S. Kerner, V. V. Osipov, and V. F. Sinkevich, *Fiz. Tekh. Poluprovodn.* **24**(10) (1990) [Sov. Phys. Semicond. **24**(10) (1990), to be published].
- <sup>36</sup> C. R. Radehaus, T. Dirksmeyer, H. Willebrand, and H.-G. Purwins, *Phys. Lett. A* **125**, 92 (1987).
- <sup>37</sup> V. P. Abramov and S. L. Klenov, *Radiotekh. Elektron.* **34**, 652 (1989).
- <sup>38</sup> A. A. Akhmetov and V. P. Baev, *Cryogenics* **24**, 67 (1984); V. E. Keilin and S. L. Kruglov, *Cryogenics* **24**, 525 (1984).
- <sup>39</sup> J. S. Langer, *Rev. Mod. Phys.* **52**, 1 (1980); D. J. Wollkind, R. Sriranganathan, and D. B. Oulton, *Physica D* **12**, 215 (1984); G. B. McFadden and S. R. Coriell, *Physica D* **12**, 253 (1984).
- <sup>40</sup> V. V. Barelko, V. M. Bebutyan, Yu. E. Volodim, and Ya. B. Zel'dovich, in *Autowave Processes in Systems with Diffusion* [in Russian], IPF Akad. Nauk SSSR, Gor'kiĭ, 1981, p. 135.
- <sup>41</sup> a) S. A. Akhmanov and M. A. Vorontsov, in *Nonlinear Waves: Dynamics and Evolution* [in Russian], Nauka, M., 1989, p. 228; b) S. A. Akhmanov, M. A. Vorontsov, and V. Yu. Ivanov, *New Physical Principles for Optical Data Processing* [in Russian], Nauka, M., 1989, Ch. 6.
- <sup>42</sup> A. A. Samarskiĭ, V. A. Galaktionov, S. P. Kurdyumov, and A. P. Mikhaĭlov, *Peaking Regimes in Problems for Quasilinear Parabolic Equations* [in Russian], Nauka, M., 1987.
- <sup>43</sup> Ya. B. Zel'dovich, *Theory of the Combustion and Detonation of Gases* [in Russian], Ivd. Akad. Nauk SSSR, L., 1944; *Selected Works: Chemical Physics and Hydrodynamics* [in Russian], Nauka, M., 1984, p. 165.
- <sup>44</sup> A. M. Turing, *Philos. Trans. R. Soc., Ser. B* **237**, 37 (1952).
- <sup>45</sup> B. S. Kerner and V. V. Osipov, *Radiotekh. Elektron.* **27**, 2415 (1982).
- <sup>46</sup> a) B. S. Kerner and V. V. Osipov, *Dokl. Akad. Nauk SSSR* **257**, 1352 (1981) [Sov. Phys. Dokl. **26**, 420 (1981)]; b) *Radiotekh. Elektron.* **28**, 132 (1983).
- <sup>47</sup> B. S. Kerner and V. V. Osipov, *Zh. Eksp. Teor. Fiz.* **71**, 1542 (1976) [Sov. Phys. JETP **44**, 807 (1976)].
- <sup>48</sup> B. S. Kerner and V. V. Osipov, *Fiz. Tekh. Poluprovodn.* **13**, 891 (1979) [Sov. Phys. Semicond. **13**, 523 (1979)].
- <sup>49</sup> B. S. Kerner and V. V. Osipov, *Fiz. Tverd. Tela (Leningrad)* **21**, 2342 (1979) [Sov. Phys. Solid State **21**, 1348 (1979)].
- <sup>50</sup> a) V. V. Gafičuk, B. S. Kerner, and V. V. Osipov, *Fiz. Tverd. Tela (Leningrad)* **23**, 2305 (1981) [Sov. Phys. Solid State **23**, 1348 (1981)]; b) *Fiz. Tekh. Poluprovodn.* **15**, 2171 (1981) [Sov. Phys. Semicond. **15**, 1261 (1981)]; c) *Fiz. Tekh. Poluprovodn.* **19**, 1871 (1985) [Sov. Phys. Semicond. **19**, 1153 (1985)].
- <sup>51</sup> B. S. Kerner and V. V. Osipov, in *Nonlinear Waves: Dynamics and Evolution* [in Russian], Nauka, M., 1989, p. 127; B. S. Kerner and V. V. Osipov, *Nonlinear Waves. I: Dynamics and Evolution*, Springer-Verlag, N.Y., 1989, p. 126 [Russ. original, Nauka, M., 1989].
- <sup>52</sup> B. S. Kerner and V. V. Osipov, *Pis'ma Zh. Eksp. Teor. Fiz.* **18**, 122 (1973) [JETP Lett. **18**, 70 (1973)]; *Mikroelektronika* **3**, 9 (1974).
- <sup>53</sup> Yu. I. Balkareĭ and M. G. Nikulin, *Fiz. Tekh. Poluprovodn.* **10**, 1455, 2039 (1976) [Sov. Phys. Semicond. **10**, 863, 1216 (1976)].
- <sup>54</sup> Yu. I. Balkareĭ and M. I. Elinson, *Mikroelektronika* **8**, 428 (1979).
- <sup>55</sup> Yu. I. Balkareĭ and M. G. Evtikhov, and M. I. Elinson, *Mikroelektronika* **14**, 67 (1985).
- <sup>56</sup> Yu. I. Balkareĭ, M. G. Nikulin, and M. I. Elinson, in *Autowave Processes in Systems with Diffusion* [in Russian], IPF Akad. Nauk SSSR, Gor'kiĭ, 1981, p. 117.
- <sup>57</sup> H.-G. Purwins, Ch. Radehaus, and J. Berkemeier, *Z. Naturforsch.* **43a**, 17 (1988).
- <sup>58</sup> K. Kardell, Ch. Radehaus, R. Dokmen, and H.-G. Purwins, *J. Appl. Phys.* **64**, 6336 (1988).
- <sup>59</sup> A. Nitzan and J. Ross, *J. Chem. Phys.* **59**, 241 (1973).

- <sup>60</sup> A. Nitzan, P. Ortoleva, and J. Ross, *J. Chem. Phys.* **60**, 3134 (1974).
- <sup>61</sup> F. V. Bunkin, N. A. Kirichenko, B. S. Luk'yanchuk, and Yu. Yu. Morozov, *Kvant. Elektron. (Moscow)* **10**, 2136 (1983) [*Sov. J. Quantum Electron.* **13**, 1430 (1983)].
- <sup>62</sup> S. V. Polyakov and V. G. Yakhno, *Fiz. Plazmy* **6**, 383 (1980) [*Sov. J. Plasma Phys.* **6**, 211 (1980)].
- <sup>63</sup> Y. Kuramoto and T. Tsuzuki, *Prog. Theor. Phys.* **54**, 687 (1975); **55**, 356 (1976).
- <sup>64</sup> A. Nitzan and P. Ortoleva, *Phys. Rev. A* **21**, 1735 (1980).
- <sup>65</sup> A. C. Newell and J. A. Whitehead, *J. Fluid Mech.* **38**, 279 (1969).
- <sup>66</sup> L. A. Segel, *J. Fluid Mech.* **38**, 203 (1969).
- <sup>67</sup> E. D. Siggia and A. Zippelius, *Phys. Rev. A* **26**, 1036 (1981).
- <sup>68</sup> J. Swift and R. S. Hohenberg, *Phys. Rev. A* **15**, 319 (1977).
- <sup>69</sup> V. S. Gertsberg and G. I. Sivashinskiy, *Prog. Theor. Phys.* **66**, 1219 (1981).
- <sup>70</sup> B. A. Malomed, *Z. Phys.* **55**, 241 (1984).
- <sup>71</sup> B. A. Malomed, in *Nonlinear Waves: Structures and Bifurcations* [in Russian], Nauka, M., 1987, p. 251.
- <sup>72</sup> A. V. Gaponov-Grekhov, A. S. Lomov, G. V. Osipov, and M. I. Rabinovich, in *Nonlinear Waves: Dynamics and Evolution* [in Russian], Nauka, M., 1989, p. 61.
- <sup>73</sup> T. S. Akhromeeva, S. P. Kurdyumov, G. G. Malinetskiy, and A. A. Samarskiy, in *Scientific and Technological Progress. Series on Current Problems in Mathematics and Latest Progress* [in Russian], Vol. 28, VINITI Akad. Nauk SSSR, M., 1987, p. 207.
- <sup>74</sup> M. I. Rabinovich and M. M. Sushchik, *Usp. Fiz. Nauk* **160**, (1), 3 (1990) [*Sov. Phys. Usp.* **33**, 1 (1990)].
- <sup>75</sup> B. S. Kerner and V. V. Osipov, *Zh. Eksp. Teor. Fiz.* **74**, 1675 (1978) [*Sov. Phys. JETP* **47**, 874 (1978)].
- <sup>76</sup> B. S. Kerner and V. V. Osipov, *Fiz. Tekh. Poluprovodn.* **13**, 721 (1979) [*Sov. Phys. Semicond.* **13**, 424 (1979)].
- <sup>77</sup> B. S. Kerner and V. V. Osipov, *Zh. Eksp. Teor. Fiz.* **79**, 2218 (1980) [*Sov. Phys. JETP* **52**, 1122 (1980)].
- <sup>78</sup> B. S. Kerner and V. V. Osipov, *Dokl. Akad. Nauk SSSR* **264**, 1366 (1982) [*Sov. Phys. Dokl.* **27**, 484 (1982)].
- <sup>79</sup> B. S. Kerner and V. V. Osipov, *Mikroelektronika* **14**, 389 (1985).
- <sup>80</sup> B. S. Kerner and V. V. Osipov, *Zh. Eksp. Teor. Fiz.* **83**, 2201 (1982) [*Sov. Phys. JETP* **56**, 1275 (1982)].
- <sup>81</sup> B. S. Kerner and V. V. Osipov, *Dokl. Akad. Nauk SSSR* **270**, 1104 (1983) [*Sov. Phys. Dokl.* **28**, 485 (1983)].
- <sup>82</sup> Z. I. Vasyunyk, V. V. Gafichuk, B. S. Kerner, and V. V. Osipov, *Fiz. Tverd. Tela (Leningrad)* **31**, 66 (1989) [*Sov. Phys. Solid State* **31**, 1875 (1989)].
- <sup>83</sup> V. V. Gafichuk, B. S. Kerner, V. V. Osipov, and Z. I. Vasyunyk, *Proceedings of the Fourth International Workshop in Nonlinear and Turbulent Processes in Physics*, Vol. 1, Naukova Dumka, Kiev, p. 107; *Noise in Physical Systems: Proceedings of the Tenth International Conference*, Budapest, 1990, p. 609.
- <sup>84</sup> M. N. Vinoslavskii, *Fiz. Tverd. Tela (Leningrad)* **31**(8), 315 (1989) [*Sov. Phys. Solid State* **31**, 1461 (1989)]; M. N. Vinoslavskii, B. S. Kerner, V. V. Osipov, and O. G. Sarbej, *J. Phys.* **2**, 686 (1990).
- <sup>85</sup> Yu. A. Astrov, "Generation of autosolitons during double injection into a high-resistivity semiconductor," (In Russian) Preprint, A. F. Ioffe Physicotechnical Institute, Academy of Sciences of the USSR, Leningrad, 1990.
- <sup>86</sup> J. Berkemeier, T. Dirksmeier, G. Klempt, and H.-G. Purwins, *Z. Phys. Kl. B* **65**, 255 (1986); H.-G. Purwins, G. Klempt, and J. Berkemeier, *Festkörperprobleme* **27**, 27 (1987).
- <sup>87</sup> a) H.-G. Purwins and Ch. Radehaus, *Neural and Synergetic Computers* (Vol. 42, *Springer Series in Synergetics*), Springer-Verlag, N. Y., 1988, p. 137; b) H.-G. Purwins, Ch. Radehaus, T. Dirksmeier, R. Dohmen, R. Schmeling, H. Willebrand, *Phys. Lett. A* **136**, 480 (1989).
- <sup>88</sup> S. Koga and Y. Kuramoto, *Prog. Theor. Phys.* **63**, 106 (1980).
- <sup>89</sup> D. S. Chernavskii and Th. W. Ruijgrok, *Biosystems* **15**, 75 (1982).
- <sup>90</sup> B. S. Kerner, E. M. Kuznetsova, and V. V. Osipov, *Dokl. Akad. Nauk SSSR* **277**, 1114 (1984) [*Sov. Phys. Dokl.* **29**, 644 (1984)].
- <sup>91</sup> B. S. Kerner, E. M. Kuznetsova, and V. V. Osipov, *Mikroelektronika* **13**, 407, 456 (1984).
- <sup>92</sup> A. Gierer and H. Meinhardt, *Kybernetik* **12**, 30 (1972).
- <sup>93</sup> H. Meinhardt and A. Gierer, *J. Cell. Sci.* **15**, 321 (1974); H. Meinhardt, *J. Cell. Sci.* **23**, 117 (1977); A. Gierer, *Naturwissenschaften* **68**, 245 (1981).
- <sup>94</sup> Yu. I. Balkarey, M. G. Evtikhov, and M. I. Elinson, *Mikroelektronika* **8**, 493 (1979); **9**, 141, 144 (1980); **10**, 78 (1981).
- <sup>95</sup> Yu. I. Balkarey, M. G. Evtikhov, and M. I. Elinson, *Mikroelektronika* **11**, 25 (1982); **12**, 65, 171 (1984).
- <sup>96</sup> G. G. Elenin, V. V. Krylov, A. A. Polezhaev, and D. S. Chernavskii, *Dokl. Akad. Nauk SSSR* **271**, 84 (1983) [*Sov. Phys. Dokl.* **28**, 542 (1983)].
- <sup>97</sup> A. A. Akhmetov and R. G. Mints, *Pis'ma Zh. Tekh. Fiz.* **9**, 1306 (1983) [*Sov. Tech. Phys. Lett.* **9**, 561 (1983)].
- <sup>98</sup> A. L. Dubitskiy, B. S. Kerner, and V. V. Osipov, *Fiz. Tekh. Poluprovodn.* **20**, 1195 (1986) [*Sov. Phys. Semicond.* **20**, 755 (1986)].
- <sup>99</sup> A. L. Dubitskiy, B. S. Kerner, and V. V. Osipov, *Fiz. Tverd. Tela (Leningrad)* **28**(5), 1290 (1986) [*Sov. Phys. Solid State* **28**, 725 (1986)].
- <sup>100</sup> V. V. Gafichuk, B. S. Kerner, V. V. Osipov, and A. G. Yuzhanin, *Pis'ma Zh. Tekh. Fiz.* **13**, 1299 (1987) [*Sov. Tech. Phys. Lett.* **13**, 543 (1987)].
- <sup>101</sup> V. V. Gafichuk, V. É. Gashpar, B. S. Kerner, and V. V. Osipov, *Fiz. Tekh. Poluprovodn.* **22**, 1836 (1988) [*Sov. Phys. Semicond.* **22**, 1161 (1988)].
- <sup>102</sup> a) V. V. Gafichuk, B. S. Kerner, I. I. Lazurchak, and V. V. Osipov, *Mikroelektronika* **15**, 180 (1986); b) **19**(6) (1990).
- <sup>103</sup> V. V. Osipov, I. I. Lazurchak, V. V. Gafichuk, and B. S. Kerner, *Mikroelektronika* **16**, 23 (1987).
- <sup>104</sup> V. V. Gafichuk, B. S. Kerner, V. V. Osipov, and A. G. Yuzhanin, *Fiz. Tekh. Poluprovodn.* **22**, 2051 (1988) [*Sov. Phys. Semicond.* **22**, 1298 (1988)].
- <sup>105</sup> Yu. I. Balkarey, M. G. Evtikhov, and M. I. Elinson, *Zh. Tekh. Fiz.* **57**, 209 (1987) [*Sov. Phys. Tech. Phys.* **32**, 127 (1987)]; *Mikroelektronika* **17**, 313 (1988).
- <sup>106</sup> Yu. I. Balkarey, A. V. Grigor'yants, and Yu. A. Rzhanov, *Kvant. Elektron. (Moscow)* **14**, 128 (1987) [*Sov. J. Quantum Electron.* **17**, 72 (1987)].
- <sup>107</sup> N. N. Rozanov and G. V. Khodova, *Opt. Spectrosk.* **65**, 761 (1988) [*Opt. Spectrosc. (USSR)* **65**, 449 (1988)]; N. N. Rozanov and G. V. Khodova, *J. Opt. Soc. Am. B* **7**(6), 1990.
- <sup>108</sup> G. G. Elenin and T. M. Lysak, *Mat. Modelirovanie* **1**, 92 (1989).
- <sup>109</sup> V. V. Gafichuk, B. S. Kerner, V. V. Osipov, and A. G. Yuzhanin, "Statistical autosolitons and dissipative structures in a hot electron-hole plasma," Preprint, IPPMM, Academy of Sciences of the Ukrainian SSR, Lvov, 1988.
- <sup>110</sup> V. V. Gafichuk, B. S. Kerner, V. V. Osipov, and A. G. Yuzhanin, *Zh. Tekh. Fiz.* **60**, 8 (1990) [*Sov. Phys. Tech. Phys.* **35**, 141 (1990)].
- <sup>111</sup> V. V. Gafichuk, B. S. Kerner, V. V. Osipov, and I. V. Tsylyuk, *Fiz. Tverd. Tela (Leningrad)* **31**(8), 46 (1989) [*Sov. Phys. Solid State* **31**, 1304 (1989)].
- <sup>112</sup> V. V. Gafichuk, B. I. Datsko, B. S. Kerner, and V. V. Osipov, *Fiz. Tekh. Poluprovodn.* **24**, 724 (1990) [*Sov. Phys. Semicond.* **24**, 455 (1990)].
- <sup>113</sup> V. V. Gafichuk, B. I. Datsko, B. S. Kerner, and V. V. Osipov, *Fiz. Tekh. Poluprovodn. No. 24(7) [*Sov. Phys. Semicond.* **24**(7) (1990) to be published].*
- <sup>114</sup> V. A. Vasil'ev, *Thermodynamics of Biological Processes* [in Russian], Nauka, M., 1976, p. 198.
- <sup>115</sup> B. S. Kerner, V. I. Krinskii, and V. V. Osipov, *Thermodynamics and Pattern Formation in Biology*, Walter de Gruyter, N.Y., 1988, p. 265.
- <sup>116</sup> V. I. Talanov, *Dokl. Akad. Nauk SSSR* **258**, 604 (1981) [*Sov. Phys. Dokl.* **26**, 522 (1981)].
- <sup>117</sup> A. V. Gurevich and A. B. Shvartsburg, *Nonlinear Theory of the Propagation of Radio Waves in the Ionosphere* [in Russian], Nauka, M., 1973.
- <sup>118</sup> V. E. Golant, A. P. Zhilinskii, and S. A. Sakharov, *Fundamentals of Plasma Physics*, Wiley, N. Y., 1980 [Russ. original, Atomizdat, M., 1977].
- <sup>119</sup> F. G. Bass and Yu. G. Gurevich, *Hot Electrons and Strong Electromagnetic Waves in Semiconductor Plasmas and Gas-Discharge Plasmas* [in Russian], Nauka, M., 1975.
- <sup>120</sup> B. S. Kerner and V. V. Osipov, *Selforganization by Nonlinear Irreversible Process* (Vol. 33, *Springer Series in Synergetics*), Springer-Verlag, N.Y., 1986, p. 118.
- <sup>121</sup> a) A. L. Hodgkin and A. F. Huxley, *J. Physiol.* **116**, 449 (1952); D. Noble, *J. Physiol.* **160**, 317 (1962); b) R. Fitz-Hugh, *Biophys.* **1**, 445 (1961); **2**, 11 (1962); H. P. Schwan (editor), *Biological Engineering*, McGraw-Hill, N.Y., 1969, p. 1; I. Nagumo, S. Arimoto, and S. Yoshizawa, *Proc. IRE* **50**, 2061 (1962); J. Rinzel and J. B. Keller, *Biophys.* **13**, 1313 (1973).
- <sup>122</sup> a) A. Scott, *Active and Nonlinear Wave Propagation in Electronics*, Wiley-Interscience, N.Y., 1970 [Russ. transl. Sov. radio, M., 1977]; L. A. Ostrovskii and V. G. Yakhno, *Biofizika* **20**, 489 (1975); b) R. G. Casten, H. Cohen, and P. A. Lagerstrom, *Quart. Appl. Math.* **32**, 365 (1975).
- <sup>123</sup> A. T. Winfree, *Sci. Am.* **230**(6), 82 (June 1974); *The Geometry of Biological Time*, Springer-Verlag, N.Y., 1980; V. I. Krinskii and K. I. Agladze, *Dokl. Akad. Nauk SSSR* **263**, 335 (1982) [*Sov. Phys. Dokl.* **27**, 228 (1982)]; *Nature (London)* **296**, 424 (1982); A. M. Pertsov and A. V. Panfilov, in: *Autowave Processes in Systems with Diffusion* [in Russian], IPF Akad. Nauk SSSR, Gor'kiy, 1981, p. 77.
- <sup>124</sup> V. S. Zykov, *Modeling of Wave Processes in Excitable Media* [in Russian], Nauka, M., 1984; V. A. Davydov and A. S. Mikhaïlov, in *Nonlinear Waves: Structures and Bifurcations* [in Russian], Nauka, M., 1987, p. 261.



- <sup>125</sup> A. A. Frolov and I. P. Murav'ev, *Neuron Models of Associative Memory* [in Russian], Nauka, M., 1987.
- <sup>126</sup> A. A. Vedenov, *Modeling of Elements of Thought* [in Russian], Nauka, M., 1988.
- <sup>127</sup> F. T. Dubinin, *Optoelectronic Models of Homogeneous Media* [in Russian], Radio i svyaz', M., 1984.
- <sup>128</sup> R. Abraham, *Lecture Notes in Mathematics*, Vol. 525, Springer-Verlag, Berlin, 1976, p. 10.
- <sup>129</sup> G. Ferraro and G. Hausler, *Opt. Eng.* **19**, 422 (1980).
- <sup>130</sup> J. P. Crutchfield, *Physica D* **10**, 229 (1984).
- <sup>131</sup> A. V. Masterov, V. N. Tolkov, and V. G. Yakhno, in *Nonlinear Waves: Dynamics and Evolution* [in Russian], Nauka, M., 1989, p. 166.
- <sup>132</sup> A. V. Masterov, M. I. Rabinovich, V. N. Tolkov, and V. G. Yakhno, in *Collective Dynamics of Excitations and Structure Formation in Biological Tissues* [in Russian], IPF Akad. Nauk SSSR, 1988, p. 89.
- <sup>133</sup> A. V. Masterov and V. G. Yakhno, in *Collective Dynamics of Excitations and Structure Formation in Biological Tissues* [in Russian], IPF Akad. Nauk SSSR, 1988, p. 198.
- <sup>134</sup> G. Nicolis and J. F. G. Auchmuty, *Proc. Natl. Acad. Sci. U.S.A.* **71**, 2748 (1974).
- <sup>135</sup> V. V. Gafichuk, *Author's Abstract, Candidate's Dissertation* [in Russian], MFTI, M., 1982.
- <sup>136</sup> B. A. Malomed and A. A. Nepomnyashchy, *Proceedings of the Fourth International Workshop in Nonlinear and Turbulent Processes in Physics*, Vol. 2, Naukova Dumka, Kiev, p. 291; *Noise in Physical Systems: Proceedings of the Tenth International Conference*, Budapest, 1990, p. 601.
- <sup>137</sup> V. I. Petviashvili and A. M. Sergeev, *Dokl. Akad. Nauk SSSR* **276**, 1380 (1984) [*Sov. Phys. Dokl.* **29**, 493 (1984)].
- <sup>138</sup> B. S. Kerner, *Mikroelektronika* **5**, 257 (1976).
- <sup>139</sup> A. L. Dubitskiĭ, B. S. Kerner, and V. V. Osipov, *Dokl. Akad. Nauk SSSR* **308**, 857 (1989) [*Sov. Phys. Dokl.* **34**, 906 (1989)].
- <sup>140</sup> B. S. Kerner and V. V. Osipov, *Pis'ma Zh. Eksp. Teor. Fiz.* **41**, 386 (1985) [*JETP Lett.* **41**, 386 (1985)].
- <sup>141</sup> B. S. Kerner and V. V. Osipov, *Dokl. Akad. Nauk SSSR* **292**, 82 (1987) [*Sov. Phys. Dokl.* **32**, 43 (1987)].
- <sup>142</sup> A. V. Gurevich, R. G. Mints, and A. L. Rakhmanov, *Physics of Composite Superconductors* [in Russian], Nauka, M., 1987.
- <sup>143</sup> B. S. Kerner, V. V. Osipov, and M. N. Shneider, *Radiotekh. Elektron.* **32**, 1909 (1987).
- <sup>144</sup> A. Nitzan, P. Ortoleva, J. Deutch, and J. Ross, *J. Chem. Phys.* **61**, 1056 (1974).
- <sup>145</sup> Yu. I. Balkarei and V. V. Sandomirskiĭ, *Fiz. Tekh. Poluprovodn.* **13**, 1006 (1979) [*Sov. Phys. Semicond.* **13**, 587 (1979)].
- <sup>146</sup> A. A. Zaitsev and Kh. A. Dzherpetov, *Zh. Eksp. Teor. Fiz.* **24**, 516 (1953).
- <sup>147</sup> B. S. Kerner and V. V. Osipov, *Biofizika* **27**, 137 (1982). [*Biophysics (USSR)* **27**, 138 (1982)].
- <sup>148</sup> Yu. I. Balkarei and M. G. Nikulin, *Fiz. Tekh. Poluprovodn.* **12**, 347 (1978) [*Sov. Phys. Semicond.* **12**, 201 (1978)].
- <sup>149</sup> B. S. Kerner and V. V. Osipov, *Zh. Eksp. Teor. Fiz.* **89**, 589 (1985) [*Sov. Phys. JETP* **62**, 337 (1985)].
- <sup>150</sup> Ch. Radehaus, K. Kordell, H. Baumann, D. Jager, and H.-G. Purwins, *Z. Phys. Kl. B* **67**, 515 (1987).
- <sup>151</sup> B. S. Kerner and V. V. Osipov, *Mikroelektronika* **6**, 337 (1977).
- <sup>152</sup> C. G. Thornton and C. D. Simmons, *IEEE Trans. Electron Devices* **ED-5**, 6 (1958).
- <sup>153</sup> F. Bergman and D. Gertsner, *Arch. Electron. Uebertragungstech.* **17**, 467 (1963).
- <sup>154</sup> R. M. Scarlett and W. Shockley, *IEEE Intern. Conv. Rec.*, 1963, Pt. 3, p. 3.
- <sup>155</sup> A. M. Nechaev, E. A. Rubakha, and V. F. Sinkevich, *Reviews of Electronic Technology* [in Russian], TsNII, M., 1978, Ser. 2, No. 10.
- <sup>156</sup> H. D. Crane, *Proc. IRE* **50**, 2048 (1962).
- <sup>157</sup> K. F. Komarovskikh, V. N. Murygin, V. V. Osipov, and V. I. Stafeev, *Elektronnaya tekhnika*, Ser. 6, "Mikroelektronika" No. 3, 11 (1967).
- <sup>158</sup> V. I. Stafeev, K. F. Komarovskikh, and G. I. Fursin, *Neuristor and Other Functional Circuits with Feedback* [in Russian], Radio i svyaz', M., 1981.
- <sup>159</sup> S. Ya. Berkovich, *Radiotekh. Elektron.* **11**, 353 (1966).
- <sup>160</sup> B. S. Kerner and V. V. Osipov, *Mikroelektronika* **10**, 407 (1981).
- <sup>161</sup> D. W. Ross, *Phys. Rev.* **146**, 176 (1966).
- <sup>162</sup> K. Blötekar and P. Weissglas, *J. Appl. Phys.* **39**, 1645 (1968).
- <sup>163</sup> V. F. Gantmakher and I. B. Levinson, *Scattering of Current Carriers in Metals and Semiconductors* [in Russian], Nauka, M., 1984.
- <sup>164</sup> B. S. Kerner, N. A. Kozlov, A. M. Nechaev, and V. F. Sinkevich, *Mikroelektronika* **12**, 217 (1983); *Fiz. Tekh. Poluprovodn.* **17**, 1931 (1983) [*Sov. Phys. Semicond.* **17**, 1235 (1983)].
- <sup>165</sup> V. V. Gafichuk, *Fiz. Tverd. Tela (Leningrad)* **26**, 2230 (1984) [*Sov. Phys. Solid State* **26**, 1355 (1984)].
- <sup>166</sup> G. K. Celler, McD. Robinson, L. E. Trimble, and D. J. Lischner, *Appl. Phys. Lett.* **43**, 868 (1983).
- <sup>167</sup> M. Von Allmen, W. Luthy, and K. Affolter, *Appl. Phys. Lett.* **33**, 824 (1978).
- <sup>168</sup> S. G. Kiyak, A. Yu. Bonchik, V. V. Gafichuk, A. G. Yuzhanin, and I. V. Tyslyuk, *Izv. Akad. Nauk SSSR, Ser. Fiz.* **52**, 1883 (1988) [*sic*].
- <sup>169</sup> A. V. Sterword, *J. Appl. Phys.* **27**, 911 (1956).
- <sup>170</sup> A. L. Dubitskiĭ, B. S. Kerner, and V. V. Osipov, *Abstracts of the All-Union Conference "Physical and Physicochemical Foundations of Microelectronics"* [in Russian], Vilnius, 1987, p. 431.
- <sup>171</sup> B. N. Klyarfel'd, *Zh. Eksp. Teor. Fiz.* **22**, 66 (1952).
- <sup>172</sup> B. S. Kerner and V. V. Osipov, *Mikroelektronika* **12**, 512 (1983).
- <sup>173</sup> A. B. Vasil'eva and V. F. Butuzov, *Asymptotic Expansions of the Solutions of Singular Equations* [in Russian], Nauka, M., 1973.
- <sup>174</sup> J. D. Murray, *Lectures on Nonlinear-Differential-Equation Models in Biology*, Oxford Univ. Press, London, 1978 [Russ. transl. Mir, M., 1982].
- <sup>175</sup> A. H. Nayfeh, *Introduction to Perturbation Techniques*, Wiley, N.Y., 1981 [Russ. transl. Mir, M., 1984].
- <sup>176</sup> P. Ortoleva and I. Ross, *J. Chem. Phys.* **63**, 3398 (1975).
- <sup>177</sup> P. C. Fife, *J. Chem. Phys.* **64**, 554 (1976).
- <sup>178</sup> G. A. Korn and T. M. Korn, *Mathematical Handbook for Scientists and Engineers*, McGraw-Hill, N.Y., 1968 [Russ. transl. Nauka, M., 1973].
- <sup>179</sup> A. I. Ansel'm, *Introduction to the Theory of Semiconductors* [in Russian], Nauka, M., 1978.

Translated by D. Parsons